

Université Mohamed Khider Biskra
Faculté des Sciences et de la Technologie
Département : Génie Electrique
Ref :.....



جامعة محمد خيضر بسكرة

جامعة محمد خيضر بسكرة كلية
كلية العلوم و التكنولوجيا
قسم: الهندسة الكهربائية
المرجع:.....

Thèse présentée en vue de l'obtention du diplôme de
Doctorat LMD en Génie Electrique

Filière : Électrotechnique

Option : Gestion de l'Énergie et Diagnostic

Distributed Control and Optimization in Electrical Smart Grids

Présentée par :

BENKHETTA Djemoui

Soutenue publiquement le : 26/02/2025

Devant le jury composé de :

YAHIA Khaled	Professeur	President	Université de Biskra
ROUINA Abdelhafid	M. C. A	Rapporteur	Université de Biskra
SAHRAOUI Mohamed	Professeur	Examineur	Université de Biskra
M'HAMDI Benalia	M. C. A	Examineur	Université de Djelfa

2024/2025

Dedication

I dedicate this work to my family: Wife, Ritej , Hazar , Mohamed, Habib and Dirar

Djemoui

Acknowledgement

First of all, I would like to express my thanks to my thesis director

Dr. ROUINA Abdelhafid, Professor at Mohamed KHIDER Biskra University, for supporting and trusting me during these years with great patience. With his experience in research and teaching, with his advice, I was able to discover the world of scientific research in the field of power system and artificial intelligence. It is indeed a great pleasure for me to work under his supervision.

I would like to sincerely thank the members of the jury:

1. Pr. YAHIA Khaled, Professor at Mohamed KHIDER Biskra University, finds here the expression of my most sincere thanks for agreeing to chair this thesis.
2. Pr. SAHRAOUI Mohamed, Professor at Mohamed KHIDER Biskra University, for the interest shown in our work and his participation in the jury as an examiner.
3. Dr. M'HAMDI Benalia , Professor at Ziane Achour Djelfa University, for the interest shown in our work and his participation in the jury as an examiner.

Publications & Communications associated with the thesis

The contributions presented in this thesis manuscript have been published in the following articles.

➤ International Publications

Benkhetta D, Rouina A, Necira A. Optimal Placement and sizing of DG Units Using LCA Algorithm. EAI Endorsed Trans Energy Web [Internet]. 2024 Jun. 24 [cited 2024 Oct. 30];11. Available from: <https://publications.eai.eu/index.php/ew/article/view/4345>.

Benkhetta, D., Rouina, A., & Necira, A. (2024). The League Championship Algorithm (LCA) for optimal placement and sizing of shunt capacitors. *STUDIES IN ENGINEERING AND EXACT SCIENCES*, 5(2), e6975. <https://doi.org/10.54021/seesv5n2-124>.

II. International communications

D.benkhetta , A.Rouina A. Necira, " Optimization of network reconfiguration by Using League Championship Algorithm (LCA)," at the 3rd International Conference on Frontiers in Academic Research, June 15-16, 2024 : Konya, Turkey.

المخلص

تهدف هذه الرسالة إلى تقديم نهج يعتمد على خوارزمية بطولة الدوري (LCA) لتحديد العدد الأمثل، والموقع، وحجم المكثفات التعويضية (SC) ووحدات توليد الطاقة الشمسية الموزعة (PV-DG) في أنظمة التوزيع. الهدف الرئيسي هو تقليل خسائر الطاقة مع تحسين ملفات الجهد وتعزيز مؤشر استقرار الجهد. يتم تحديد المواقع المثلى لوحدات PV-DG و SC باستخدام عامل حساسية الخسارة (LSF)، بينما يتم تطبيق LCA لتحديد الأحجام المثلى لوحدات DG. تم التحقق من الطريقة المقترحة باستخدام أنظمة التوزيع الشعاعية-33 IEEE حافلة و69-حافلة، وتمت مقارنة النتائج بتقنيات أخرى من الأدبيات. تُظهر المحاكاة أن طريقة LCA فعالة للغاية، حيث تقدم أداءً متفوقاً في تحديد المواقع الأمثل وحجم وحدات PV-DG و SC داخل الشبكة الشعاعية.

Résumé

Cette thèse vise à introduire une approche basée sur l'Algorithme de Championnat de Ligue (LCA) pour déterminer le nombre optimal, le placement et la taille des condensateurs shunt (SC) et des unités de génération distribuée photovoltaïque (PV-DG) dans les systèmes de distribution. L'objectif principal est de minimiser les pertes d'énergie tout en améliorant les profils de tension et en renforçant l'indice de stabilité de la tension. Les emplacements optimaux des unités PV-DG et SC sont identifiés à l'aide du Facteur de Sensibilité aux Pertes (LSF), tandis que le LCA est appliqué pour déterminer les tailles optimales des unités DG. La méthode proposée a été validée en utilisant les systèmes de distribution radiale IEEE 33-bus et 69-bus, et les résultats ont été comparés à d'autres techniques de la littérature. Les simulations montrent que la méthode LCA est très efficace, offrant des performances supérieures dans la détermination de l'emplacement optimal et de la taille des unités PV-DG et SC au sein du réseau radial.

Mots-clés : génération d'énergie photovoltaïque distribuée (PV-DG) ; condensateurs en dérivation (SC) ; algorithme de championnat de ligue (LCA) ; réseau de distribution radial (RDS).

Abstract

This thesis aims to introduce an approach based on the League Championship Algorithm (LCA) to determine the optimal number, placement, and size of Shunt Capacitors (SC) and PV-DG (Photovoltaic Distributed Generation) units in distribution systems. The primary goal is to minimize power losses while improving voltage profiles and enhancing the voltage stability index. The optimal locations of PV-DG and SC units are identified

using the Loss Sensitivity Factor (LSF), while the LCA is applied to determine the optimal sizes of the DG units. The proposed method was validated using IEEE 33-bus and 69-bus radial distribution systems, with the results compared to other techniques from the literature. Simulations show that the LCA method is highly effective, delivering superior performance in determining the optimal location and sizing of PV-DG and SC units within the radial network

Keywords: Photovoltaic Distributed Generation (PV-DG); Shunt Capacitors (SC); League championship algorithm (LCA); Radial distribution network (RDS).

Abbreviations

ABC : Artificial Bee Colony

ANN : Artificial Neural Network

Ap : Awareness probability

BFS : Backward/Forward Sweep

CA : Culture Algorithm

CEED : Combined Economic and Emission Dispatch

CSA : Crow Search Algorithm

DCSA : Developed Crow Search Algorithm

DG : Distributed Generation

FA : Firefly Algorithm

Fl : Flight length

GA : Genetic Algorithm

IWO : Invasive Weed Optimization

LSF : Loss Sensitivity Factor

PSO : Particle Swarm Optimization

PSSE : Power System State Estimation

Pu : Per unit

RDN : Radial Distribution Networks

TLBO : Teacher Learner Based Optimization

VD : Voltage Deviation

VSI : Voltage Stability Index

LIST OF FIGURES:

Figure. 1.1. Basic structure of a power system	3
Figure. 1.2. Radial distribution network.....	3
Figure. 1.3. Network conFigureuration of a distribution network.....	4
Figure.1.4. Loop conFigureuration of a distribution network	4
Figure. 1.5. Concentrated and distributed power generation	5
Figure.1.6. Connection of a DG to a sub-branch of a distribution feeder.....	17
Figure. 1.7. Connection of a DG to the load bus.....	18
Figure. 1.8. Voltage profile of a distribution network at minimum and maximum loads.....	24
Figure. 1.9. The changes in the voltage with respect to the system angle and power factor	38
Figure. 1.10. The changes in the voltage with respect to the short circuit ratio for different values of power factor	38
Figure 2.1 Flux linkage of conductor i with n adjacent conductors.....	42
Figure 2.2 Two unbalanced conductors with virtual path for the return current flow.....	43
Figure 2.3 Four wire line section of grounded neutral	47
Figure 2.4 Daily load curve of certain 11kV distribution feeder in per-unit values.....	49
Figure 2.5 Simulation of load curves at the nodes of radial distribution feeder.....	50
Figure 2.6 Single line diagram of 5-nodes radial distribution feeder.....	51
Figure 2.7 Line section in four wire feeder of 3-phase unbalanced loads.....	53
Figure 2.8 Single line diagram of 3-phase four-wire distribution feeder.....	55
Figure. 3.1 Flowchart of the basic LCA.....	63
Figure. 3.2 A simple example of league championship scheduling.....	64
Figure. 3.3 Procedure of the artificial match analysis in LCA.....	66
Figure 4.1. A two bus system one line diagrams	74

Figure 4.2. Voltage profile of the 33-bus system with optimal number of distributed generators.....79

Figure 4.3. voltage profile of the 69-bus system with the optimal number of distributed generation (DG) units installed.81

Figure 4.4 . Voltage profile improvement with single capacitor 33-bus.....82

Figure 4.5. Voltage profile improvement with single capacitor 69-bus.....84

LIST OF TABLES

Table 1.1. Classification of DG sources6

Table.2.1 Real and reactive daily load demands of actual 11kV distribution feeder.....48

Table 3.1 Characteristics of the LCA.....61

Table 3.2 Hypothetical SWOT analysis derived from the artificial match analysis.....67

Table 4.1. LSF values for the 33-bus system.....77

Table 4.2. Results comparison of the 33-bus system with predetermined number of DG units.....78

Table 4.3. Results for the 33-bus system with 12 DG units obtained using both the SOS and LCA methods.....79

Table 4.4. Evaluating of results for the 69-bus system with Predetermined number of DG units.....80

Table 4.5. Results comparison for the 69-bus system with 8 distributed generation (DG) units81

Table 4.6. Single capacitor placement for 33-bus system.82

Table 4.7. Multi capacitors placement for 33-bus system.....83

Table 4.8. Single capacitor placement for 69-bus system.83

Table 4.9. Multi capacitors placement for 69-bus system.....84

Table 4.10. Results of 33-bus Distribution System for Reconfiguration in the Presence of PV-DG and Capacitors.85

Table 4.11. Results of 69-bus Distribution System for Reconfiguration in the Presence of PV-DG and Capacitors86

TABLE OF CONTENTS

Abstract	III
List of figures.....	VI
List of tables.....	VI
GENERAL INTRODUCTION.....	1
Chapter 1: Smart Grid Technology.....	4
1.1 Introduction.....	4
Distribution network.....	4
1.3 Distributed generation (DG)	6
1.3.1 DG application in the distribution network.....	8
Distributed generation benefits.....	7
Distributed generation limitations.....	8
1.3.2 DG types.....	9
Micro-turbine.....	10
Diesel generator.....	14
Wind turbine.....	11
Fuel cell.....	15
Geothermal energy.....	15
Biomass.....	16
1.3.3 DG effects.....	16
The effects of DGs on power flow components.....	17
The effect of DGs on line currents.....	18
The effect of DGs on voltage profile.....	20
The effect of DGs on network loss.....	22
The effect of different operation modes of DGs on power flow.....	22
Constant power factor operation mode.....	23
Voltage control mode.....	24

The effect of DG on voltage regulation devices.....	25
Control method.....	25
Tap adjustment.....	25
The effect of DG on capacitors.....	26
Reactive power flow.....	27
Capacitor control methods.....	28
The effect of DG on voltage regulators.....	29
1.3.4 Study of different loadings in the network.....	29
Without DGs and with maximum loading.....	30
With DGs and with maximum loading.....	30
With DGs and with minimum loading.....	31
1.3.5 DG application in distribution system based on optimization algorithm.....	32
Particle Swarm Optimization (PSO)	33
Genetic Algorithm (GA)	34
Ant Colony Optimization (ACO)	35
Artificial Bee Colony Algorithm (ABC)	35
Fireworks Algorithm (FWA)	36
Backtracking Search Optimization Algorithm (BSOA)	37
Ant Lion Optimizer (ALO)	38
1.3.6 Analysis of Power Quality (PQ) Features with DGs in the network.....	41
PQ problems in distribution systems with DGs.....	41
Gradual changes in the voltage.....	42
1.4 Conclusion.....	43
Chapter 2: Modeling Of Radial Distribution Feeder.....	44
Introduction.....	44
Series Impedance for Radial Distribution Feeder.....	44
2.2.1 Balanced Load Feeder... ..	44

2.2.2 Unbalanced load feeder.....	45
Load and PVDG Production Curves.....	50
2.3.1 Load Curve Modeling.....	50
2.3.2 PVDG Production Curve Modeling.....	50
Application of Backward/Forward Sweep Power Flow.....	53
2.4.1 Balanced Load Consideration.....	54
Calculation of Line Power Loss.....	59
Conclusion.....	60
Chapter 3: League Championship Algorithm (LCA).....	62
Introduction.....	62
Review of LCA and Its Terminology	63
League Championship Algorithm.....	65
Generating League Schedule.....	69
Determining the Winner or Loser.....	70
Setting Up a New Team Formation.....	71
Pseudo Code of LCA.....	76
Conclusions.....	78
Chapter 4: Simulation Results and Discussions.....	79
4.1 Introduction.....	80
4.2 Loss Sensitivity Factor.....	80
4.3 Objective Function.....	81
4.3.1 Constraints.....	82
Load Balancing Constraints.....	82
Voltage Constraints.....	83
DG Constraints.....	83
4.4 Results And Analysis Of Numerical Data.....	85
4.4.1 Only DG.....	85

The IEEE 33-Bus Radial Distribution Network.....	86
Predetermined number of DG units.....	86
Optimal Number of DG Units.....	87
The IEEE 69-Bus Radial Distribution Network.....	87
Predetermined Number of DG Units.....	88
Optimal Number of DG Units.....	88
4.4.2 Only Capacitors.....	89
THE IEEE 33-Bus Radial Distribution Network.....	90
Single Capacitor Placement.....	90
Multi Capacitor Placements.....	94
The IEEE 69-bus radial distribution system.....	96
Single Capacitor Placement.....	96
Multi Capacitor Placements.....	97
4.4.3 Simultaneous PV-DG And Capacitors.....	98
The IEEE 33-bus radial distribution network.....	98
The IEEE 69-bus radial distribution network.....	99
4.5 CONCLUSION.....	100
Appendix I: IEEE 33-Bus Radial Distribution Network.....	102
Appendix II: IEEE 69-Bus Radial Distribution Network.....	104
References.....	106

GENERAL INTRODUCTION

The growth of any power system grid in the world is and always has been on an accelerating pace, feeding the almost insatiable demand for electrical power for the past century or so [1, 2]. This in turn forces a certain level of intricacy on the power system and that intricacy compounds with time; to the point where the power systems face the inability to progress with ease due to introductions of new transmission systems and construction of generating plants near load centres. As the system grows more complex and burdened with increasing load; various issues regarding cost, pollution, power quality and voltage stability takes centre stage [2].

Distributed Generation (DG) is an electrical power generation unit that is directly connected to a distribution network or placed as nearly as possible to its consumer. The technologies adopted in distributed generation vary in methods of generation including small-scaled gas turbines, wind, fuel cells, solar energy and hydro, etc [1]. DG is both beneficial to the consumers and utilities, much so in places where centralized generations are unfeasible or where deficiencies can be found in transmission systems. Optimally allocating DG units may address all the issues stated before, resulting in reduced power system losses, improved voltage profile, enhance power transfer capability, reduce pollution and cut generation and transmission cost [3,4].

Benefit-wise, DG may offer solutions to the majority of power systems crave. However, installation of a unit at a non-optimal place may have the reverse effect instead to the system; such as increases in system losses followed by an increase in cost [5-8]. With that in mind, selecting the most appropriate place for installation paired with the ideal size of a DG unit is of utmost importance in a large power system. Nevertheless, the optimum choice and allocation of DG is a complex integrative optimization method for which common or older optimization method falls short in implementing such a concept in the system [9].

Radial distribution networks, which are commonly used in low and medium-voltage networks, have a very high resistance-to-reactance ratio (R/X ratio). Traditional power flow techniques such as Gauss-

Seidel (GS), Newton-Raphson (NR), and Fast Decoupled Load Flow (FDLF) are not operative in this scenario and most of time fails to converge. Therefore, alternative algorithms have been proposed to address this issue. The Backward Forward Sweep (BFS) approach is the most widely used algorithm

In optimization, many techniques are used to solve the problem in power system. In this study, the League Championship Algorithm (LCA), a powerful optimization method, was utilized to define the optimal location and size of DG units in radial distribution systems. The effectiveness of the suggested method was demonstrated through testing on various real networks, including the 33-bus and 69-bus test systems. The results were then compared to recently published articles.

The objectives of the project are as follow:

1. To study about Distribution Generation, load flow by using backward forward sweep method and optimization technique using League championship Algorithm (LCA).
2. To solve sizing and location of Distribution Generation and shunt capacitors with standard IEEE 33-bus and IEEE 69-bus installation by using MATLAB programming.
3. To minimize the losses and improve the voltage profile in a distribution network.

This thesis is organized around four chapters which deal with all the questions raised:

In the first chapter, a reminder of smart grid technology is discussed. The Distributed generator and shunt capacitors and different algorithms used.

The second chapter of this work concerns modeling of radial distribution feeder, application of backward forward sweep power flow.

Third chapter presents the league championship algorithm.

We present in the fourth chapter the development of the league championship algorithm and we prove its superiority against basic LCA and other well-known algorithms. Afterwards, the results of the application of LCA to the optimization of the placement and sizes of PV-DG and capacitors, as well as a comparative study of the results obtained by other optimization methods. In other hand, the integration effect of a photovoltaic PV generators and capacitors on the radial distribution system IEEE 33 bus and IEEE 69

bus (test system) is presented, Finally, we end this essay with a conclusion and perspectives to complete this work.

Chapter 1:

Smart Grid Technology

1.1 Introduction

Numerous studies have delved into harnessing distributed networks powered by distributed generation resources, particularly renewable energy sources [22-75]. Various metrics have been explored to assess the impact of distributed generation resources on the distribution network. In the operation of distribution networks, diverse methods have been proposed to determine the optimal location and size of energy resources, alongside offering different objective functions. Optimization methods have been suggested based on their intelligent characteristics among analytical approaches. This chapter reviews selected research topics concerning the optimization process of distributed generation (DG) and its influence on diverse parameters such as power loss, power quality (PQ), among others, within the distribution network. Furthermore, recent studies analyzing the optimization of hybrid distributed generation (HDG) systems in both isolated and grid-connected operations are examined in this chapter. Additionally, the chapter presents the limitations of these methods and strategies for overcoming them.

1.2 Distribution network

The primary objective of a power system is to ensure the consistent supply of voltage and frequency to customers without any disruptions. Achieving this goal requires various components to function effectively:

Firstly, the generation system must produce the necessary power. Secondly, the transmission system must efficiently transfer this power over long distances without overheating. Lastly, distribution networks are responsible for delivering electricity to the input nodes of customers' internal systems.

Traditionally, power generation involves injecting power into the transmission system, which acts as the conduit for power from generating stations to the sub-transmission system, operating at voltage levels of 230 kV and higher. The sub-transmission system then transfers power to distribution networks, which ultimately supply electricity to consumers at voltages typically below 34.5 kV.

An illustration of this conventional bulk electrical power system is depicted in Figure. 1.1

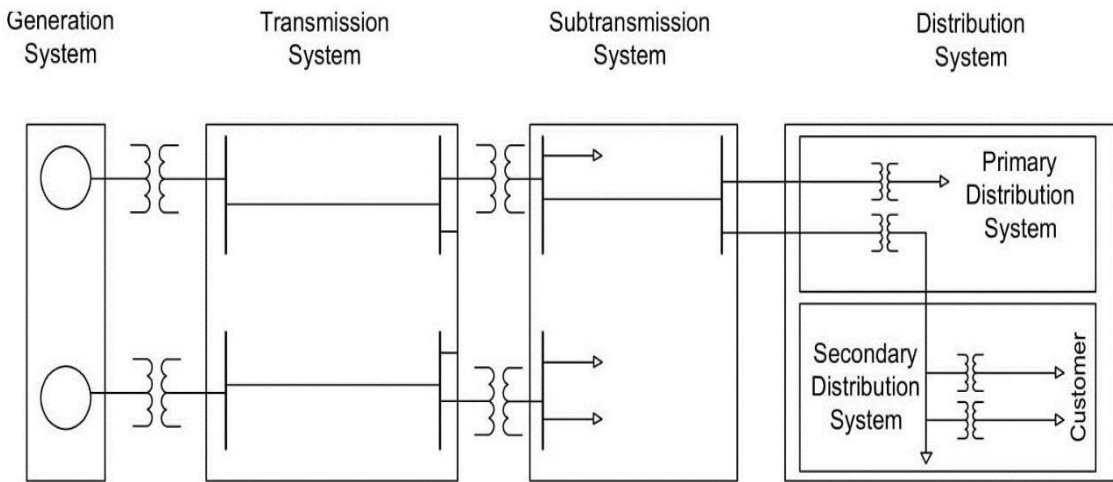


Figure. 1.1. Basic structure of a power system [22].

An important aspect of distribution networks is their configuration, or how their lines are interconnected. There are three conventional configurations: radial, network, and loop. In radial configurations, the lines are sequentially branched out and the power flow is unidirectional as shown in Figure. 2.2. This configuration imposes the lowest cost; however, it has the minimum reliability, because any fault in the feeders will cause service interruptions at all downstream locations.

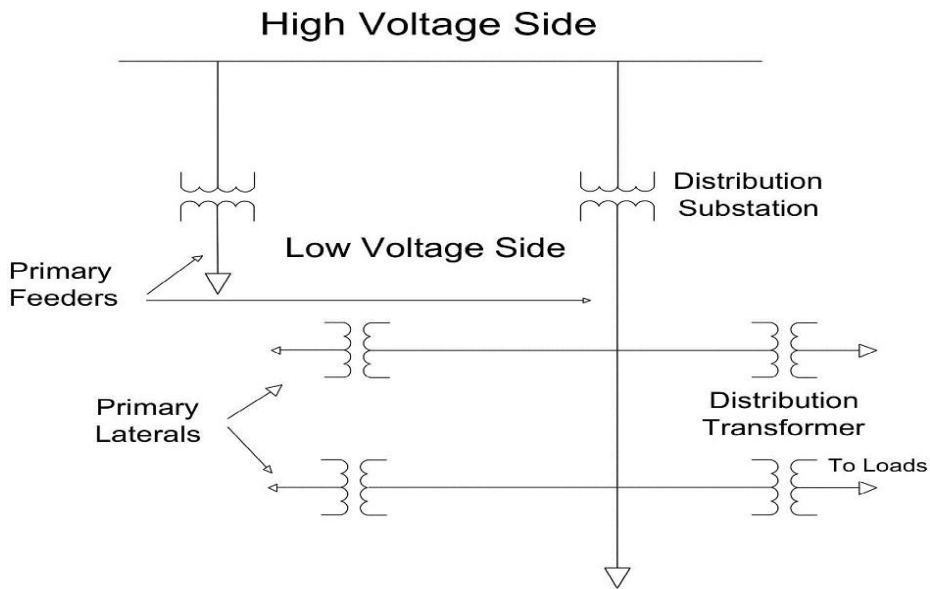


Figure. 1.2. Radial distribution network [18].

In a network configuration, there are typically a greater number of connections, resulting in multiple paths between two points and forming loops within the system. Figure. 1.3 demonstrates a network configuration of a distribution network

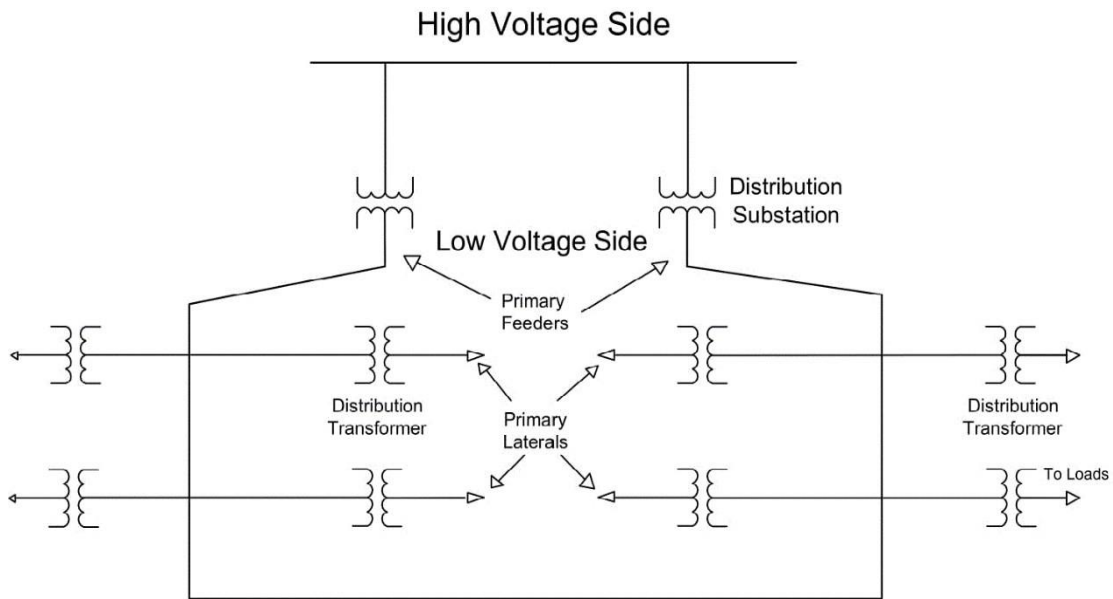


Figure 1.3. Network configuration of a distribution network [21].

Loop configuration distribution networks lie between the radial and network configurations in terms of cost and reliability. As depicted in Figure 1.4, loop configurations can be conceptualized as two radial systems separated by a normally open switch. In the event of a failure in one of the two substation transformers, the switch can be closed, allowing part of the distribution network to be energized through another transformer.

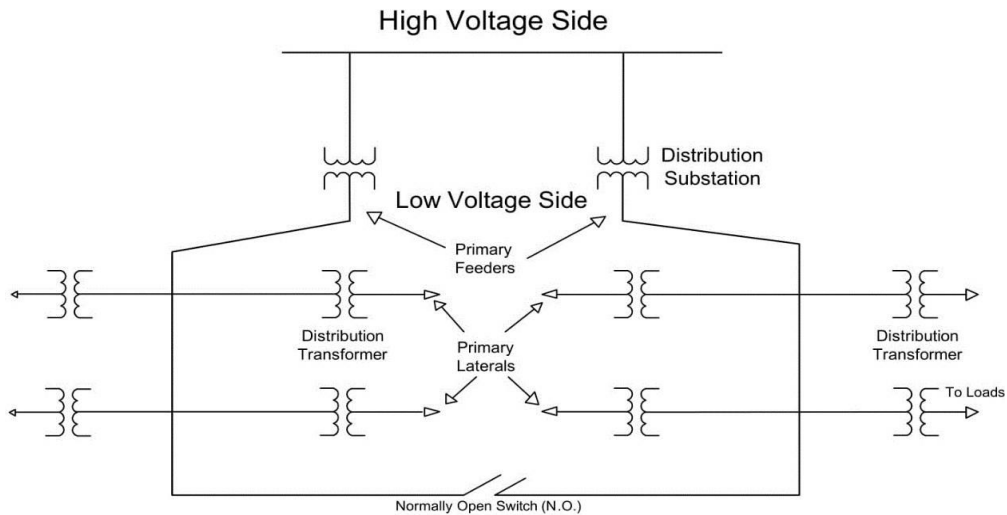


Figure 1.4. Loop configuration of a distribution network [21].

Designing and planning the distribution network presents a significant challenge in the current model, largely due to the restructuring of the power industry, policy shifts, and advancements in distributed generation (DG) technologies. Effective planning and design

of the distribution network represent the optimal approach for network development, ensuring reliable services and minimizing economic costs for customers. Presently, the rapid evolution of DG technology, along with its myriad benefits, has rendered it a feasible and appealing option for distribution companies in their planning endeavors.

1.3 Distributed generation (DG)

Distributed generation, also known as locally generated or distributed energy, involves generating electricity from small-scale sources. Historically, industrialized nations have relied heavily on fossil fuels like coal, gas, nuclear, and large hydroelectric plants for their electricity needs. However, with the advent of restructuring in the energy sector, there's a growing emphasis on utilizing renewable sources such as solar and wind power within the newly restructured system. Concentrated distributed generation units leveraging renewable energies offer economic benefits and have minimal negative environmental impacts.

Distributed generation resources encompass various small-scale power technologies that can enhance power quality (PQ) in traditional electrical networks. They achieve this by injecting active and reactive power into the network, necessitating optimal placement and capacity to improve network characteristics, including PQ. Additionally, distributed generation serves as an alternative to extending electricity transmission to rural areas, thus reducing transmission and distribution costs. These small-scale distributed generation units play a crucial role in meeting incremental load demand changes and addressing demand shortages across the power system.

Technologies utilized in distributed generation include small gas turbines, micro-turbines, fuel cells, wind and solar energy, biomass power plants, hydroelectric power, among others. Distributed generation can operate either in an isolated mode, catering to local customer demand, or as part of an integrated electrical system connected to the grid. Within the distribution network, distributed generation can be strategically deployed to fulfill customer needs, particularly in areas where the power transmission system is inadequate. Figure. 1.5 illustrates the distinction between conventional centralized generation and today's distributed generation approaches.

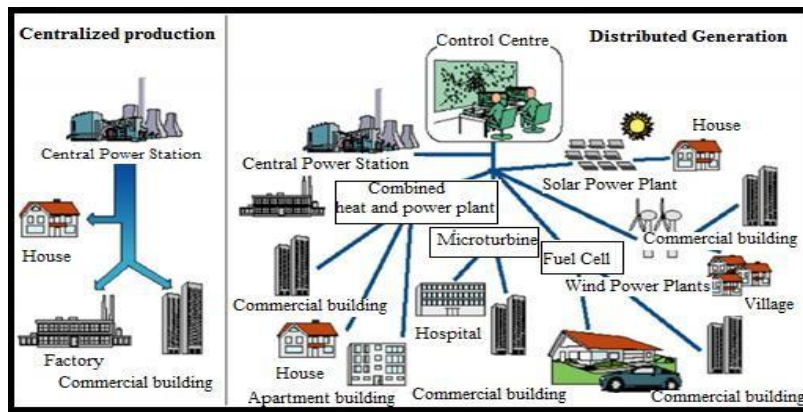


Figure. 1.5. Concentrated and distributed power generation [24].

The widespread application of distributed generation (DG) in conducted studies can be attributed to several key factors:

Power generation at the load site by DG helps in reducing distribution and transmission costs.

In an integrated restructured system where both the network and DGs are included, distribution and transmission costs tend to rise as DG costs decrease.

Recent advancements in energy resources technology have facilitated access to power plants with higher efficiency and capacity, ranging from a few kilowatts to several hundred megawatts, for various DGs.

Within the restructured system, it is essential to determine the optimal location and size of DG resources to maximize their effectiveness and efficiency.

DGs usually require less installation time than traditional power plants or transmission lines to supply remote loads and have low investment risk; and DGs have relatively good efficiency, especially in hybrid combustion and combined cycle (larger power plants).

When considering the operation of distribution networks and the impact of distributed generation (DG), particular attention is focused on the location and sizing of DG units. Installing DG units in suboptimal locations can lead to increased power loss and reduced reliability in meeting customer demand, ultimately weakening the power quality (PQ) of the network. Therefore, employing appropriate tools to locate and size DG units optimally is crucial to reducing system costs and improving PQ.

At the endpoint level of power consumption, various DG technologies, including internal combustion engines, can be utilized. These technologies enable DG to function either independently as an "island" or as a small component of the grid. Studies generally indicate that DG penetration of up to 10-15% of peak load can be seamlessly integrated into the power grid without necessitating major structural changes.

Table 1.1 provides a classification of DGs based on their generation capacity, taking into account parameters such as fuel type, capacity, electrical efficiency, installation cost, maintenance cost, peak load correction, reliability, and power quality.

Classification	Generation level
Micro DG	1 W to 5 kW
Small DG	5 kW to 5 MW
Average DG	5 MW to 50 MW
Large DG	50 MW to 300 MW

Table 1.1. Classification of DG sources [24].

1.3.1 DG application in the distribution network

The application of different DG technologies is determined by various factors. Some of these factors are as follows:

- *Base load: Systems operating in parallel with the distribution network continuously inject energy into the grid and can also sell energy to the grid. This constant operation reduces network energy consumption;*
- *Peak load supply: DG is utilized to supply electricity during peak load periods when energy costs are typically higher, thereby reducing peak demand;*
- *Distribution network support: Power companies or large customers sometimes install small power plants to reinforce their power grid and alleviate congestion or network failures at different times of the year;*
- *Power supply quality: DGs are employed to compensate for power shortages if the quality of power supply in the distribution network falls below the demand of electricity customers*
- *Energy storage: DGs serve as alternative sources when the cost of using this technology is low or when the network experiences frequent interruptions. Consequently, they are utilized as backup resources.*

➤ **Distributed generation benefits**

Distributed power generation presents numerous opportunities, particularly in the realm of clean energy production devoid of environmental pollution. Many distributed generation (DG) sources utilize renewable energy, operating on the cogeneration of electric power and heat. Renewable sources like wind and solar energy are freely obtained from nature, as is the case

with thermal power plants. Due to their high efficiency and environmentally-friendly nature, DG technologies aid in reducing greenhouse gas emissions.

The deployment of DG in existing distribution networks offers a plethora of benefits with economic and technical implications that are interconnected. These benefits are typically categorized into three main areas: technical, economic, and environmental. Technical benefits encompass a wide range of issues, including peak load correction, maintaining proper voltage levels, continuous load supply, and addressing power quality (PQ) problems.

In developing countries, where energy losses during transmission and distribution are significant (15 to 20% of generation), DG installations can contribute to system loss reduction. In contrast, developed power systems typically experience lower losses (around 10%). However, the optimal location and sizing of DG units play critical roles in minimizing losses, an aspect that has been extensively studied.

Some of the technical benefits associated with employing DG include:

- Reduction of distribution network losses;
- Improvement of voltage profile in the distribution network;
- Improvement of energy efficiency;
- Improvement of network reliability and security;
- Improvement of PQ; and
- Minimizing transmission and distribution costs.

The economic benefits include saving on fuel consumption, saving on transmission and distribution costs, and reducing electricity sales prices. The major economic benefits of utilizing DG are as follows:

- Deferred investment to upgrade facilities;
- Reduced maintenance and operation costs of some DG technologies;
- Reduced healthcare costs due to environmental improvements;
- Reduced fuel costs due to increased overall efficiency;
- Reduced storage requirements and associated costs;
- Lower operating costs due to load peak correction; and
- Increased security for critical loads.

➤ **Distributed generation limitations**

When the DG penetration level is noticeable, the dynamics of the system can be affected. DG connection analysis becomes complicated, especially given the wide range of DG technology and distribution network configuration designed to operate with unidirectional power flow. When large-scale DG is connected to the grid, researchers and Operators of distribution networks encounter various challenges and limitations, including:

- Reverse power flow: Connection of distributed generation (DG) to the system can disrupt protective circuits in the network configuration.
- Reactive power: Many DG technologies, particularly those using synchronous generators, do not inject reactive power into the grid.
- System frequency: Imbalances between supply and demand can cause frequency deviations from the system's nominal frequency. Increasing DG capacity can affect system frequency, complicating the control process.
- Voltage levels: Installed DG units can improve the voltage profile of the distribution network, potentially leading to increased voltage levels. While this is not an issue in congested networks with low-voltage problems, it may require adjustments in other scenarios.
- Protection design: Distribution networks are often configured in radial or loop forms, accommodating unidirectional power flow. The installation of DG units introduces bidirectional power flow, necessitating adjustments to the protection system and network resizing.
- Islanding protection: Ensuring protection against islanding, where a part of the system remains energized by DG while isolated from the rest of the network, is crucial. This situation poses risks during maintenance or repairs. Protective devices such as relays and transition switches are employed to address this issue.
- Harmonic injection: Asynchronous DG sources using inverters for connection can inject harmonics into the system.
- Network instability: The presence of DG units can contribute to network instability under certain conditions.

- **Increased fault currents:** The location of DG units can lead to increased fault currents in the distribution network.
- **High financial costs per kW of power generation:** The financial costs associated with DG installations can be relatively high compared to centralized power generation.
- **Power quality (PQ) concerns:** The use of power electronics in controlling wind energy technologies can pose PQ risks.

1.3.2 DG types

➤ **Micro-turbine**

A micro-turbine is a device that utilizes gas flow to convert thermal energy into mechanical energy. Typically fueled by combustible gases such as natural gas, the fuel is pumped by a compressor and mixed in an air combustion chamber. The resulting gases from combustion drive the turbine to rotate, which in turn rotates the generator and compressor simultaneously. In the commonly used design, the compressor and turbine are mounted on the same shaft as the generator.

The output voltage of micro-turbines cannot be directly connected to the grid or urban facility. Instead, it must be converted to direct current (DC) to achieve the rated voltage and frequency before being converted back to alternating current (AC). Micro-turbines offer several advantages, including clean operation with low gas emissions, suitable performance, fast response time, moderate startup time, high availability, and convenient dispatching capability. However, there are also disadvantages associated with micro-turbines, such as high maintenance costs and limited experience in this field. Few micro-turbines have been deployed for a sufficient duration to establish a reliable database on their reliability. Furthermore, load control and power flow methods have not been fully developed for a large number of micro-turbines, especially regarding the sale of excess energy generated.

➤ **Diesel generator**

Diesel generators serve as essential Uninterruptible Power Supplies (UPS) or backup sources for a wide range of applications, from low to large-scale public and industrial use. They combine a diesel engine with an electric generator (commonly referred to as a dynamo) to

produce electricity. Diesel generators are deployed during network failures or as emergency power sources connected to the power grid. They find utility in various scenarios, including construction sites (for auxiliary electricity) and mobile residential power supply.

A diesel generator set typically includes a diesel engine, generator, and auxiliary components like a stand or chassis, control systems, circuit breakers, and water heaters to ensure system operation. Diesel generators with rated power ranging from 8 to 30 kW are commonly used for residential homes, small offices, shops, as well as larger office complexes, factories, and industrial centers.

Photovoltaic cells, also known as solar cells, form an integral part of photovoltaic systems. These systems convert solar radiation energy into electricity through the photovoltaic effect. Solar cells are often interconnected electrically and assembled into modules. With advancements in solar technology and research, electricity generation from solar power has become increasingly competitive with other conventional methods. Solar power generation plays a significant role in reducing greenhouse gas emissions.

Solar power systems can operate in both grid-connected and grid-independent modes. In grid-connected systems, electrical energy generated by the photovoltaic system is converted from DC to AC using inverters and injected into the grid at specified voltage and frequency levels. In grid-independent mode, the solar power system operates autonomously, supplying electricity directly to the load without relying on the main grid. In this mode, power is supplied by PV panels, energy storage systems, and energy control systems with high reliability.

The major advantages of solar power plants include:

- No required for fossil fuel and refueling ability to install and operate different capacities to meet the needs of consumers;
- Longevity;
- Ease of operation;
- Ability to install and operate on the roof of homes; and
- storage capability.

➤ **Wind turbine**

In the process of generating electrical power from wind kinetic energy, a specific cycle is

involved between the input and output of the wind turbine. When the turbine blades are driven by wind energy, the mechanical power is transmitted to the gearbox through the main shaft. The output of the gearbox is then transmitted to the generator via a coupling mechanism, resulting in the generation of electrical energy through the rotation of the generator.

The wind turbine typically comprises a tower, a nacelle (or yoke), a generator, and a compartment. The power flow path starts from the wind, which is converted into mechanical energy and then into electrical energy.

The tower supports the main components of the wind turbine. However, part of the wind power is initially lost and does not enter the system due to inefficiencies in the turbine. Additionally, some power is lost mechanically in the turbine, shaft, and generator. Another portion of the power, dependent on speed changes, is stored as inertia in the mechanical system. Finally, the remaining portion is lost as electrical losses in components such as generators, cables, brushes, etc..

➤ **Fuel cell**

Fuel cells operate similarly to batteries, continuously charged with high-hydrogen gas fuel while incorporating air to provide the necessary oxygen for the chemical reaction. The process involves a reaction between hydrogen and oxygen within the fuel cell, resulting in the generation of DC voltage through an electrolytic conductive ion. This DC voltage is then converted to AC voltage using an inverter before being delivered to the grid.

One notable characteristic of fuel cells is their ability to produce electricity, heat, and water without any moving parts, which enhances the technology's reliability and ensures noise-free operation. Moreover, fuel cells can operate more efficiently than many other electricity generation devices by utilizing a wide range of fossil fuels.

However, fuel cells also come with drawbacks, particularly high operating costs. Additionally, it is essential to assess the impact of rapid contamination and hardening of electrolyte properties on cell efficiency and longevity. These factors represent significant considerations in evaluating the overall performance and viability of fuel cell technology.

➤ **Geothermal energy**

Geothermal energy, sourced from the thermal energy within the earth's solid crust, is a pivotal

resource [31]. The earth's core serves as a vast reservoir of thermal energy, evident through phenomena like volcanic eruptions and warm waters. The prevailing hypothesis suggests that over 4 billion years ago, the earth was a molten mass that has since cooled gradually, a process that persists today. Presently, geothermal energy, readily accessible, finds widespread use across the globe in various applications. Researchers continually develop new energy supply methods in response to emerging energy technologies, emphasizing the essential role of technology transfer in future advancements. Geothermal energy exploitation, stemming from the earth's depths, remains unaffected by climate conditions and proves adaptable to current and future human energy demands.

Regions with geothermal energy potential are typically found in volcanic and earthquake-prone areas worldwide. The earliest endeavors to harness this energy for electricity generation date back to Italy in 1904, sparking widespread interest and activities globally. Generally, areas possessing three key attributes— a heat source, intermediary fluid, and porous media— show promise for geothermal energy exploitation. Both power plant and non-power plant methods can be employed to utilize geothermal energy effectively. Non-power plant methods are versatile, finding applications in greenhouse facilities, fishponds, thermal pumps, ice prevention in passageways, as well as for home heating and snow melting. Electricity generation at geothermal power plants is categorized into two main groups: two-phase and single-phase geothermal power plants. In certain countries, it is crucial to harness geothermal energy in regions with the appropriate potential. However, many of these generation methods in these countries are primarily studied in the context of distributed generation (DG), and their integration into the main grid requires careful evaluation. This involves assessing their placement, determining the appropriate objective function, and analyzing the impacts of their presence on the overall power system.

➤ **Biomass**

Biomass [32] stands out as one of the most suitable energy sources for environmental preservation, as it not only qualifies as renewable but also promotes environmental cleanliness and health. With its various forms and methods of utilization, biomass technology offers a significant contribution to reducing environmental pollution through energy generation. Biomass is essentially the result of solar energy collection, conversion, and storage by plants,

along with surplus residues from nature. Despite its relatively low process efficiency, the utilization of biomass as a source of energy is on the rise, largely owing to the availability of its raw material (fuel) at no cost, coupled with its additional benefits. Presently, considerable efforts are underway to enhance efficiency and advance this technology further. Diverse technologies have been developed to convert biomass into heat in thermal power plants, with typical efficiency levels ranging from 36 to 47%.

➤ **DG effects**

Distribution systems are typically designed under the assumption that electrical charge flows from the power system to the load. Therefore, the presence of Distributed Generation (DG) can lead to output fluctuations or reverse current flow from the generator, potentially affecting the distribution system. These impacts encompass various aspects such as power losses, voltage profile, reliability, power quality, protection, and safety. Some key effects of DGs include [24, 33]:

Because of its proximity to the load center, Distributed Generation (DG) plays a substantial role in reducing electrical losses. Ideally, DG units should be positioned in areas where additional loss reduction is needed. Similar to the placement of capacitors, the location of DG units is determined with the aim of minimizing losses. The primary distinction lies in the fact that DG units impact both active and reactive power, whereas capacitor banks only affect reactive power flow. In feeders characterized by high losses, strategically placing a small amount of DG (approximately 10-20% of the feeder load) can lead to a significant reduction in network losses.

Voltage regulation in distribution systems is typically managed through tap changers on substation transformers and the use of voltage regulators and capacitors within the feeder. This traditional voltage regulation method assumes power flow from the substation to the loads. However, the introduction of Distributed Generation (DG) with continuous power flow can disrupt this conventional approach to voltage regulation. Improper placement of DG can lead to under-voltage or overvoltage conditions in the network, as voltage regulation control is typically based on radial power flow.

Nevertheless, DG installation can have positive effects on the distribution network by supplying reactive power for voltage control, reducing losses, regulating frequency, and

serving as a spinning reserve [34].

Power Quality (PQ) refers to the degree to which power characteristics align with the ideal sinusoidal waveform of current and voltage, with balanced current and voltage. To safeguard the system from PQ degradation, the system operator must ensure the minimum specified short circuit capacity [35]. The relationship between DG and PQ is multifaceted. On one hand, many researchers highlight the impact of DG on power quality. For instance, in areas where voltage support is challenging, DG can be beneficial as it generally raises grid voltage, potentially aiding voltage support and power factor correction. However, excessive DG connections in a given line may widen the power flow distance among feeder lines due to backward current flow, potentially causing voltage profiles to exceed acceptable limits.

Distribution line voltage is typically controlled by a programmable timer or Line Drop Compensator (LDC) [36]. Since a distribution transformer serves multiple feeder lines, voltage is set collectively for these lines. Rapid changes in DG output can lead to voltage fluctuations in the system, resulting in overvoltage and under-voltage conditions for end-users. This issue is particularly pronounced when generation systems rely on natural conditions, such as wind and photovoltaic (PV) generators, whose inputs are subject to the uncertainty of wind speed and solar radiation intensity, leading to concerns about voltage fluctuations caused by changes in the power output of these units [37].

The reliability of power supply sources is crucial for both power distribution companies and end-users, as interruptions in power supply can result in significant economic losses. In the past, outages and interruptions in distribution systems were perceived as less severe compared to those in generation and transmission systems. However, extensive data collected over many years have demonstrated that power interruptions at the distribution level have a dramatic impact on the entire power supply chain. Consequently, Distributed Generation (DG) units are often integrated into distribution networks with the aim of improving power supply reliability [38]. DGs can serve as support and backup systems, or in some cases, they can function as the primary power source for supplying loads. Another objective of deploying DGs is to reduce costs during peak demand hours.

Assessing reliability at the distribution level involves estimating the impact of past service levels. To address this, the effects of service deficiencies on system performance indices must be determined. Power system operators utilize reliability indices to enhance service levels and

meet users' requirements. These indices also aid in identifying the requirements of generation and transmission systems, determining additional capacity needed at the distribution level, and assessing system robustness against adverse faults and events. Furthermore, power engineers and operators extensively rely on reliability indices to make operational decisions and implement changes in emergency situations [39].

➤ **The effects of DGs on power flow components**

Distribution networks are traditionally designed under the assumption that the primary side of sub-transmission substations connected to the transmission system is the sole power source from which the short circuit capacity of the system can be obtained. However, the integration of Distributed Generation (DG) units throughout the distribution network challenges this assumption. Consequently, new operational paradigms emerge, introducing complexities not present in traditional systems. Nevertheless, precise engineering practices can mitigate potential disadvantages associated with DGs and maximize their efficiency [40]. Some of the disadvantages of DGs include [41]:

- Increase probability of failure in system equipment and customers;
- Reduction of PQ (especially overvoltage);
- Reduction of reliability;
- Increased substation -fault restoration time; and
- Reduced safety of the system and personnel.

This subsection examines the impacts of Distributed Generators (DGs) on various components of power flow within the distribution network, including line currents, voltage profiles, and system losses. Given that distribution systems utilize specific equipment to adjust voltage profiles, the subsequent discussion addresses the effect of DGs on voltage regulation devices. Different loading scenarios are derived from studies focusing on the influence of DGs.

Traditional unidirectional radial distribution networks typically rely on a single power supply originating from the primary side of the substation, which is connected to the transmission network. However, the introduction of DGs disrupts this structure, giving rise to new challenges in these networks that affect various power flow component.

➤ The effect of DGs online currents

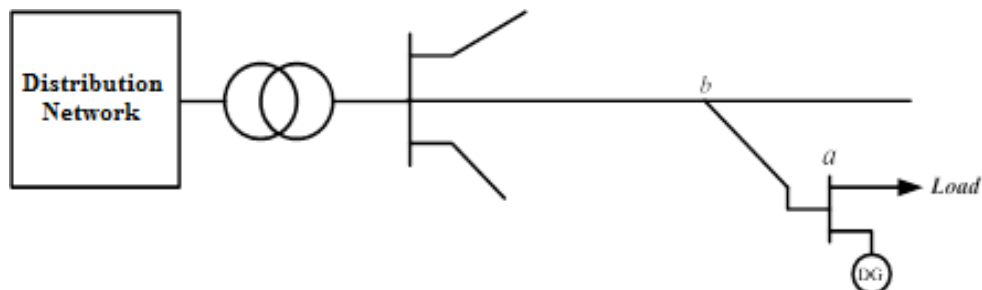
The presence of Distributed Generators (DGs) typically leads to a reduction in network loading and frees up capacity on various lines, which is a significant benefit of these resources. However, poor engineering design conditions may result in some lines becoming overloaded. Therefore, studying the network with DGs in terms of line overcurrent is essential.

In a traditional network, the conductors typically weaken as they move away from the substation. This design relies on the assumption that the network is radial and unidirectional, with power supplied from the substation. Normally, DGs decrease line currents by supplying part of the network load. However, depending on the network's size and condition, DG current may flow in the opposite direction. If the DG is larger than the load downstream, some current may return to the substation. While this alone may not be problematic, excessive current flow toward the substation can exceed conductor capacity.

Under certain conditions, such as load curtailment after the DG due to unforeseen faults, the entire DG current may flow back to the substation. If the DG size is substantial and the network is designed based on traditional defaults, an overcurrent problem may arise. Therefore, careful consideration of DG integration and network design is crucial to avoid such issues.

Another scenario that can lead to an overcurrent problem is when a dedicated Distributed Generator (DG) is installed to supply specific customers. In such cases, if the conductors leading to the DG are chosen based on the released capacity of the line, challenges may arise during load outage conditions.

For instance, consider Figure. 1.6, where the DG is connected to bus a to supply a three-phase load. When the load is disconnected, the DG current flows toward point b. Consequently, if the line between points a and b is selected based on the released capacity of the line, it may not be able to transmit DG energy to point b and could become overloaded. This situation



highlights the importance of careful conductor selection and network planning to avoid overloading issues when integrating dedicated DGs to feed specific loads.

Figure.1.6. Connection of a DG to a sub-branch of a distribution feeder.

Indeed, while Distributed Generators (DGs) generally reduce line current and free up capacity on the line, poor design can lead to overloading in certain cases. This issue can be examined by considering the maximum and minimum loading conditions of both the DG and the network, respectively. Studying various scenarios for network loading allows for a comprehensive investigation of potential overloading issues and helps identify optimal design solutions to ensure efficient and reliable operation of the system.

➤ **The effect of DGs on voltage profile**

DGs located near the load centers in distribution networks can improve voltage profile due to the following reasons:

- Because of the proximity to the load, the impedance of the load feeding path is thus reduced, DGs reduce the voltage drop according to the impedance reduction;
- By supplying the loads, DGs reduce the power transfer from the sub-transmission substation or distribution substation toward the end of the feeders, thereby reducing the voltage drop by reducing the active and reactive power supply; and
- By operating in the PV mode, DGs can regulate the voltage of the network.

While Distributed Generators (DGs) offer numerous advantages to the grid, they can also introduce some drawbacks. One such disadvantage arises from the fact that most DGs supply constant power to the network, thereby enhancing the voltage profile during peak load hours. However, during low load conditions, DGs can increase voltage levels by reversing the power flow.

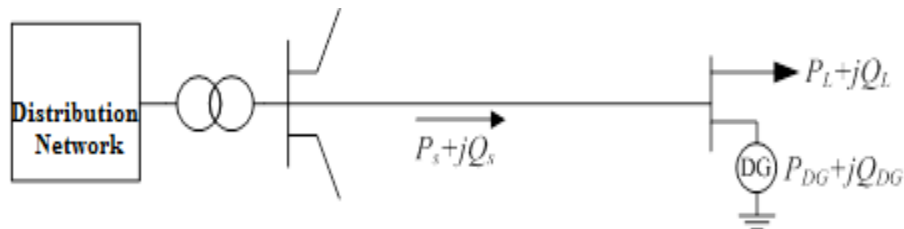


Figure. 1.7. Connection of a DG to the load bus.

For example, in Figure. 1.7, a DG is connected to the load bus. The amount of injected power

from the distribution substation can be calculated as follows:

$$S_s = P_s + jQ_s = (P_L - P_{DG}) + (Q_L -) \quad (1.1)$$

where, S_s is apparent power, P_s and Q_s , are active and reactive powers respectively, j is an imaginary number and Q_L and Q_{DG} are reactive powers of the load and DG respectively.

Therefore, the voltage drop in the feeder is calculated as follows:

$$\Delta V = (r(P_L - P_{DG}) + x(Q_L -)) / V_s \quad (1.2)$$

Where, ΔV is voltage difference, r and x are resistance and reactance from the primary point of view of the circuit respectively and V_s is considered as the reference voltage of the network. During peak consumption hours, if the power injected by the Distributed Generator (DG) is lower than the peak power consumption by the loads, the voltage difference (ΔV) is positive. Consequently, the DG aids in improving the voltage profile, bringing the load busbar voltage closer to the substation voltage.

Conversely, during low-load hours, if the injected power from the DG exceeds the load demand, ΔV becomes negative, leading to overvoltage at the load busbar compared to the substation voltage. Adjusting the transformer tap-changers becomes challenging in this scenario. To prevent overloading the feeder during low-load hours when a DG is installed on one of the feeders, the transformer tap-changer should be set to lower taps. However, this adjustment causes voltage drop on the other feeders during peak loads, making it difficult to find a balance point for the transformer tap-changer.

When the DG operates in Photovoltaic (PV) mode, it injects or absorbs reactive power to maintain voltage levels. A large DG operating in lag mode may receive significant reactive power from the network, necessitating a solution to offset this reactive power drawn from the network. Absorbing such reactive power affects network losses and loads, which must be considered by distribution utilities.

Moreover, sudden power outages of the source can cause transient overvoltage, and the duration the primary side of the transformer takes to react and restore the network should be taken into account. In such instances, distribution utilities may employ switching capacitors and other reactive power compensation devices to recover network voltage.

➤ **The effect of DGs on network loss**

Distributed Generators (DGs) typically reduce network losses by shortening the load supply path. When a DG is sized proportionally to a local load and installed nearby, it can significantly reduce losses by minimizing injected powers. The impact of DG on the voltage profile is intertwined with its effect on network losses, as these two components are closely correlated. However, in certain situations, an inadequately sized DG or its improper placement may lead to increased network losses. If the DG is situated too far from the substation and supplies power to the substation or returns power to the transmission network, distribution network losses may increase while transmission network losses are reduced. [41].

➤ **The effect of different operation modes of DGs on power flow**

A DG connected to the circuit, depending on the DG's nature and the common goals of the seller and buyer (distribution utility), can usually operate in two different modes as follows:

➤ **Constant power factor operation mode**

In this scenario, the Distributed Generator (DG) is connected to the circuit with a constant power factor. This mode of operation is commonly used to study synchronous generator DGs, where the active power produced remains constant, and the reactive power of the DGs is determined by assuming a constant power factor. Consequently, DGs can be modeled as PQ buses or loads in power flow equations.

In many power systems, buses operate under such operating modes for simplicity and reduced control device requirements. In this setup, both the active and reactive powers of the bus are specified, while the unknowns include the magnitude and phase angle of the bus voltage. These quantities can be determined using conventional power flow equations, and the resulting voltage drop or increase at the bus can be analyzed.

However, a significant drawback of this operating mode is the lack of control over the bus voltage. Consequently, in cases where the DG power injection exceeds the local load consumption power, leading to reversed current flow, the bus voltage tends to increase uncontrollably. This situation highlights the limitation of this mode in regulating bus voltage under certain operating conditions.

In fact, this operating mode is the main cause of the voltage increase. However, according to

the IEEE P1547 standard [42], the DG should not be used for voltage control, this operation mode is the most common operating mode of DGs.

➤ **Voltage control mode**

In certain cases, the voltage control mode is utilized to enhance the voltage profile. This mode involves determining the voltage magnitude and active power injection of the bus using control devices. The unknowns at the bus include the amount of reactive power injected and the phase angle of the bus voltage. Since the voltage at the bus connected to the Distributed Generator (DG) must remain constant, the calculations for voltage drop will differ.

In the scenario depicted in Figure. 1.7, the magnitude of the load voltage can be expressed as:

$$V_S = |V_L| + (r (P_L - P_{DG}) + x (Q_L -)) / V_S \quad (1.3)$$

where, $|V_L|$ is the magnitude of the bus voltage. Now, if $|V_L|$ is assumed to be equal with the reference bus voltage, Equation (1.3) changes to the following equation:

$$r (P_L - P_{DG}) + x (Q_L - Q_{DG}) = 0 \quad (1.4)$$

In this case, the following situations can occur:

- If the injected power by the DG is less than the active power of the load and the load is also inductive then, the load consumes reactive power or on the other hand, reactive power of DG will be positive as follows:

$$Q_{DG} = (r (P_L - P_{DG}) + x ()) / x > 0 \quad (1.5)$$

- If the injected power by the DG is greater than the active power of the load and the load is also capacitive, which means it produces reactive power as follows:

$$Q_{DG} = -r \frac{(P_{DG} - P_L)}{x} + Q < 0 \quad (1.6)$$

- If the active power injection by the DG is less than the active power of the load and the load is capacitive, depending on the value of the parameters, the sign of Equation (1.6) can be positive or negative.

- If the active power injection by the DG is greater than the active power of the load and the load is inductive, depend on the value of the parameters the sign of Equation (1.6) can be positive or negative.

The advantage of operating DGs in this mode is the ability to adjust the voltage profile by

injecting reactive power. However, problems may arise when DGs absorb reactive power, as this can lead to operational challenges.

Additionally, each DG has limitations regarding reactive power generation, which must be carefully observed. When the reactive power injection by a DG exceeds these limitations, the DG transitions from the PV (constant power factor) operation mode to the PQ (specified active and reactive power) operation mode.

The disadvantages of DG operation in this mode can be described as follows:

- Unavailability of DG control by the network operator; and
- Feeding the fault location. Suppose that a three-phase symmetric ground fault occurs near the DG. The voltage of the fault location is assumed to be zero. Thus, the relevant Equation will be as follows:

$$|V_{DG}| - 0 = (r_{sc} P_{DG} + X_{sc} Q_{DG}) / |V_{DG}| \quad (1.7)$$

where, r_{sc} and X_{sc} are short circuit resistance and reactance respectively. Apart from the reactive power, all other parameters of Equation (1.7) are constants, so it is possible to obtain the reactive power of DG as follows:

$$Q_{DG} = (|V_{DG}|^2 - r_{sc} P_{DG}) / X_{sc} \quad (1.8)$$

In the aforementioned Equation, the real and imaginary terms of the impedance are small, and on the other hand, if DG is considered a synchronous generator then, the voltage of the DG bus is obtained as follows:

$$V_{DG} = E_f - j X_s I_a \quad (1.9)$$

where, E_f is the electromotive force of the generator and I_a is the injection current of the generator that feeds the fault location. In Equation (1.9), if the voltage of the generator bus is to remain about one p.u., then the reactive power injection will be as follows:

$$Q_{DG} = 1 / X_{sc} \quad (1.10)$$

that will be a large amount, which means the generator will strongly feed the fault location. By following Equations (1.8) and (1.9), the electromotive force according to the fault is obtained as follows:

$$I_a = \frac{E_f}{r_{sc} + j(X_s + X_{sc})} \quad (1.11)$$

Certainly, in order to maintain the voltage of the generator terminal (VDG) at one per unit (p.u.), the electromotive force (EMF) must exceed one p.u. For the EMF to surpass one p.u., the injection current, as defined in Equation (1.11), must also exceed one p.u., indicating that the generator actively supplies the fault point.

However, in practice, both the terminal voltage and the electromotive force (EMF) tend to sharply drop and fall below one p.u. In voltage control systems, the excitation current is increased when the terminal voltage falls below the desired value. Consequently, based on Equation (1.11), the generator current increases as the EMF increases. This increase in generator current, as per Equation (1.9), results in a further drop in terminal voltage, initiating a repetitive cycle. This cycle forms a closed loop that intensifies the supply to the fault point. With the consent of the distribution operator and the DG owner, these sources can be employed as voltage regulators, aiding in regulating grid voltage by injecting or absorbing reactive power. However, generally, any attempt by the DG to control voltage may disrupt the voltage regulation scheme implemented by the grid operator for controlling the same bus or a nearby bus. The network operator's voltage control scheme may include the use of capacitor banks, Step Voltage Regulators (SVRs), or online tap-changers on sub-transmission transformers.

When the utilization of DG as a voltage regulator is permitted, the reactive power output of the DG can be adjusted to regulate the voltage, stabilizing it at a specified limit. However, the range of DG variations may not be adequate to control large voltage variations. In such cases, the DG switches its operation mode similar to any other PV bus. The efficacy of the voltage control at the generator's common connection point hinges on the ratio between the short-circuit powers of the DG and the grid. A small ratio results in a low impact of the DG on voltage changes, necessitating high reactive power injection or absorption to stabilize its bus voltage below or above standard voltage levels. Therefore, the DG should operate at a low power factor by restricting its ability to generate active power. In practical applications, DGs for voltage control should not operate at low power factors [41].

➤ **The effect of DG on voltage regulation devices**

Voltage regulation equipment typically relies on conventional distribution network configurations, meaning the integration of Distributed Generators (DGs) can impact their

effectiveness. In particular, DGs, supplying power bidirectionally, can significantly influence the operation of voltage control devices tasked with managing network voltage levels. This subsection aims to explore the impact of Distributed Generators (DGs) on key voltage profile adjustment devices, such as automatic tap-changers in sub-transmission substations. The integration of DGs into distribution networks affects the tap-changers of sub-transmission transformers in two distinct ways, as outlined below:

➤ **Control method**

Sub-transmission substations' online tap-changers employ various methods to regulate secondary voltage. The presence of DGs can impact certain methods used for voltage control, particularly those employing line-drop compensation and/or negative reactance compounding. In the presence of DGs, tap-changers utilizing these methods may encounter operational challenges [43].

➤ **Tap adjustment**

In traditional methods, the tap-changer of the sub-transmission transformer is adjusted to ensure that the voltage drop at the end of feeders remains within an acceptable range. Typically, this adjustment focuses solely on the voltage drop of the feeders, with the tap setting usually set to the maximum permissible voltage to maintain compliance. The primary concern in this scenario is managing the voltage drop at the buses.

However, the integration of DGs into distribution networks alters the regulation of transformer taps. DGs contribute active power, thereby reducing bus voltage drops and enhancing the voltage profile. Nonetheless, during periods of low load when DGs cause reverse power flow, they can result in overvoltages. Consequently, in such instances, consideration must be given not only to the voltage drop of the feeders but also to potential overvoltages, particularly on feeders hosting DGs.

To maintain an optimal condition for the transformer taps and ensure that all feeder voltages remain within permissible limits under varying load conditions, a comprehensive approach is required. Managing DGs at their maximum power generation capacity necessitates careful

management of the voltage profile to prevent unacceptable overvoltages.

Setting the sub-transmission transformer taps to lower steps is a crucial and effective means of increasing DG power in the network. However, this approach must be balanced against potential voltage drop issues in adjacent feeders, It may not always be feasible for operators to implement such conditions. Nevertheless, it can be stated that adjusting sub-transmission transformer taps is indeed one effective method to increase DG power in the network without causing overvoltages.

Figure 1.8 illustrates a typical voltage profile mode in the distribution network. In this depiction, the sub-transmission transformer tap voltage is set at 1.04 p.u. As per the Figure, the minimum voltage at the end of the feeder during peak and low load hours is 0.96 p.u. and 1.03 p.u., respectively. This implies that if a DG is introduced into the network, it is permitted to increase the network voltage by only 0.02 p.u. during low load hours.

In the Medium Voltage (MV) section, the minimum voltage at maximum and minimum loads is 0.99 p.u. and 1.02 p.u., respectively. Consequently, at this stage, the DG is only allowed to increase the voltage by 0.03 p.u.

Now, if the same transformer tap is adjusted to 1.0 p.u on the same network, then the permissible increase in voltage in the MV and Low Voltage (LV) sections would be 0.04 p.u. and 0.03 p.u., respectively. Correspondingly, on the MV side, the minimum voltage values at minimum and maximum loads will reach 1.01 p.u. and 0.98 p.u., respectively. In the LV section, these values will be 1.02 p.u. and 0.95 p.u., respectively.

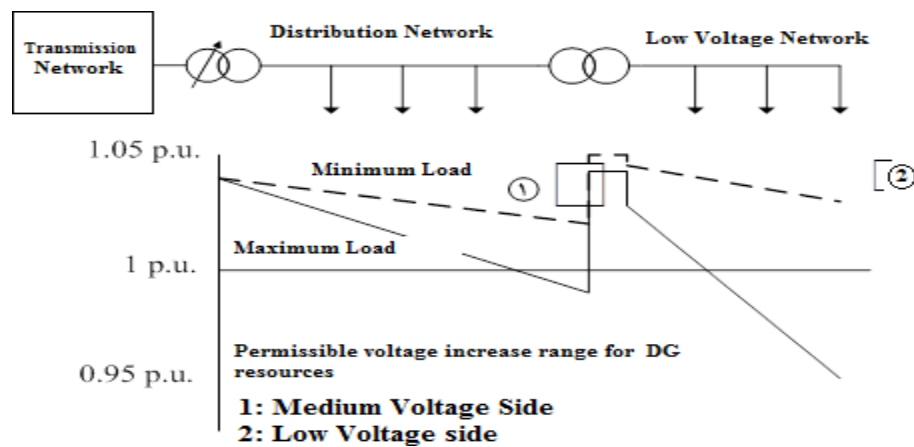


Figure. 1.8. Voltage profile of a distribution network at minimum and maximum loads.

These numbers are approximate and are utilized solely to demonstrate that appropriate tap settings can enhance DG penetration in the network. The difference in the amount of power generated by a DG when allowed to increase the voltage by 0.04 or 0.03 p.u. is significantly higher compared to when it is permitted to increase the voltage by 0.02 p.u. Therefore, the most crucial factor in increasing DG penetration in the network is the proper adjustment of transformer taps.

Figure 1.8 highlights a different issue arising from setting the distribution transformer tap, which may pose challenges to the network. In the Figure, it is assumed that the distribution transformer tap will always regulate the voltage to 1.0 p.u. Obviously, such a scenario cannot be the case for non-automatic taps, and it is depicted in the Figure solely for studying LV network conditions at high voltage levels. The Figure demonstrates that it is not feasible to set the automatic distribution transformer tap without coordination with the offline distribution transformer tap.

Suppose the distribution transformer tap is set to 0.05 p.u. Then, on the MV side, neglecting the transformer voltage drop, the maximum voltage should be 1 p.u. Similarly, when the DG is implemented on the LV side, it should not increase the voltage beyond this value.

➤ **The effect of DG on capacitors**

Capacitors, as vital reactive power compensation components, are instrumental in mitigating voltage drop and power loss in traditional distribution networks. However, their application in DG networks poses a challenge, as DGs not only serve as voltage drop compensators but can also induce overvoltages in the network. The impacts of DGs on capacitors can be analyzed in two distinct aspects.

➤ **Reactive power flow**

One crucial parameter for voltage control is the flow of reactive power. With the integration of DGs into distribution networks, the dynamic of reactive power flow shifts from being a constant that always requires compensation and is considered undesirable in the network, to a variable that can sometimes be beneficial and is even demanded for further flow. Essentially, due to the voltage increase induced by DGs, this increase must be compensated for using a quantity, and reactive power flow can serve this purpose.

Conversely, one of the simplest methods employed by DGs for voltage control is to adjust the reactive power flow they adopt in the PV mode. Therefore, controlling reactive power flow emerges as one of the simplest yet effective methods of voltage control in the presence of DGs.

In the presence of DGs, which typically raise voltage levels upon increased penetration, the installation of capacitors to compensate for reactive power becomes ineffective. In fact, capacitor placement may even exacerbate voltage levels, rendering it counterproductive. Therefore, in such networks, rather than compensating for reactive power, it becomes necessary to consume it to ensure that the resulting voltage drop falls within acceptable limits. This can be achieved by installing reactors to increase reactive power consumption, consequently inducing a voltage drop that allows for higher DG penetration levels.

However, it's important to note that increasing reactive power consumption and the resulting voltage drop will also lead to higher network losses. Additionally, issues such as overvoltage and potential network instability following a sudden DG outage may arise.

Conversely, when DGs operate in voltage control mode, they can either generate or consume reactive power to regulate voltage levels. Generators typically consume reactive power when there's a risk of overvoltage. However, this increased reactive power flow can escalate network losses and pose challenges for network stability in the event of a sudden DG outage.

To mitigate these challenges, capacitors, reactors, and other reactive power compensation devices in the network must be carefully coordinated and studied to prevent overvoltage or voltage drop below acceptable levels.

➤ **Capacitor control methods**

The impact of Distributed Generators (DGs) on capacitive banks varies depending on factors such as the type, operation mode, and location of the DG, as well as the control methods employed for switching capacitor banks.

Voltage-controlled capacitors are typically unaffected by DGs if the DGs do not operate in voltage control mode. To prevent rapid voltage fluctuations between the DG and capacitors, adjustments should be made to the set-point and time delay increased.

However, if the line current control method is utilized, DGs can affect capacitors by altering line currents and occasionally reversing them. Consequently, the current monitored by the

capacitor may not accurately reflect downstream network currents. The switching set-point is adjusted based on the assumption that the current at any point on the feeder maintains a reasonable ratio to the current at the control site.

When DGs operate at unity power factor, the reactive power flow control method of capacitors remains unaffected. However, DGs with non-unity power factors can significantly influence this control mode [41].

➤ **The effect of DG on voltage regulators**

The control methods of voltage regulators, similar to automatic tap-changers, can be influenced by the presence of Distributed Generators (DGs). As mentioned earlier for automatic tap-changers, the Line-Drop Compensation (LDC) method, a common control method of voltage regulators, can encounter challenges in the presence of DGs. Additionally, capacitors can impact the performance of voltage regulators and may occasionally lead to malfunctions.

1.3.3 Study of different loadings in the network

The loading of distribution networks varies based on load characteristics, which in turn depend on factors like time of day and weather conditions. Typically, early evening hours witness maximum loads due to lighting needs, while load drops to its minimum during late night hours. In traditional distribution networks, network power flow analysis is conducted under maximum load conditions, which result in the highest voltage drop and line currents. Since the network operates unidirectionally, this scenario represents the worst-case scenario for the network. Consequently, if the voltage profile and line currents remain within standard ranges under maximum load conditions, these standards can generally be applied to other loadings as well.

However, the introduction of Distributed Generators (DGs) transforms the network from unidirectional to multi-directional supply. This configuration change alters the direction of current flow in the lines, thereby affecting the voltage profile. Consequently, it can no longer be definitively stated that if the voltage profile under overload conditions is within standard limits, then the network load will also fall within the standard range.

Alternatively, it can be noted that the active injection power by a DG is typically constant and can be returned to the substation, leading to reduced overload consumption. Under such

conditions, the current flowing in the opposite direction can alter the voltage profile and, in some cases, lead to overvoltage. Therefore, it becomes necessary to analyze the network power flow in the presence of DGs under three different cases:

➤ **Without DGs and with maximum loading**

This scenario is utilized to assess the network when DGs are disconnected. However, it can also serve to analyze the network's condition prior to the introduction of DGs. DG disconnection may occur due to maintenance, vendors ceasing sales to the network, unforeseen faults, and other reasons. If the network is designed assuming the continuous presence of DGs, it may experience voltage drops or line overcurrents following DG disconnection.

When DGs are disconnected, there is an increase in current flow from the beginning of the substation to the end of the feeders. This heightened current flow leads to elevated voltage drops, potentially resulting in the aforementioned issues.

➤ **With DGs and with maximum loading**

In this scenario, the network is examined during peak hours with the presence of DGs, representing an intermediate state. On one hand, there is an increase in voltage drop due to heightened consumption. On the other hand, the presence of DGs can somewhat mitigate this voltage drop. However, if there isn't proper coordination between the automatic tap-changer of the sub-transmission substation, the offline tap-changer of the substation, and the location and operation mode of the DGs, it can lead to overvoltage in one feeder and excessive voltage drop in another feeder.

➤ **With DGs and with minimum loading**

DGs and network loads have contrasting effects on the voltage profile. DGs tend to increase the voltage profile, whereas network loads have the opposite effect of reducing it. Consequently, when the network load decreases to a minimum, the network may experience an increase in voltage. The reduction in load results in a flow of current by DGs towards the beginning of the feeder. Since this reverse flow induces an inverse voltage drop, the buses near these DGs may encounter elevated voltages.

However, it's worth noting that some studies treat the lost load in the network as the minimum network load, especially when considering load outages.

1.3.4 DG application in distribution system based on optimization algorithm

The introduction of Distributed Generators (DGs) into the electricity industry has brought about significant changes in the design of distribution networks. The utilization of DGs reduces the need for newly installed feeders in subsequent periods. Moreover, they contribute to delays in system upgrades or the installation of new infrastructure in subsequent periods, thereby reducing losses and potentially freeing up network capacity.

Grid-connected distributed generation systems are integrated into distribution networks by transferring power to them. As with other generation units and electrical network components, they impact network characteristics and variables such as voltage, losses, and reliability.

However, it's important to note that the cost of DGs is relatively high in the design and development of distribution networks. Therefore, the design and development of distribution networks, considering DGs, are carried out based on distribution constraints and to minimize investments, operational costs, and maintenance expenses.

In the process of designing and operating the network, the optimal siting and sizing of these resources have been thoroughly investigated to ensure efficient utilization.

To optimize the optimal siting and capacity of Distributed Generators (DGs), various methods have been employed in distribution networks. Optimization methods are intelligent approaches used to determine the optimum solution to a problem, which can be either a minimum or maximum value. Formulating an appropriate function for the problem is essential to ensure the effectiveness and efficiency of these methods.

Meta-heuristic methods, which encompass repetitive intelligent algorithms within computational intelligence, are commonly utilized in this context. These methods employ specific rules and techniques to search for the best site and size of DGs within the distribution network. Optimization methods involve a repetitive production process that utilizes search approaches to effectively identify near-optimal solutions through various intelligent computing methods, thereby facilitating exploration of the search space. This approach is

crucial for finding optimal or near-optimal solutions.

This subsection outlines the desirable methods utilized in addressing the application of DGs in distribution networks. In recent years, meta-heuristic algorithms have gained prominence for optimizing DG resources in distribution networks. Some of these methods are presented in subsections 2.3.7.1-2.3.7.4.

➤ **Particle Swarm Optimization (PSO)**

The meta-heuristic Particle Swarm Optimization (PSO) algorithm is widely applied in solving various optimization problems. Inspired by the behavior of birds or fish, PSO involves generating particles with random positions and velocities. These particles' positions and velocities are then updated based on their search experience compared to other particles, with the optimal solution obtained through repeated iterations of this process.

In a study by [47], the PSO method was employed to determine the optimal site and size of DG units in a multi-phase imbalanced distribution grid. Actual experiments utilized a combination of DGs. The results were compared with those obtained using the Repetitive Load Flow (RLF) method, revealing that the PSO method was more effective in locating DGs and faster in terms of computational time. Additionally, the optimized distributed generation enhanced the voltage profile and reduced losses.

Another study by [48] utilized the PSO algorithm in optimizing two distribution networks, one with 33 buses and the other with 69 buses. After applying the PSO algorithm for optimization, an analysis approach was employed. The results demonstrated that the PSO method led to fewer complications in solving optimization problems. In addition to comparing PSO with genetic algorithms and artificial bee colony (ABC) algorithms for the 69-bus system, it was found that all methods yielded similar results in terms of losses. Wind turbines are commonly integrated into networks to reduce power loss, mitigate congestion, and enhance voltage stability and supply during peak load conditions. Proper sizing and siting of wind turbines are crucial for minimizing losses in distribution networks.

In a study by [49], PSO was applied to determine the optimal installation site of wind turbines, considering their maximum power capacity to minimize losses. The site and maximum allowable size of wind units were calculated to minimize power loss while adhering to operational constraints. This approach involved optimizing the location of wind units as a

variable and evaluating losses under various scenarios based on the number of wind units. The feasibility of this method was validated using two sample networks of 84- and 32-bus. Results indicated that determining the optimum size of wind units reduced losses and decreased voltage deviations. Moreover, increasing the number of turbines positively impacted loss reduction and improved voltage profile. Notably, considering the capacity of wind turbines instead of their maximum allowable production capacity as a variable resulted in greater loss reduction and voltage profile improvement.

In another study by [48], PSO was utilized to optimize the location of wind units and photovoltaic (PV) systems for reducing losses and improving voltage stability. This was formulated as a multi-objective optimization problem using weight coefficients. The optimal siting and sizing of wind and PV sources were determined to minimize losses while enhancing voltage stability. Results demonstrated that this approach effectively reduced losses by deploying optimal PV panels and wind turbines capable of reactive power injection, consequently improving voltage stability and the overall voltage profile in the network.

Furthermore, PSO was employed in [50] to investigate optimal responses for the problem of capacitor placement in a 16-bus IEEE-based wind energy distribution network considering cost functions. Siting and sizing capacitors led to loss reduction and voltage improvement. Results indicated that using PSO for the 16-bus network resulted in lower power loss costs and voltage deviations compared to genetic algorithms.

In [51], a method is proposed to determine the optimal size and location of renewable distributed and non-distributed sources in a network. In this study, Distributed Generation (DG) units based on wind energy and photovoltaic (PV) are categorized as non-DGs, while DGs utilizing biomass energy are classified as distributed units.

The multi-objective approach involves considering various factors such as power losses, allowable current in branches, voltage, environmental impact, and economic indices. Weight coefficients for different indices are determined using the Analytical Hierarchical Process (AHP) to ensure their proper consideration in the optimization process.

To solve the extended formula encompassing these factors, a Particle Swarm Optimization (PSO)-based method has been employed for a 51-bus network. The results obtained from this method are compared with those obtained from other multi-objective methods, where different weight coefficients have been assigned to the indices. It is noted that the PSO-based method

is deemed simple and efficient for this optimization problem.

➤ **Genetic Algorithm (GA)**

The Genetic Algorithm (GA) serves as an optimization technique, mimicking nature's processes. It operates by managing a population of distinct individuals, each assessed for its "fitness." Those individuals demonstrating greater fitness are afforded more opportunities for reproduction, blending their traits with others in the population. By selecting the fittest members and combining their traits, a new population with improved characteristics is generated. Through successive iterations of reproduction and population generation, individual traits evolve towards a desirable state, leading the population towards an optimal solution.

In [52], the goal is to optimize the siting of Distributed Generators (DGs) by minimizing investment and utilization costs, reducing the purchase cost of electric power, and minimizing voltage deviation. The Pareto optimization strategy, employing fuzzy theory, addresses this multi-objective problem. The allocation and optimal capacity determination of DG units are handled using a GA, with penalty coefficients incorporating voltage deviation constraints, DG unit power generation, and line overloads into the objective function. An enhanced GA is proposed to tackle multi-objective problems, determining the optimal site and capacity of DG units by altering their locations and capacities and evaluating their fitness using objective functions. The resulting Pareto front is analyzed using fuzzy methods to extract optimal solutions.

In [53], the optimal capacity of wind turbines is determined to minimize losses in the distribution network. A GA is utilized for optimization, while load flow analysis computes energy losses, considering load characteristics and turbine power profiles. Weight coefficients are assigned to candidate buses to determine the number of turbines per bus, with the method applied to a 30-bus network. Results demonstrate decreased losses with wind turbine integration, albeit with a slight increase in losses due to clustering.

In [54], a hybrid optimization approach is proposed, combining GA and the Optimal Power Flow (OPF) method based on electricity market dynamics, to determine the optimal placement and size of wind turbines. This method minimizes overall energy losses by considering both wind production and load. The GA selects optimal capacities, while the OPF method, based

on electricity market conditions, determines the optimal number of wind turbines per candidate bus.

In [55], a method is proposed for the optimal siting of wind turbines in the distribution network. The GA and PSO are combined to optimize the cost of investments made by wind turbine developers as well as social welfare in the distribution network operator (DNO) benefit market environment simultaneously. The GA has been used to select optimal capacities between the different capacities of wind turbines, while the market has been used to find the number of wind units to maximize social welfare, taking into account network constraints. The results have shown that wind turbine developers can improve their benefit by optimizing the location of wind units and the consumers' benefit will also be increased with decreasing the energy cost.

➤ **Ant Colony Optimization (ACO)**

The Ant Colony Optimization (ACO) draws inspiration from the intricate relationships and behaviors observed in real ant colonies. Ants exhibit a remarkable and efficient foraging behavior, naturally discovering the most optimal paths to food sources. This innate ability enables ant colonies to explore and efficiently access food supplies. ACO algorithm, rooted in this behavior, serves as a novel meta-heuristic approach for tackling complex combinatorial optimization (CO) problems, delivering viable solutions within reasonable computational timeframes.

Employing principles akin to ants seeking food, the ACO algorithm seeks to find the shortest paths in problem spaces by simulating ant behavior, where ants communicate through pheromone trails to determine optimal routes from their nest to food sources. This methodology has found application across various domains, including electrical engineering, where it has been utilized for optimizing tasks such as reducing losses and enhancing load balancing in distributed radial distribution networks.

Studies have demonstrated that ACO outperforms traditional genetic algorithms (GA) in certain scenarios. For instance, in evaluating the impact of distributed generation on network performance, ACO yielded an average loss reduction of 44.626%, surpassing the average of 43.803% achieved using GA. While the study primarily focuses on the influence of distributed generation on losses, it assumes constant values for the site and size of distributed generation.

Nonetheless, the results underscore the effectiveness of ACO as a highly proficient method for optimization tasks.

➤ **Artificial Bee Colony Algorithm (ABC)**

The Artificial Bee Colony (ABC) method draws inspiration from the collective intelligence observed in honey bee swarms during their search for food sources. This optimization approach mimics the behavior of bees in seeking out optimal solutions. The model for this method comprises three key elements: scout bees, onlooker bees, and food sources. These elements guide the movement towards productive nectar sources while disregarding less fruitful options, ultimately leading to the convergence of social intelligence.

The ABC algorithm has been extensively applied across various domains to address practical optimization problems. For instance, in a study focusing on loss reduction and optimal determination of Distributed Generation (DG) capacity [64], the ABC method was employed on networks featuring three distributed generation units. The results demonstrated simultaneous reductions in power losses and computational time, without getting trapped in local optima.

In another study [65], the ABC algorithm was utilized for the location and planning of DG systems based on hybrid diesel-photovoltaic resources within distribution networks. This application showcases the versatility of the ABC method in tackling diverse optimization challenges across different domains. The optimization problem's objective function aims to minimize various costs associated with system equipment investment, replacement, operation, and maintenance, as well as reducing losses, power transfer amounts in the network, and unsupplied loads. This methodology was applied to radial systems consisting of 33- and 45-bus configurations.

In this study, the Particle Swarm Optimization (PSO) algorithm was employed for comparison with the Artificial Bee Colony (ABC) algorithm. Simulation results indicate that the ABC optimization method exhibits superior problem-solving capabilities compared to the PSO method. It achieves lower system costs along with higher convergence rates, highlighting its effectiveness in addressing the optimization objectives outlined.

➤ **Fireworks Algorithm (FWA)**

The Fireworks Algorithm (FWA) is a randomized search method based on collective intelligence, suitable for solving optimization problems by exploring response spaces. Inspired by the explosive phenomenon of fireworks and the sparks generated around them, this algorithm mimics the search behavior observed in such scenarios. The FWA is considered a novel approach due to its ability to mimic the explosive nature of fireworks during the search process, allowing it to efficiently explore solution spaces. Additionally, the algorithm can organize resources into a hierarchical community for more effective solution searches.

In a related study [67], a new hybrid method was introduced for minimizing losses and improving voltage stability by strategically installing Distributed Generators (DGs) within a network. Leveraging the FWA, this method determines the optimal locations and capacities of DGs based on the Voltage Stability Index (VSI), ensuring efficient optimization of the system's performance and stability.

➤ **Backtracking Search Optimization Algorithm (BSOA)**

The placement of Distributed Generators (DGs) is determined to optimize loss reduction and voltage profile enhancement using the Bee Swarm Optimization Algorithm (BSOA) based on fuzzy rules and loss sensitivity factors. Fuzzy expert rules are utilized to determine the initial locations and priorities of candidate bus sites for DG placement. Additionally, the Loss Sensitivity Factor (LSF) is employed to identify critical bus locations for DG placement, thereby reducing computational time.

The LSF predicts areas with the highest losses due to active and reactive power injections at specific buses and normalizes this information for use in fuzzy logic. The proposed method is implemented on a 33-bus system, considering two scenarios for DG units. In Scenario A, DGs can only inject active power, while in Scenario B, DGs have the capability to inject both active and reactive power.

Results indicate that employing two DGs improves voltage, reduces losses, and enhances power factor. However, adding a third DG does not significantly alter the system's performance compared to having two DGs. Furthermore, employing two DGs with active and reactive power injection capabilities effectively reduces losses and improves voltage profiles.

➤ **Ant Lion Optimizer (ALO)**

The optimization of siting and sizing for Photovoltaic (PV) and wind units within the network is explored using the Ant Lion Optimization (ALO) algorithm in [69]. The study aims to determine the optimal locations and capacities for distributed wind and PV units through an intelligent approach. Multi-objective optimization, along with weight factors, is utilized to address the problem effectively.

The proposed method is applied to radial distribution networks, specifically the 33-bus and 69-bus IEEE standard systems. To address the challenge of integrating renewable sources into the distribution network, the optimal locations and capacities of PV and wind units are crucial. The ALO optimization algorithm is introduced as a novel solution for this problem, enabling the optimization of hybrid Distributed Generators (DGs) incorporating PV and wind resources.

A loss sensitivity index is introduced to identify buses with significant loss implications, reducing the search area and optimization time. This index helps pinpoint problematic buses in terms of losses, guiding the selection of DG installation sites. The objective function aims to minimize losses and voltage deviations while improving voltage stability across the network.

The proposed approach employs multi-objective optimization with weighted factors using the ALO algorithm. Results demonstrate that the ALO algorithm yields lower losses and outperforms alternative methods in enhancing voltage profiles and achieving minimum voltage levels. Comparisons illustrate that ALO effectively achieves significant objectives in terms of loss reduction and associated cost savings.

1.3.5 Analysis of Power Quality (PQ) Features with DGs in the network

The integration of Distributed Generators (DGs) utilizing renewable energy sources into medium- and low-voltage distribution systems is a key strategy in modern energy generation. As DG resources become more prevalent in distribution systems, it becomes imperative to consider various technical parameters of the system. The deployment of renewable energy resources like solar and wind plants in distribution systems plays a crucial role in addressing contemporary concerns regarding environmental pollution and reducing fuel consumption.

However, it's essential to analyze Power Quality (PQ) issues and strive to improve them under

both normal and faulty operating conditions. This subsection focuses on PQ problems in distribution systems arising from the presence of DGs and investigates the underlying causes such as harmonics, voltage waveform oscillations, voltage flicker, and increased short circuit levels in the system.

Since individual DGs can introduce harmonics into the distribution system, it's important to prevent these harmonics and voltage oscillations from exceeding predefined standard limits. Therefore, there is a need for methods to determine the maximum allowable power output from DGs. This approach helps avoid overloading the system with excessive DGs and ensures PQ is maintained even during severe disruptions.

➤ **PQ problems in distribution systems with DGs**

through the examination of distribution systems incorporating Distributed Generators (DGs), several Power Quality (PQ) issues can be detected, such as oscillations and fluctuations, voltage and current waveform distortion and harmonics, and heightened short circuit levels within the system. Broadly speaking, integrating DGs into Low Voltage (LV) distribution systems may lead to the subsequent challenges [71- 72]:

- Increase or decrease in the voltages of conductors;
- Increase in the voltage harmonic distortions;
- Increase in the system short circuit level;
- Disoperation of protective systems; and

Increase in the temperature of LV system conductors. These cases are true for radial and ring distribution systems.

➤ **Gradual changes in the voltage**

The examination of voltage stability at the interface between Distributed Generators (DGs) and overhead line feeders or underground cables within distribution systems is pivotal in system analysis. Consequently, standards have been established to govern voltage magnitude variations in both Low Voltage (LV) and Medium Voltage (MV) systems incorporating DGs. One approach involves assessing the average voltage change (%) over 10-minute intervals at the connection point. The calculation of voltage magnitude at the connection point under steady-state conditions is determined as follows [71-72]:

$$\varepsilon\% = 100 S_n / S_k \cos(\phi_K + \phi) = 100/R \cos(\phi_K + \phi) \leq 3\% \quad (1.12)$$

In the equation (1.12), where S_n represents the rated power of the DG source, S_k is the short-circuit capacity at the connection point, ϕ_K denotes the network impedance angle, ϕ signifies the output current angle of the DG, and $R = S_k/S_n$ indicates the short-circuit ratio at the connection point. As per the standards in European countries, the value specified in Equation (1.12) should not surpass 2-3% in Medium Voltage (MV) systems to ensure that voltage variations in Low Voltage (LV) systems remain below 10%. The variations in voltage magnitude at the connection point of DGs to the distribution system, concerning power factor ϕ , system angle ϕ_K , and short-circuit ratio R , are depicted in Figure 1.9 for various values. Furthermore, the power factor of the DG affects the Root Mean Square (RMS) voltage. Figure 1.10 illustrates the voltage variations in relation to the short-circuit ratio at the connection point for different power factors of the DG.

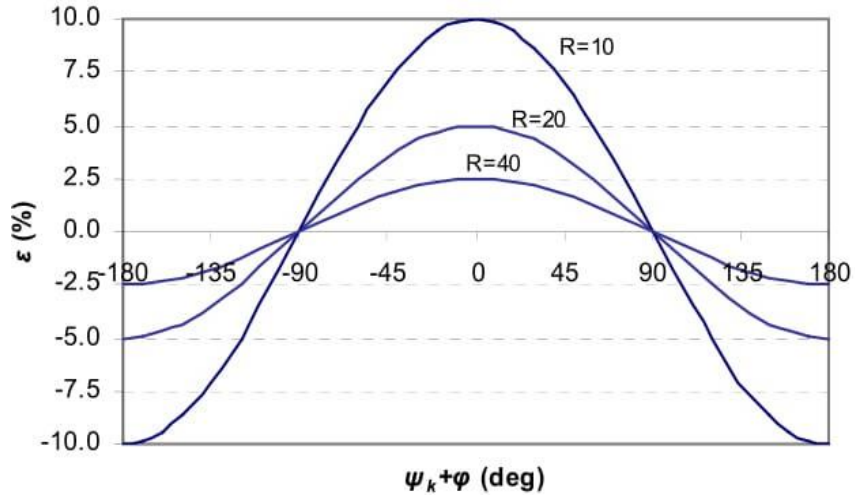


Figure. 1.9. The changes in the voltage with respect to the system angle and power factor [71-72].

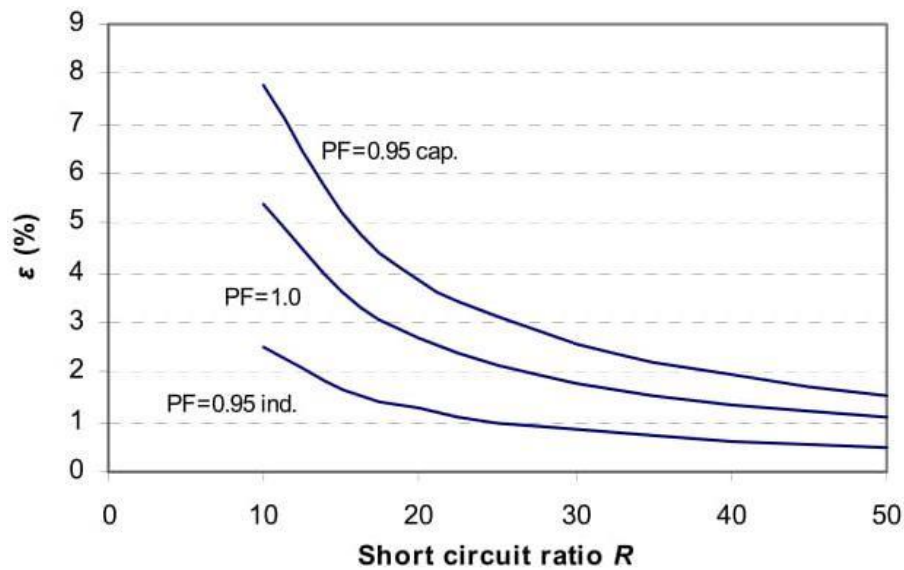


Figure. 1.10. The changes in the voltage with respect to the short circuit ratio for different values of power factor [71-72].

When multiple DGs are utilized within a system and connected to a single feeder, it's crucial to account for voltage variations caused by all DGs. Therefore, conducting a precise power flow analysis becomes essential for the system. When the power generated by DGs reaches its maximum (or minimum) and the power consumed by system loads is at its minimum (or maximum), the resulting voltage changes at the connection point will be at their maximum (or minimum) levels. It's imperative that the average voltage at the connection point does not

exceed 5% of the rated voltage, allowing for compensation through adjustment of tap-changers on Medium Voltage (MV) to Low Voltage (LV) transformers as follows [71]:

$$0.95V_n < V_{med} = \frac{V_{min} + V_{max}}{2} \leq 1.05 V_n \quad (1.13)$$

where, V_n , V_{med} and V_{max} are rated voltage, medium voltage and maximum voltage respectively. The change in the voltage of the connection point around the average voltage should not exceed 3% of the rated voltage so that the voltage changes in the LV system is maintained less than 10% that is presented as follows [71]:

$$2\Delta V = V_{max} - V_{min} \leq 0.06 V_n \quad (1.14)$$

1.4 Conclusion

This chapter presents studies on the application of DG in distribution networks including analytical and bio-inspired methods. The studies are evaluated in terms of objective functions, constraints, and optimization methods. Finally, the limitations of previous studies and the proposed method for overcoming these limitations are presented.

Chapter 2:

Modeling Of Radial Distribution Feeder

2.1 Introduction

The local distribution substations cater to their nearby consumers through primary distribution feeders, typically configured in a radial fashion. These feeders extend via overhead wires, underground cables, or a combination of both. They commonly operate within a 3-phase system, yet lateral feeders branching off may include 1-phase, 2-phase, and 3-phase systems. Consequently, distribution feeders often operate under unbalanced load conditions, primarily due to the diverse natures and demands of the loads served by each phase. Therefore, achieving more accurate results necessitates modeling line impedance and conducting distribution power flow calculations while considering unbalanced load conditions. Moreover, correct modeling of load demands along the feeder and the output of interfaced PVDG units is essential for precise analysis.

2.2 Series Impedance for Radial Distribution Feeder

Accurate power flow calculations hinge significantly on modeling the series impedance along radial distribution feeders, a matter of considerable importance. Numerous references delve into this topic extensively. In this study, the pertinent modeling is chiefly constructed based on reference [1]:

2.2.1 Balanced Load Feeder

The series impedance of both overhead and underground distribution lines comprises the resistance of the conductors and the self and mutual inductive reactance resulting from the magnetic fields surrounding the conductors. The resistance component is typically obtained from product specification sheets. Conversely, the self and mutual reactance are determined based on several parameters characterizing the type and configuration of the line.

Referring to Figure. 2.1, the inductance of conductor 'i' in the magnetic field of 'n' adjacent conductors is calculated by determining its flux linkage with each of the other conductors.

Thus, the following equation for total flux linkage is applied:

$$\lambda_i = 2 \cdot 10^{-7} \left(I_1 \times I_n \frac{1}{D_{i1}} + I_2 \times \frac{1}{D_{i2}} + \dots + I_i \times I_n \frac{1}{GMR_i} + \dots + I_n \times I_n \frac{1}{D_{in}} \right) \quad (2.1)$$

Where,

λ_i -Flux linkage of conductor 'i' with 'n' adjacent conductors (Wb- t/m)

D_{in} - Distance between conductor i and conductor n (ft)

GMR_i - Geometric Mean Radius of conductor i (ft)

If the currents in the lines are balanced then, $I_1 + I_2 + \dots + I_i + \dots + I_n = 0$.

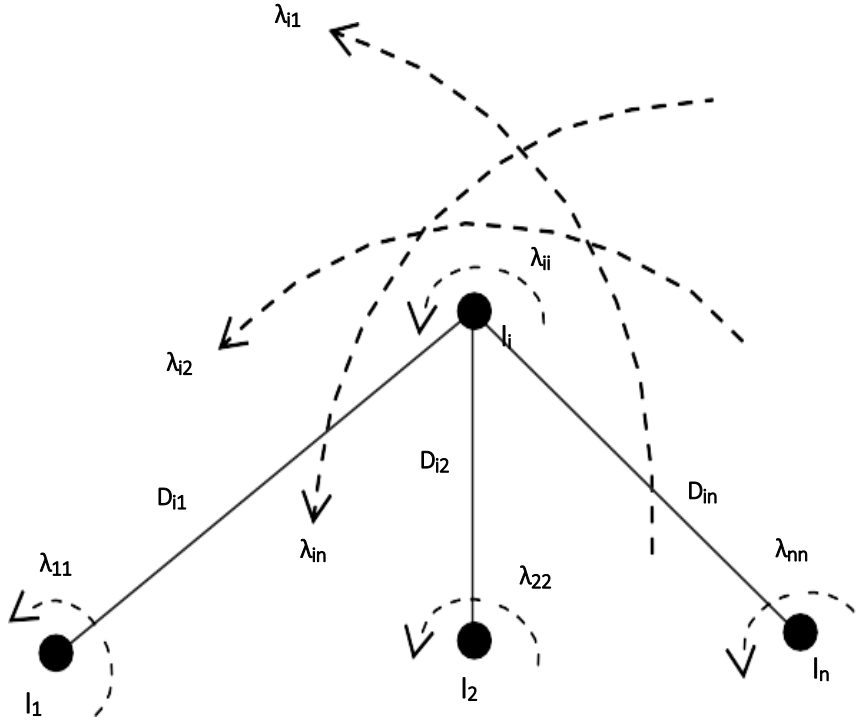


Figure 2.1 Flux linkage of conductor i with n adjacent conductors

The inductance of conductor 'i' consists of the self inductance (L_{ii}) and the mutual inductance (L_{ij}) between the conductor and all of the adjacent conductors. By definition:

$$L_{ii} = \frac{\lambda_{ii}}{I_i} = 2 \cdot 10^{-7} \ln \frac{1}{\text{GMR}_i} \text{ H/m} \quad (2.2. a)$$

$$L_{ij} = \frac{\lambda_{ij}}{I_i} = 2 \cdot 10^{-7} \ln \frac{1}{D_{ij}} \text{ H/m} \quad (2.2. b)$$

In the event that the 3-phase conductors of the feeder are equally loaded, the self and mutual inductances can be combined in one equation for each phase as follows [1]:

$$L_i = 2 \cdot 10^{-7} \ln \frac{D_{eq}}{\text{GMR}_i} \text{ H/m} \quad (2.3)$$

$$D_{eq} = \sqrt[3]{D_{ab} D_{bc} D_{ca}} \text{ ft} \quad (2.4)$$

Where,

l_i - phase inductance of any of the 3-phase conductors 'a, b, c'

D_{ab} - Distance between phase conductors 'a' and 'b' (ft)

For 50Hz system frequency, the reactance of any of the three phases (x_i) per one km length is expressed by multiplying Eq.3.3 in $2\pi f \times 1000$. Thus, for $f=50\text{Hz}$,

$$x_i = 0.06285 \ln \frac{D_{eq}}{GMR_i} \quad \Omega/\text{km} \quad (2.5)$$

Hence, the series phase impedance of any of the three phases (z_i) in 3-phase balanced load feeder is given below, where r_i is the ac series resistance of the conductor.

$$z_i = r_i + j0.06285 \ln \frac{D_{eq}}{GMR_i} \quad \Omega/\text{km} \quad (2.6)$$

2.2.2 Unbalanced load feeder

Previously, it was noted that distribution feeders can be installed as 1-phase, 2-phase, and 3-phase lines to serve unbalanced loads. This often leads to unbalanced loading in the 3-phase primary lines. In such scenarios, it is logical to model the series phase impedances of the lines in terms of self and mutual values. Additionally, the unbalanced loading will induce specific current flows in the ground/neutral return path, which should also be taken into account.

Referring back to Eq. 2.2 of self and mutual inductances, the following equations for series phase impedances can be derived,

$$z_{ii} = r_i + 0.06285 \ln \frac{1}{GMR_i} \quad \Omega/\text{km} \quad (2.7)$$

$$z_{ij} = j0.06285 \ln \frac{1}{D_{ij}} \quad \Omega/\text{km} \quad (2.8)$$

A derivation was given in [1] to calculate the self and mutual impedances of a line with ground return path. The derivation was developed based on Figure.2.2 illustrating two conductors with currents I_i and I_j connected to ground together from their ends. A virtual path 'd' is assumed carrying the return current I_d , resulting from the unbalance of I_i and I_j .

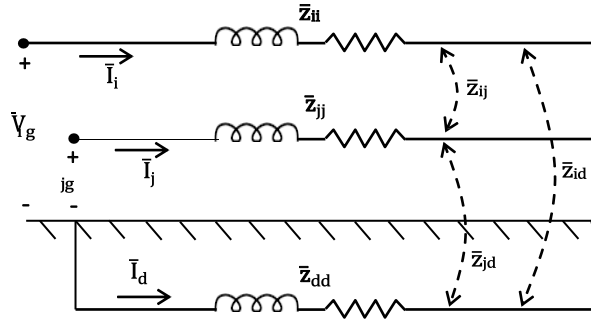


Figure 2.2 Two unbalanced conductors with virtual path for the return current flow
The application of Kirchhoff's voltage and current laws (KVL&KCL) for the voltage V_{ig} of Figure.2.2 can result in:

$$V_{ig} = \hat{Z}_{ii} \times I_i + \hat{Z}_{ij} \times I_j \quad (2.9)$$

Where,

$$I_i + I_j = -I_d$$

$$\hat{Z}_{ii} = \bar{Z}_{ii} + \bar{Z}_{dd} - \bar{Z}_{di} - \bar{Z}_{id} \quad (2.10)$$

$$\hat{Z}_{ij} = \bar{Z}_{ij} + \bar{Z}_{dd} - \bar{Z}_{dj} - \bar{Z}_{id} \quad (2.11)$$

Where \hat{Z}_{ii} and \hat{Z}_{ij} are called the primitive self and mutual impedances, which include the impact of the impedances in the virtual return path 'd'.

The impedance on the right hand side of Eq.2.10 and Eq.2.11 can be substituted by Eq.2.7 and Eq.2.8. Hence, the following derivations for the primitive impedances are expressed:

$$\hat{Z}_{ii} = r_i + jx_{ii} + r_d + jx_{dd} - jx_{di} - jx_{id} \quad (2.12)$$

$$\hat{Z}_{ii} = r_i + r_d + j0.06285 \left(\ln \frac{1}{GMR_i} + \ln \frac{1}{GMR_d} - \ln \frac{1}{D_{di}} - \ln \frac{1}{D_{id}} \right) \Omega/\text{km} \quad (2.13)$$

$$\hat{Z}_{ii} = r_i + r_d + j0.06285 \left(\ln \frac{1}{GMR_i} + \ln \frac{D_{di} \times D_{id}}{GMR_d} \right) \Omega/\text{km} \quad (2.14)$$

Similarly,

$$\hat{Z}_{ij} = r_d + j0.06285 \left(\ln \frac{1}{D_{ij}} + \ln \frac{D_{di} \times D_{id}}{GMR_d} \right) \Omega/\text{km} \quad (2.15)$$

However, applying Eqs.2.14 and 2.15 requires the values related to the virtual return path

'd' that are still unknown. In order to solve the problem, the work published by John Carson [2] is applied, where a technique was developed to determine the self and mutual impedances for an arbitrary number of conductors. The technique can be applied on both overhead and underground conductors.

According to the work in [1], the original Carson's equations for the self and mutual impedances are given as follows:

$$\hat{z}_{ii} = r_i + 4wP_{ii}G + j(x_i + 2wG \ln \frac{S_{ii}}{RD_i} + 4wQ_{ii}G) \Omega/\text{km} \quad (2.16)$$

$$\hat{z}_{ij} = 4wP_{ij}G + j(2wG \ln \frac{S_{ij}}{RD_{ij}} + 4wQ_{ij}G) \Omega/\text{km} \quad (2.17)$$

And

$$X_i = 2wG \ln \frac{RD_i}{GMR_i} \quad (2.18)$$

$$P_{ij} = P_{ii} = \pi/8 \quad (2.19)$$

$$Q_{ij} = -0.0386 + 0.5 \ln \frac{2}{K_{ij}} \quad (2.20)$$

$$K_{ij} = 8.565 \times 10^{-4} \cdot S_{ij} \sqrt{f/\rho} \quad (2.21)$$

$$Q_{ii} = 0.5 \times (7.6786 - \ln S_{ii} + 0.5 \ln \frac{\rho}{f}) \quad (2.22)$$

Where,

- \hat{z}_{ii} - Self impedance of conductor i (Ω/mile),
- \hat{z}_{ij} - Mutual impedance between conductors i and j (Ω/mile),
- r_i - resistance of conductor i (Ω/mile),
- $w = 2\pi f$ - angular frequency (rad/sec),
- $G = 0.1609344 \times 10^{-3}$ (Ω/mile),
- RD_i - Radius of conductor i (ft),
- GMR_i - Geometric Mean Radius of conductor i (ft),
- f - System frequency (Hz),
- ρ - Resistivity of earth ($\Omega \cdot \text{meter}$),
- D_{ij} - Distance between conductor i and j (ft),
- S_{ij} - Distance between conductor i and the image of conductor j (ft),

Equations 2.18 to 2.22 are substituted wherever required into the original Carson's Eqs.2.16 and 2.17. The resulting expressions are solved and simplified accordingly giving the following equations of self and mutual primitive impedances (in Ω/mile) [1]:

$$\hat{Z}_{ii} = r_i + 0.001588 \cdot f + j0.0020223 \cdot f \left(\ln \frac{1}{GMR_i} + 7.6786 + 0.5 \ln \frac{\rho}{f} \right) \quad (2.23)$$

$$\hat{Z}_{ij} = 0.001588. f + j0.0020223. f \left(\ln \frac{1}{D_{ij}} + 7.6786 + 0.5 \ln \frac{\rho}{f} \right) \quad (2.24)$$

Where, ρ is the Earth resistivity = 100 Ω /meter,

The unit of Eqs.2.23 and 3.24 can be changed to Ω /km by multiply the two equations in (1/1.609344). Hence, for $f=50$ Hz the equations are simplified in Ω /km as follows:

$$\hat{Z}_{ii} = r_i + 0.04934 + j0.06285 \left(\ln \frac{1}{GMR_i} + 8.02517 \right) \Omega/\text{km} \quad (2.25)$$

$$\hat{Z}_{ij} = 0.04934 + j0.06285 \left(\ln \frac{1}{D_{ij}} + 8.02517 \right) \Omega/\text{km} \quad (2.26)$$

As observed, Carson's modified equations 2.25 and 2.26 offer a solution for the primitive impedances of the lines without explicitly involving terms related to the virtual return path 'd'. However, the influence of 'd' is implicitly incorporated within the terms of these two equations. Notably, this impact becomes apparent upon comparing the terms of equations 2.25 and 2.26 with their counterparts in equations 2.14 and 2.15.

Primitive Impedance Matrix:

At this point, Carson's modified equations 2.25 and 2.26 are employed to create what is termed a "Primitive Impedance Matrix" for the line. For instance, an overhead four-wire line section with a grounded Y setup produces a 4x4 matrix. Conversely, the grounded Y configuration of an underground line section with three concentric neutrals results in a 6x6 matrix.

With this context, the primitive impedance matrix for an unbalanced 3-phase line section with 'm' neutrals is expressed as follows:

$$[Z_{\text{Primitive}}] = \begin{bmatrix} [\hat{Z}_{pp}] & [\hat{Z}_{pn}] \\ [\hat{Z}_{np}] & [\hat{Z}_{nn}] \end{bmatrix} \quad (2.27)$$

And,

$$[\hat{Z}_{pp}] = \begin{bmatrix} \hat{Z}_{aa} & \hat{Z}_{ab} & \hat{Z}_{ac} \\ \hat{Z}_{ba} & \hat{Z}_{bb} & \hat{Z}_{bc} \\ \hat{Z}_{ca} & \hat{Z}_{cb} & \hat{Z}_{cc} \end{bmatrix} \quad (2.28.a) \quad [\hat{Z}_{pn}] = \begin{bmatrix} \hat{Z}_{a,n1} & \hat{Z}_{a,n2} & \dots & \hat{Z}_{a,nm} \\ \hat{Z}_{b,n1} & \hat{Z}_{b,n2} & \dots & \hat{Z}_{b,nm} \\ \hat{Z}_{c,n1} & \hat{Z}_{c,n2} & \dots & \hat{Z}_{c,nm} \end{bmatrix} \quad (2.28.b)$$

$$[\hat{Z}_{np}] = \begin{bmatrix} \hat{Z}_{n1,a} & \hat{Z}_{n1,b} & \hat{Z}_{n1,c} \\ \dots & \dots & \dots \\ \hat{Z}_{nm,a} & \hat{Z}_{nm,b} & \hat{Z}_{nm,c} \end{bmatrix} \quad (2.28.c) \quad [\hat{Z}_{nn}] = \begin{bmatrix} \hat{Z}_{n1,n1} & \hat{Z}_{n1,n2} & \hat{Z}_{n1,nm} \\ \dots & \dots & \dots \\ \hat{Z}_{nm,n1} & \hat{Z}_{nm,n2} & \hat{Z}_{nm,nm} \end{bmatrix} \quad (2.28.d)$$

Where,

$[\hat{Z}_{pp}]$ - Primitive impedance matrix of the three phases,

$[\hat{Z}_{pn}]$ - Primitive impedance matrix of the three phase conductors with the „m“ neutrals,

$[\hat{Z}_{np}]$ - Primitive impedance matrix of the „m“ neutrals with the three phases,

$[\hat{Z}_{nn}]$ - Primitive impedance matrix of the „m“ neutrals,

Phase Impedance Matrix:

To facilitate the three phase calculations it is very helpful if the primitive impedance matrix can be reduced to equivalent 3x3 matrix namely „Phase Impedance Matrix“. In this case the effect of the neutral is included implicitly in the equivalent values of this matrix.

One of the potential methods that can realize this reduction is the *Korn reduction* [1]. To apply this method, a four-wire section with grounded Y system is assumed, as shown in Figure.2.3.

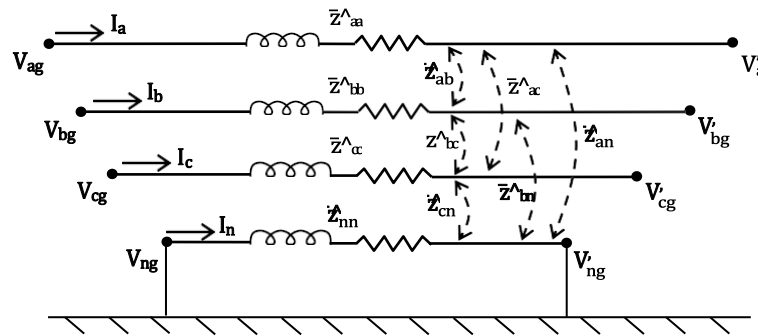


Figure 2.3 Four wire line section of grounded neutral

Application of KVL on the circuit of the Figure yields:

$$\begin{bmatrix} V_{ag} \\ V_{bg} \\ V_{cg} \\ V_{ng} \end{bmatrix} = \begin{bmatrix} V'_{ag} \\ V'_{bg} \\ V'_{cg} \\ V'_{ng} \end{bmatrix} + \begin{bmatrix} \hat{Z}_{aa} & \hat{Z}_{ab} & \hat{Z}_{ac} & \hat{Z}_{an} \\ \hat{Z}_{ba} & \hat{Z}_{bb} & \hat{Z}_{bc} & \hat{Z}_{bn} \\ \hat{Z}_{ca} & \hat{Z}_{cb} & \hat{Z}_{cc} & \hat{Z}_{cn} \\ \hat{Z}_{na} & \hat{Z}_{nb} & \hat{Z}_{nc} & \hat{Z}_{nn} \end{bmatrix} \times \begin{bmatrix} I_a \\ I_b \\ I_c \\ I_n \end{bmatrix} \quad (2.29)$$

Comparing the sub-matrices of Eqs.2.27 with the primitive impedance matrix in Eq.2.29

shows that $[\hat{Z}_{pp}]$ consist of 3x3 elements, while $[\hat{Z}_{pn}]$, $[\hat{Z}_{np}]$ and $[\hat{Z}_{nn}]$ consist of 3x1, 1x3 and 1x1 elements respectively. Accordingly, Eq.2.29 can be rewritten as follows:

$$\begin{bmatrix} [\mathbf{V}_{abc}] \\ [\mathbf{V}_{ng}] \end{bmatrix} = \begin{bmatrix} [\mathbf{V}'_{abc}] \\ [\mathbf{V}'_{ng}] \end{bmatrix} + \begin{bmatrix} [\hat{\mathbf{Z}}_{pp}] & [\hat{\mathbf{Z}}_{pn}] \\ [\hat{\mathbf{Z}}_{np}] & [\hat{\mathbf{Z}}_{nn}] \end{bmatrix} \times \begin{bmatrix} [\mathbf{I}_{abc}] \\ [\mathbf{I}_n] \end{bmatrix} \quad (2.30)$$

For grounded neutral, $[\mathbf{V}_{ng}]$ and $[\mathbf{V}'_{ng}]$ are equal to zero. Hence,

$$[\mathbf{V}_{abc}] = [\mathbf{V}'_{abc}] + [\hat{\mathbf{Z}}_{pp}] \cdot [\mathbf{I}_{abc}] + [\hat{\mathbf{Z}}_{pn}] \times [\mathbf{I}_n] \quad (2.31)$$

$$[0] = [0] + [\hat{\mathbf{Z}}_{np}] \cdot [\mathbf{I}_{abc}] + [\hat{\mathbf{Z}}_{nn}] \times [\mathbf{I}_n] \quad (2.32)$$

Solving Eq.2.32 for $[\mathbf{I}_n]$ and substitute into Eq.2.31, gives:

$$[\mathbf{V}_{abc}] = [\mathbf{V}'_{abc}] + ([\hat{\mathbf{Z}}_{pp}] - [\hat{\mathbf{Z}}_{pn}] \cdot [\hat{\mathbf{Z}}_{nn}]^{-1} \cdot [\hat{\mathbf{Z}}_{np}]) \times [\mathbf{I}_{abc}] \quad (2.33)$$

Based on Eq.2.33, the equivalent 3x3 phase impedance matrix $[\mathbf{Z}_{abc}]$ is given as follows:

$$[\mathbf{Z}_{abc}] = [\hat{\mathbf{Z}}_{pp}] - [\hat{\mathbf{Z}}_{pn}] \cdot [\hat{\mathbf{Z}}_{nn}]^{-1} \cdot [\hat{\mathbf{Z}}_{np}] \quad (2.34)$$

And

$$[\mathbf{V}_{abc}] = [\mathbf{V}'_{abc}] + [\mathbf{Z}_{abc}] \cdot [\mathbf{I}_{abc}] \quad (2.35)$$

It is important to mention that $[\mathbf{Z}_{abc}]$ for three wire line section containing no neutral is determined with no need to Kron reduction. In other words, $[\mathbf{Z}_{abc}]$ of such line section is directly equal to $[\hat{\mathbf{Z}}_{pp}]$ of Eq.2.28.a.

2.3 Load and PVDG Production Curves

Connecting PVDG (Photovoltaic Distributed Generation) units to specific distribution feeders necessitates appropriate modeling to accommodate variations in feeder load demand and PVDG unit production. This section focuses on such modeling, expressed in terms of daily curves, specifically the load curve and PVDG production curve.

2.3.1 Load Curve Modeling

The load curve of a specific feeder is typically segmented into equal time intervals spanning a certain duration, often on a daily basis. These intervals could range from 15 minutes to 1 hour or longer. Within each interval, the feeder's load demand is typically

calculated as the average load over that period. Alternatively, in some cases, the load curve may be represented by the maximum or minimum load demand values recorded in each interval. The load curve values can be expressed in various units such as kilo/megaVoltampere (kVA/MVA), kilo/megaWatt (kW/MW), kilo/megaVAr (kVAr/MVAr), kilo/Amperes (kA/A), or per-unit. In per-unit representation, the load curve values are expressed relative to the peak load demand recorded over the entire duration of the curve.

Table 2.1 provides an example of the summer daily load demand for a specific 11kV distribution feeder in Abu Dhabi city.

Time	MW	MVAr	Time	MW	MVAr
01:00	1.77	0.60	13:00	2.10	0.67
02:00	1.69	0.54	14:00	2.14	0.69
03:00	1.66	0.54	15:00	2.19	0.69
04:00	1.59	0.50	16:00	2.21*	0.69
05:00	1.63	0.55	17:00	2.14	0.69
06:00	1.54	0.56	18:00	2.06	0.69
07:00	1.47	0.63	19:00	1.86	0.65
08:00	1.57	0.63	20:00	2.14	0.73
09:00	1.73	0.67	21:00	2.17	0.77
10:00	1.87	0.67	22:00	2.12	0.79*
11:00	1.91	0.67	23:00	1.98	0.66
12:00	1.99	0.71	24:00	1.91	0.63

Table.2.1 Real and reactive daily load demands of actual 11kV distribution feeder
* MW & MVAr Peak load demands

In the same connection, it is a usual practice representing the load curve in per-unit values. Thus, Eq.2.36 is applied to convert the actual load demand of certain distribution feeder into per-unit-values.

$$LD_{Fj-pu} = \frac{LD_{Fj}}{LD_{Fp}} \Big|_{j=1:24} \quad (2.36)$$

Where,

- LD_{Fj} – Load demand of the feeder at interval j,
- LD_{Fp} – Peak load demand of the feeder,
- LD_{Fj-pu} – LD_{Fj} in per-unit of LD_{Fp} ,

Equation.2.36 is applied on the data of Table.2.1. The results are depicted in Figure.2.4.

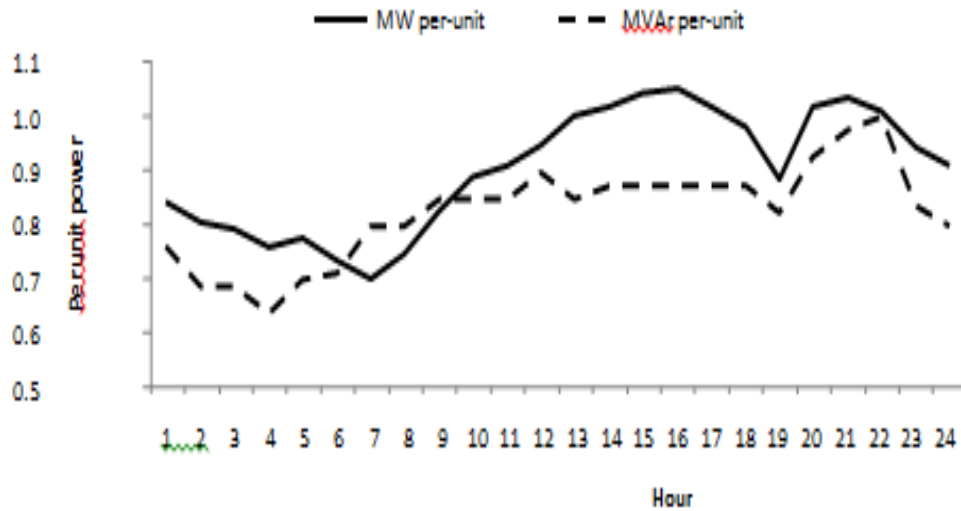


Figure 2.4 Daily load curve of certain 11kV distribution feeder in per-unit values

The furthest point on the distribution network monitored by power distribution companies is typically the input of distribution feeders. However, for this study, load demand data along the feeder is required. To address this, it is assumed that the load demand of each node along the feeder follows the same pattern as the feeder load demand but at a lower level. This assumption is reasonable given that distribution feeders often serve loads of similar nature, including residential, commercial, and industrial loads.

Hence, the actual load curve values at each node are adjusted based on Equation 2.36 and the peak load demand at that node, as follows:

$$LD_{ij} = LD_{ip} \times LD_{Fj-pu} \tag{2.37}$$

Where,

- LD_{ij} – Load demand of node i at interval j ,
- LD_{ip} – Peak Load demand of node i ,

As a result, Equations 2.36 and 2.37 are utilized to generate realistic load curves for the nodes along the feeder. Figure 2.5 illustrates examples of real power load curves at the nodes of a radial distribution feeder. It's important to note that when detailed load demands along the feeder are readily available, the corresponding load curves can be generated directly without the need to apply Equation 2.37.

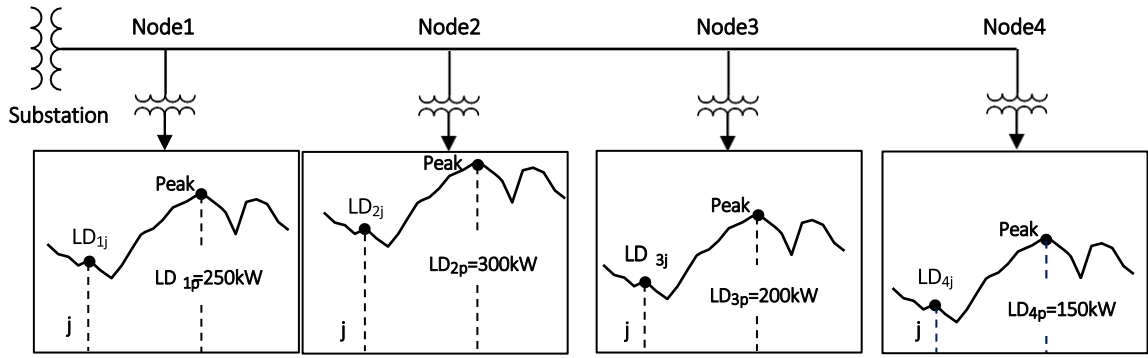


Figure 2.5 Simulation of load curves at the nodes of radial distribution feeder

At this point, the load curves for all nodes along the feeder have been reasonably generated. Subsequently, the currents and voltages along the feeder throughout the daily duration can be determined by applying power flow calculations in each time interval. In this scenario, the feeder nodes are treated as PQ buses in the calculation process, with their values for each interval being substituted from the generated load curves.

2.3.2 PVDG Production Curve Modeling

The production of PVDG units is directly correlated with the solar irradiance (SI) rates falling on the PV modules of the system. While the cell temperature of PV modules may also have an impact, its effect is relatively minor compared to that of solar irradiance. Consequently, the daily solar irradiance curve predominantly determines the daily PVDG production curve, exhibiting a similar pattern.

Given the above, the values of the solar irradiance curve are recalled and represented in per-unit of solar irradiance at standard conditions (SISTC) as follows:

$$SI_{j-pu} = \frac{SI_j}{SI_{STC}} \Big|_{j=1:24} \quad (2.38)$$

Where,

- SI_j – Solar irradiance at interval j ,
- SI_{STC} – Solar irradiance at standard conditions ($1kW/m^2$),
- SI_{j-pu} – Solar irradiance at interval j in per-unit of SI_{STC} ,

Thus, the results of Eq.2.38 are substituted directly to represent the daily PVDG production curve in per-unit of the PVDG output at SI_{STC} , as follows:

$$PVDG_{j-pu} = SI_{j-pu} \Big|_{j=1:24} \quad (2.39)$$

Where, $PVDG_{j-pu}$ is the output of the PVDG unit at j in per-unit of its output at SI_{STC} .

2.4 Application of Backward/Forward Sweep Power Flow

The primary characteristics of radial distribution feeders include their radial structure, utilization of multi-phase conductors, and operation under unbalanced load conditions. These attributes often render traditional power flow methods, typically used for transmission systems, inadequate due to poor convergence characteristics and failure to meet the requirements of distribution systems.

In instances where the primary distribution feeder and all its laterals consist of a 3-phase system, some power companies may assume that the feeder operates under balanced load conditions. Alternatively, specialized power flow methods tailored for radial distribution systems are employed. Among these methods are the backward/forward sweep and ladder iterative methods. While their basic principles are similar, each method requires specification of the voltage magnitude and phase angle of the source, along with the complex values of load demands at each node along the feeder.

Beginning from the end of the feeder, the backward sweep calculates the line section currents and node voltages using Kirchhoff's Current Law (KCL) and Kirchhoff's Voltage Law (KVL) back to the source. The calculated voltage at the source is then compared with its originally specified value. If the error exceeds a certain limit, the forward sweep is executed to update the node voltages along the feeder. In this step, the specified source voltage and previously calculated line section currents from the backward sweep are utilized. This process continues iteratively until the voltage error at the source falls within the specified limit.

2.4.1 Balanced Load Consideration

As previously mentioned, it is feasible to consider the primary distribution feeder with 3-phase laterals as operating under balanced load conditions. Thus, it is prudent to initiate the application of the backward/forward power flow method on such a 3-phase balanced load feeder. In this scenario, calculations are carried out in terms of line voltages and currents using a single line diagram model, akin to traditional power flow methods. Referring to Figure. 2.6, which illustrates a radial distribution feeder with five nodes, the backward sweep commences from node 5 as outlined below:

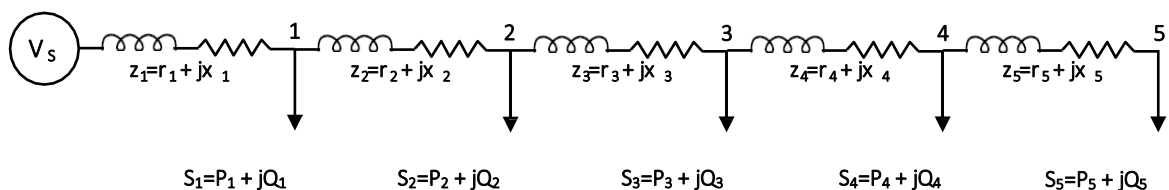


Figure 2.6 Single line diagram of 5-nodes radial distribution feeder

Backward Sweep

Before starting the backward sweep, an initial flat voltage equal to the specified substation voltage (V_{SS}) is assumed along the feeder.

The network is traced in the backward direction using KCL & KVL to calculate the currents and voltages in all sections and nodes respectively. Let the initial flat voltage is $V_{SS} \angle 0$; then the first iteration will start from node 5 calculating the relevant line current and voltage as follows:

$$I_5^1 = I_{4,5}^1 = \left(\frac{S_5}{\sqrt{3} V_5^1} \right)^* = \left(\frac{P_5 + jQ_5}{\sqrt{3} V_5^1} \right)^* \quad (2.40)$$

$$V_4^1 = V_5^1 + z_5 \cdot I_{4,5}^1 \quad (2.41)$$

Setting initial voltage at node 5 as,

$$V_5^1 = V_{SS} \angle 0$$

Where,

- I_5^1 - Load current of node 5 at iteration 1
- $I_{4,5}^1$ - Section current from node 4 to 5 at iteration 1
- S_5 - Specified complex load demand of node 5
- V_5^1 - Line voltage of node 5 at iteration 1

Then, in the upstream direction,

$$I_4^1 = \left(\frac{S_4}{\sqrt{3} V_4^1} \right)^* \quad (2.42)$$

$$I_{3,4}^1 = I_4^1 + I_{4,5}^1 \quad (2.43)$$

$$V_3^1 = V_4^1 + z_4 \cdot I_{3,4}^1 \quad (2.44)$$

In general form; with i and t denoting the node and iteration numbers respectively,

$$I_i^t = \left(\frac{S_i}{\sqrt{3} V_i^t} \right)^* \quad (2.45)$$

$$I_{i-1,i}^t = I_i^t + I_{i,i+1}^t \quad (2.46)$$

$$V_{i-1}^t = V_i^t + z_i \cdot I_{i-1,i}^t \quad (2.47)$$

Bearing in mind that z_i is determined in Ω/km by applying Eq.2.6

The procedure continues until V_{SS} is calculated. At that stage, if the difference between the calculated and specified V_{SS} is within the convergence tolerance, the procedure stops at the last calculated values in hand. Otherwise, it shall continue with the forward sweep.

Forward Sweep

The substation is set to its specified V_{SS} and the voltages of the downstream nodes are updated using the currents already calculated from the backward sweep. Thus, the updated voltages are calculated as follows:

$$V_1^2 = V_{SS} - z_1 \cdot I_{SS,1}^1 \quad (2.48)$$

Where, V_1^2 - Updated line voltage of node 1 at iteration 2
 $I_{SS,1}^1$ - Section current from the substation to node 1 calculated at iteration 1

Then, in the downstream direction,

$$V_2^2 = V_1^2 - z_2 \cdot I_{1,2}^1 \quad (2.49)$$

In general form, with i and t denoting the node and iteration numbers respectively,

$$V_i^t = V_{i-1}^t - z_i \cdot I_{i-1,i}^{t-1} \quad (2.50)$$

The procedure proceeds until V^2 is calculated initiating the next backward sweep. At the end of the next backward sweep, the most recent calculated V_{SS} is compared with its specified value. If the error is within the convergence tolerance the procedure stops, adopting the results of the last iteration. Otherwise, the procedure continues with new iteration and so on.

2.4.2 Unbalanced Load Consideration

Essentially, the same procedure applied to a 3-phase balanced load distribution feeder is also applied to an unbalanced load feeder. However, in the case of an unbalanced load condition, the calculations should be conducted separately for each phase along the feeder's wire conductors. In this process, the series impedances of the line sections are determined in terms of the phase impedance matrix derived in Section 2.1.2. To illustrate this, Figure. 2.7 depicts line sections in a certain four-wire feeder with 3-phase unbalanced loads.

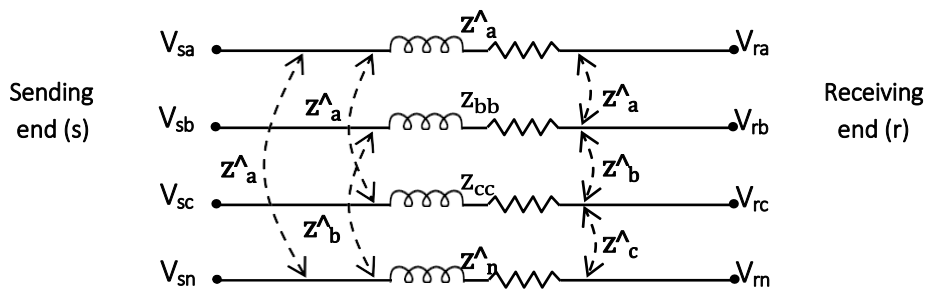


Figure 2.7 Line section in four wire feeder of 3-phase unbalanced loads

At the beginning, the primitive impedance matrix of the line section is formulated according to Eqs.2.27 & 2.28:

$$[\hat{Z}_{primitive}] = \begin{bmatrix} \hat{Z}_{aa} & \hat{Z}_{ab} & \hat{Z}_{ac} & \hat{Z}_{an} \\ \hat{Z}_{ba} & \hat{Z}_{bb} & \hat{Z}_{bc} & \hat{Z}_{bn} \\ \hat{Z}_{ca} & \hat{Z}_{cb} & \hat{Z}_{cc} & \hat{Z}_{cn} \\ \hat{Z}_{na} & \hat{Z}_{nb} & \hat{Z}_{nc} & \hat{Z}_{nn} \end{bmatrix} \quad (2.51)$$

Then, the line section of Figure.2.7 is converted to equivalent three wires configuration by applying Korn's reduction method of Eq.2.34. This will result in the equivalent phase impedance matrix $[Z_{abc}]$ as follows:

$$[Z_{abc}] = \begin{bmatrix} \hat{Z}_{aa} & \hat{Z}_{ab} & \hat{Z}_{ac} \\ \hat{Z}_{ba} & \hat{Z}_{bb} & \hat{Z}_{bc} \\ \hat{Z}_{ca} & \hat{Z}_{cb} & \hat{Z}_{cc} \end{bmatrix} - \begin{bmatrix} \hat{Z}_{an} \\ \hat{Z}_{bn} \\ \hat{Z}_{cn} \end{bmatrix} \cdot [\hat{Z}_{nn}]^{-1} \cdot [\hat{Z}_{na} \ \hat{Z}_{nb} \ \hat{Z}_{nc}] \quad (2.52)$$

Each of the elements on the right hand side of Eq.3.52 is determined by using Carson's modified Eqs.3.25 & 3.26 for the primitive impedance matrix. Hence, the resulting equivalent 3X3 phase impedance matrix of the line section is.

$$[Z_{abc}] = \begin{bmatrix} Z_{aa} & Z_{ab} & Z_{ac} \\ Z_{ba} & Z_{bb} & Z_{bc} \\ Z_{ca} & Z_{cb} & Z_{cc} \end{bmatrix} \quad (2.53)$$

Backward Sweep

The backward sweep starts with the setting of an initial flat voltage along the feeder, equal to the specified substation voltage by phase ($[V_{abc}]_{SS}$). The same procedure of tracing the feeder back and forth is applied until the error between the calculated and specified substation voltages becomes within the convergence tolerance.

Hence, back to Figure.3.6 assuming the 5 node radial distribution feeder is now operating under unbalanced load condition. Starting from the far end node,

$$[I_{abc}]_5^1 = \left[\frac{[S_{abc}]_5}{[V_{abc}]_5^1} \right]^* = \left[\frac{(P+jQ)_5}{[V_{abc}]_5^1} \right]^* \xrightarrow{\text{yields}} \begin{bmatrix} I_a < \theta_a \\ I_b < \theta_b \\ I_c < \theta_c \end{bmatrix}_5^1 \quad (2.54)$$

$$[V_{abc}]_4^1 = [V_{abc}]_5^1 + [Z_{abc}]_{5,4} \cdot [I_{abc}]_{4,5}^1 \xrightarrow{\text{yields}} \begin{bmatrix} V_a < \alpha_a \\ V_b < \alpha_b \\ V_c < \alpha_c \end{bmatrix}_4^1 \quad (2.55)$$

Setting initial voltage at node 5,

$$[V_{abc}]_5^1 = [V_{abc}]_{SS} = \begin{bmatrix} V_a \\ V_b \\ V_c \end{bmatrix}_{SS} \xrightarrow{\text{set}} \left\{ \begin{array}{l} \text{At the substation the voltage is specified as} \\ |V_a| = |V_b| = |V_c| \text{ and} \\ < V_a = \theta, < V_b = (\theta - 120), < V_c = (\theta + 120), \end{array} \right\} \quad (2.56)$$

- Where,
- $[I_{abc}]_5^1$ - Phase currents of node 5 at iteration 1
 - $[S_{abc}]_5$ - Specified complex load demands of node 5 by phase
 - $[V_{abc}]_5^1$ - Phase voltages of node 5 at iteration 1
 - $[I_{abc}]_{4,5}^1$ - Phase currents from node 4 to 5 at iteration 1
 - $[Z_{abc}]_5$ - Phase impedance matrix of line section 5
 - $[Z_{abc}]_5$ - Specified phase voltages of the substation
 - (*) - For conjugate complex values

In general form; with i and t denoting the node and iteration numbers respectively,

$$[I_{abc}]_i^t = \left(\frac{[S_{abc}]_i}{[V_{abc}]_i^t} \right)^* \quad (2.57)$$

$$[I_{abc}]_{i-1,i}^t = [I_{abc}]_i^t + [I_{abc}]_{i,i+1}^t \quad (2.58)$$

$$[V_{abc}]_{i-1}^t = [V_{abc}]_i^t + [Z_{abc}]_i \cdot [I_{abc}]_{i-1,i}^t \quad (2.59)$$

The procedure proceeds until $[V_{abc}]_{SS}$ is calculated. At that stage, if the difference between the calculated and specified $[V_{abc}]_{SS}$ is within the convergence tolerance, the procedure stops at the last calculated values in hand. Otherwise, it goes to the forward sweep

Forward Sweep.

The forward sweep is commenced by setting the substation voltage to its specified value. The node voltages by phase are then updated in the downstream direction using the currents from the previous backward sweep. Thus, the updated voltages are calculated as follows:

$$[V_{abc}]_1^2 = [V_{abc}]_{SS} - [Z_{abc}]_1 \cdot [I_{abc}]_{SS,1}^1 \xrightarrow{\text{yields}} \left[\begin{array}{l} V_a < \alpha_a \\ V_b < \alpha_b \\ V_c < \alpha_c \end{array} \right]_1^2 \quad (2.60)$$

Where,

$[I_{abc}]_{SS,1}^1$ - Phase currents from the substation to node 1 calculated at iteration 1

$[V_{abc}]_1^2$ - Updated voltages by phase of node 1 at iteration 2

Then, in the downstream direction,

$$[V_{abc}]_2^2 = [V_{abc}]_1^2 - [Z_{abc}]_2 \cdot [I_{abc}]_{1,2}^1 \quad (2.61)$$

In general form, with i and t denoting the node and iteration numbers respectively,

$$[V_{abc}]_{i-1}^t = [V_{abc}]_{i-1}^{t-1} - [Z_{abc}]_i \cdot [I_{abc}]_{i-1}^{t-1} \quad (2.62)$$

The procedure continues until $[V_{abc}]_5^2$ is calculated, initiating the next backward sweep. At the end of the next backward sweep, the most recent calculated $[V_{abc}]_{SS}$ is compared with its specified value. If the error is within the convergence tolerance the procedure stops adopting the results of the last iteration. Otherwise, the procedure continues with new iteration and so on.

2.5 Calculation of Line Power Loss

The calculation of line power loss along a certain wire is typically determined using the I^2R formula. However, for feeders of a 3-phase system, this formula is not always applicable. It may work under a 3-phase balanced load condition, as the series resistance per phase is determined individually for each section along the feeder. Consequently, the total line power loss is the summation of I^2R losses in the conductors of the three phases, assuming zero current in the neutral wire (in the case of a four-wire system).

Figure 2.8 shows a single line diagram of 3-phase four-wire distribution feeder of 'n' sections.

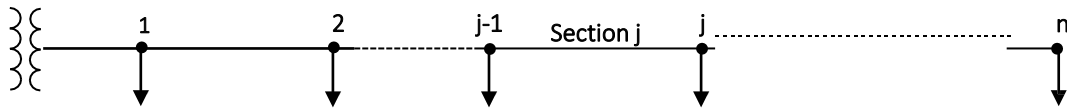


Figure 2.8 Single line diagram of 3-phase four-wire distribution

feeder The total line power loss (PL_T) along the feeder under balanced load

condition is then:

$$PL_T = 3 \cdot \sum_{j=1}^n I_j^2 \cdot R_j \quad (2.63)$$

Under unbalanced load condition, each four-wire line section is represented by equivalent 3×3 phase impedance matrix, by the means of Carson's equations and Korn's reduction. However, substituting the resistances of the equivalent 3×3 matrices into the I^2R formula will lead to incorrect results. Alternatively, the line power loss should be computed as the difference between the sending and receiving power of the line section by phase [8].

Assume the same 3-phase four-wire feeder is now operating under unbalanced load

condition. The line power loss (PL_j) for line section j in this feeder is:

$$[PL_j]_{abc} = \begin{bmatrix} |(S_a)_{j-1} - (S_a)_j| \\ |(S_b)_{j-1} - (S_b)_j| \\ |(S_c)_{j-1} - (S_c)_j| \end{bmatrix} \quad (2.64)$$

$$[PL_j]_{abc} = \begin{bmatrix} |(V_a)_{j-1} \times (I_a)_j - (V_a)_j \times (I_a)_j| \\ |(V_b)_{j-1} \times (I_b)_j - (V_b)_j \times (I_b)_j| \\ |(V_c)_{j-1} \times (I_c)_j - (V_c)_j \times (I_c)_j| \end{bmatrix} = [|\Delta V_j \times I_j|]_{abc} \quad (2.65)$$

Where,

$(V_a)_{j-1}$ - Sending end voltage of section j at phase 'a'

$(V_a)_j$ - Receiving end voltage of section j at phase 'a'

$(I_a)_j$ - Current flows in section j at phase 'a'

ΔV_j - Voltage drop in section j by phase

I_j - Current flows in section j by phase

| | - Gives positive power loss value even if the current flows from j to $j-1$

Hence, the total line power loss along the feeder (PL_T) is,

$$PL_T = \text{sum} \left(\sum_{j=1}^n [PL_j]_{abc} \right) \quad (2.66)$$

Where, 'sum' is the summation of line power loss across the three phases.

2.6 Conclusion

The sizing and placement of PVDG units on distribution feeders necessitate thorough modeling of the physical structure of the line sections along the feeder. Equally important are the load curve of the feeder and the PVDG production curve. Concerning the physical structure, the series impedances are modeled taking into account both 3-phase balanced and unbalanced load conditions.

For a balanced load feeder, the self and mutual inductances of the conductors are typically combined into a single formula, while the resistances are determined from the product specification sheet of the conductors. However, distribution feeders are most likely operated under unbalanced load conditions, necessitating reflective modeling.

Hence, a suitable procedure is applied to model the series impedances of unbalanced load feeders. This procedure calculates the self and mutual inductances of the line sections based on Carson's equations. The result is a "primitive impedance matrix" for the

conductors of each line section along the feeder. Furthermore, the work is enhanced by utilizing Korn's reduction method to generate an equivalent 3×3 "phase impedance matrix" from any $n \times n$ "primitive impedance matrix".

Suitable modeling is developed for the load curve of the feeder, assuming that the load demand of each node along the feeder varies in the same pattern as the feeder load demand. Consequently, the feeder load curve is generated in per-unit of the feeder's peak load demand and then applied to each node in per-unit of that node's peak load demand.

The modeling of PVDG production is based on the fact that production is directly proportional to the solar irradiance (SI) rates falling on the PV modules of the system. Therefore, the daily solar irradiance curve can largely determine the daily PVDG production curve. With this in mind, the values of the solar irradiance curve are represented in per-unit of SI at standard conditions. Consequently, the results reflect the PVDG production in per-unit of the PVDG output due to SI at standard conditions.

At this stage, the aforementioned modeling components can be integrated by means of suitable power flow techniques. The backward/forward sweep power flow is one of the most potential techniques for dealing with radial distribution feeders.

Chapter 3:

League Championship Algorithm (LCA)

3.1 Introduction

Since 1970s that the idea of a general algorithmic framework emerged, many algorithms have been introduced. With the aim of being applicable with relatively few modifications to different optimization problems, these algorithms have got their source of inspiration from nature, society, culture, politics, human, etc. The term “metaheuristic” is used for such methods that combine rules and randomness while imitating natural, social, cultural and political phenomena. These methods are from now on regularly employed in all sectors of business, industry, engineering, etc. However, besides all of the interest necessary to applications of metaheuristics for solving difficult and complex optimization problems, occasionally a new metaheuristic algorithm is introduced which uses a novel metaphor as a guide for solving optimization problems. For example, particle swarm optimization algorithm (PSO) , introduced in 1995, models the flocking behavior of birds; harmony search (HS) , introduced in 2001, is conceptualized using the musical process of searching for a perfect state of harmony; bacterial foraging optimization algorithm (BFOA) , introduced in 2002, models foraging as an optimization process where an animal seeks to maximize energy per unit time spent for foraging; artificial bee colony algorithm (ABC) [61], introduced in 2005, simulates the intelligent foraging behavior of a honeybee swarm; central force optimization algorithm (CFO) , introduced in 2007, makes an analogy between the process of searching a decision space for the maxima of an objective function and flying probes through 3-dimensional physical space under the influence of gravity; fire fly algorithm (FA) introduced in 2007, performs based on the idealization of the flashing characteristics of fireflies; group search optimizer (GSO), introduced in 2009, simulates the animal searching behavior (an active movement by which animals find or attempt to find resources such as food, mates, oviposition, or nesting sites); krill herd algorithm (KH) , introduced in 2012, works based on the simulation of the herding of the krill swarms in response to specific biological and environmental processes; and optics inspired optimization (OIO) , introduced in 2013, treats the surface of the numerical function to be optimized as a reflecting surface in which each peak is assumed to reflect as a convex mirror and each valley to reflect as a concave one.

The League Championship Algorithm (LCA) is a recently proposed algorithm for global optimization, which mimics the championship process in sport leagues . Beside the nature,

Chapter 3: League Championship Algorithm (LCA)

culture, politics, human, etc as the typical sources of inspiration of various algorithms, the metaphor of sporting competitions is used for the first time in LCA. The methodology of LCA can be described as follows. A number of individuals making role as sport teams compete in an artificial league for several weeks (iterations). Based on the league schedule in each week, teams play in pairs and their game outcome is determined in terms of win or loss (or tie), given the playing strength (fitness value) along with the particular team formation/arrangement (solution) followed by each team. Keeping track of the previous week events, each team devises the required changes in its formation/playing style (a new solution is generated) for the next week contest and the championship goes on for a number of seasons (stopping condition). LCA is a population based algorithm where its “teams” are similar to PSO’s “particles” but with a quite different way of performing their search. The way in which a new solution associated to an LCA’s team is generated is governed via imitating the match analysis process followed by coaches to design a suitable arrangement for their forthcoming match. In a typical match analysis, coaches will modify their arrangement on the basis of their own game experiences and their opponent’s style of play.

The above rationale is modeled by some LCA-specific paradigm as follows. To determine the winner/loser individuals to bias the search toward/outward them, LCA focuses on the relative comparison of individuals, and not their absolute fitness gains. Such a mechanism ensures that the win portion for the better solution (team) is greater than the win portion of the weaker solution (team). Therefore the search direction is expected to be toward winner (more likely the better solution) and in opposition of loser (more likely the weaker solution). Such a mechanism allows that the algorithm moves the population toward promising areas and at the same time escapes from local or fruitless areas. Modeling artificial match analysis mathematically in LCA yields four equations which generate new solutions in the search space. The development of these equations is closely related to develop a balance between intensification and diversification. Unlike many algorithms which only allow a given solution approaches to better solutions in the search space, LCA also allows retreat from solutions in a scheduled manner (supplied by the league schedule module). For this reason, we will see that LCA performs well on various types of problems. To preserve diversity and avoid premature convergence, LCA uses a truncated geometric probability distribution to choose the number of elements in a given solution that their value should change via one

of the four equations to generate a new solution. Using a truncated geometric distribution we can set the number of changes dynamically with more emphasis given to the smaller or larger rate of changes.

3.2 Review of LCA and Its Terminology

The basic idea of LCA was inspired by the concept of league championship in sport competitions. Following terms related to the league, team and its structure are commonly used in LCA.

League: 'league' means a group of sport teams that are organized to compete with each other in a certain type of sport. A league championship can be held in different ways. For example, the number of games that each team should play with other teams may vary. At the end of the league championship, the champion is determined based on the win, loss and tie records during the league's competition with other teams.

Formation: formation of a team refers to the specific structure of the team when playing with other teams, such as the positions of players, and the rule of each player during match. For any sport teams, coaches arrange their teams based on their players' abilities to achieve the best available formation to play with other teams.

Match analysis: match analysis refers to the examination of behavioral events occurring during a match. The main goal of match analysis after determining the performance of a team is to recognize the strengths and weaknesses and to improve. The important part of the match analysis process is to send the feedback of last matches (their own match and the opponent's match) to players. The feedback should be given to the player, pre-match and post-match to build up team for next match. One of these analyses is the strength/weakness/opportunity/threat (SWOT) analysis which links the external (opportunities and threats) and internal (strengths and weaknesses) factors of the team's performance. Identification of SWOTS is necessary because next planning step is based on the results of the SWOT analysis to achieve the main objective. The SWOT analysis evaluates the interrelationships between the internal and external factors of match in four basic categories:

S/T matches illustrate the strengths of a team and the threats of competitors. The team

should use its strengths to defuse threats.

S/O matches illustrate the strengths and opportunities of a team. The team should use its strengths to take opportunities.

W/T matches illustrate the weaknesses and threats of a team. The team should try to minimize its weaknesses and defuse threats.

W/O matches show the weaknesses coupled with opportunities of a team. The team should attempt to overcome weaknesses by use of opportunities.

The SWOT analysis provides a structure for conducting gap analysis. A gap refers to the space between the place where we are and the place where we want to be. The identification process of a team's gap contains an in-depth analysis of the factors that express the current condition of the team and subsequently help to make a plan for improvement of the team.

3.3 League Championship Algorithm

LCA is a population-based algorithm that is used for solving global optimization problems with a continuous search space. Like other population-based algorithms, LCA tries to move populations from possible areas to promising areas during searching for the optimum in the whole decision space. Table 3.1 presents a list of the characteristics of the LCA.

General algorithm	League championship algorithm
Decision variable	Player's strength in each team's formation
Solution	Team's formation
Old solution	Old team's formation
New solution	New team's formation
Best solution	The winner of league championship
Fitness function	Team's playing strength

Chapter 3: League Championship Algorithm (LCA)

Initial solution	Random formation for each team
Selection	Match analysis process
Process of generating new solution	SWOT matrix

Table 3.1 Characteristics of the LCA

In the optimization process of LCA, a set of L (an even number) solutions are first created randomly to build initial population. Then, they evolve gradually the composition of the population in sequential iterations. In LCA, league refers to population; formation of a team stands for solution; and week refers to iteration. So, team i denotes the i th solution of the population. A fitness value is then calculated for each team based on the team's adaption to the objectives (determined by the concepts of player strength and team's formation). In LCA, new solutions are generated for next week by applying operators to each team based on the results of match analysis which are used by coaches to improve their team's arrangements. An evolutionary algorithm (EA) is a population-based one that uses the Darwin's evolution theory as selection mechanism. Based on a pseudo code of EA and according to the selection process of LCA (greedy selection), in which the current team's formation is replaced by the best team's formation, LCA can be classified as an EA group of the population-based algorithms. LCA terminates after a certain number of seasons (S), each of which is composed of $(L-1)$ weeks. Note that the number of iterations in LCA is equal to $S(L-1)$.

LCA models an artificial championship during the optimization process of the algorithm based on some idealized rule that can be expressed as follows:

1. The team with better playing strength (ability of the team to defeat competitors) has more chances to win the game.
2. The weaker team can win the game but its chance to win the game is very low (the playing strength does not determine the final outcome of the game exactly).
3. The sum of the win's probabilities of both teams that participate in a match is equal to one.

Chapter 3: League Championship Algorithm (LCA)

4. The outcome of the game only can be win or loss (tie is not acceptable as the outcome of the game in the basic version of LCA).
5. When teams i and j compete with each other and eventually team i wins the match, any strength helps team i to win and dual weakness causes team j to lose the match (weakness is a lack of specific strength).
6. The teams just focus on their forthcoming match without consideration of other future matches and the formation of team arranged only by previous week results.

Figure 3.1 shows the flowchart of LCA, which illustrates the optimization process of the basic LCA. As shown in Figure. 3.1, first of all a representation for individuals must be chosen. Solutions (team's formation) are represented with n decision variables of real numbers. Each element of the solutions depends on one of the team's players and shows the corresponding values of the variables with the aim of optimization. Changes in each value can be the effect of changes in the responsibility of the corresponding player. $f(x_1, x_2, \dots, x_n)$ denotes an n variable function to be minimized during the optimization running of LCA over a decision space (a subset of R^n). The solution of team i at week t can be represented by $X_{it} = (x_{it1}, x_{it2}, \dots, x_{itn})$ and the value of its fitness function (player strength) is $ff(x_{it})$. $Bit-1 = (bit_1^{t-1}; bit_2^{t-1}; \dots; bit_n^{t-1})$ and $ff(B_i^{t-1})$ denote the best formation of team i before

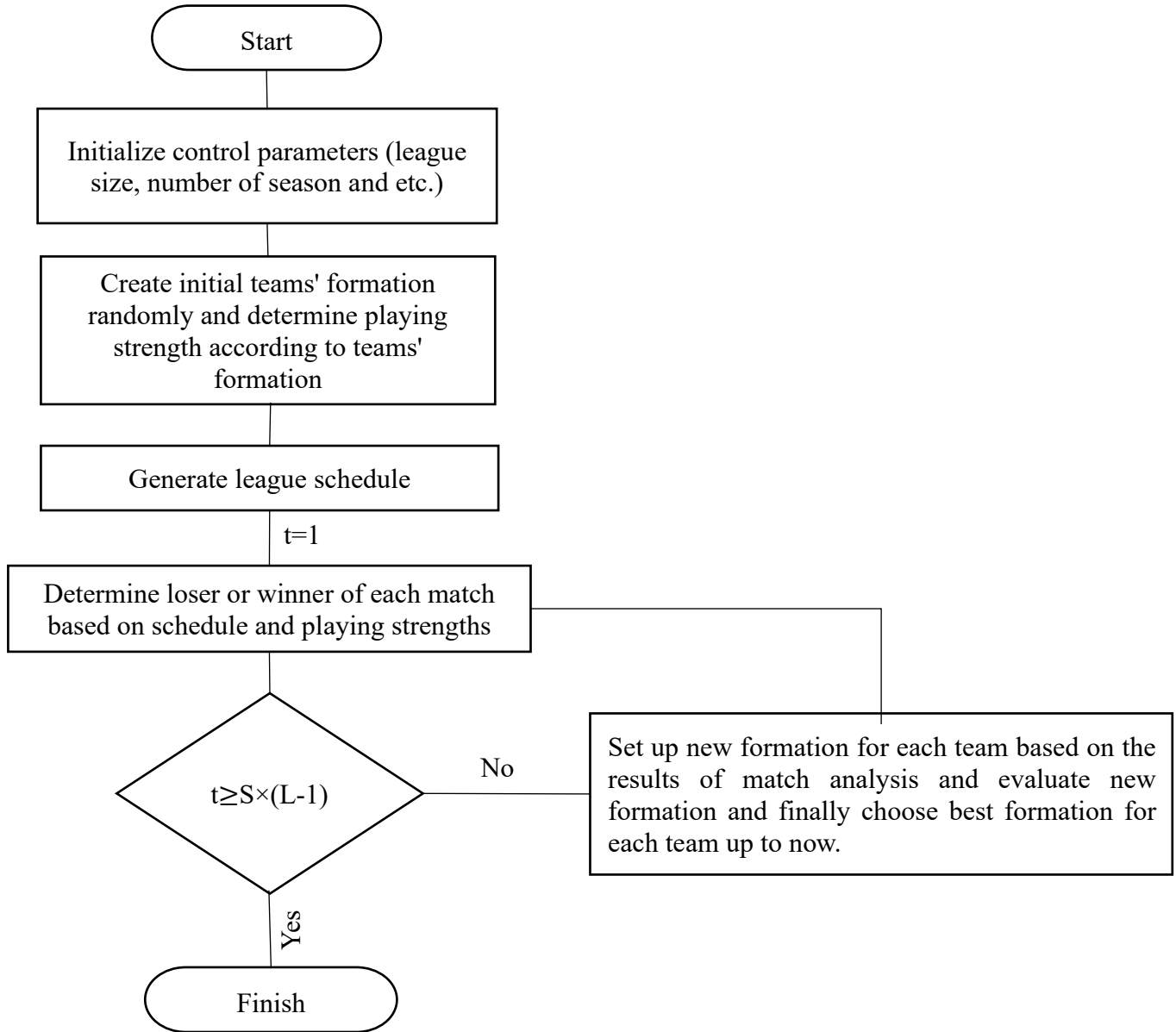


Figure. 3.1 Flowchart of the basic LCA

week t and its fitness function, respectively. The greedy selection in LCA can be made between $ff(x_{ti})$ and $ff(B_{ti-1})$. The modules of LCA, generation of league schedule, determination of the winner or loser, and setup of new formation are detailed in the following section.

3.4 Generating League Schedule

The common aspect of different sport leagues is the structure, in which teams can compete with each other in a nonrandom schedule, named season. Therefore, the first and the most

Chapter 3: League Championship Algorithm (LCA)

important step in LCA, is to determine the match schedule in each season. A single-round robin schedule can be applied in LCA to determine the team's schedule, in which each team competes against other teams just once in a certain season. In a championship containing L teams with the single-round robin schedule rule, there are $L(L-1)/2$ matches in a certain season. In each of $(L-1)$ weeks, $(L/2)$ matches will be held in parallel (if L is odd, in each week $(L-1)/2$ matches will be held and one team has to rest).

The procedure of scheduling of the algorithm can be illustrated by a simple example of league championship of 8 teams. The teams have named from a to h. In the first week, the competitors are identified randomly. Figure 3.2a shows the competitors in the first week. For example, team a competes with team d and team b competes with team g. In the second week, in order to identify the pairs of competitors, one of the teams (team a) is fixed in its own place and all other teams turn round clockwise. Figure 3.2b indicates the procedure of identifying the pairs of competitors for week 2. This process continues until the last week (week 7) shown Figure. 3.2c. In LCA, the single-round robin tournament is applied for scheduling L teams in $S(L-1)$ weeks.

3.5 Determining the Winner or Loser

During the league championship, teams compete with each other in every week. The outcome of each match can be loss, tie, or win. The scoring rules for the outcome of the matches can be different for different sports. For instance, in soccer the winner gets three, and the loser gets a zero score. By the end of the match, both teams get one if the outcome is tie. According to the idealized rule 1, the chance of a stronger team to win the match is higher than its competitor, but occasionally a weaker team may win the match. Therefore, the outcome of the match is associated with different reasons. The most important one is the playing strengths of the teams. So we can consider a linear relationship between the playing strengths and the outcome of the match (idealized rule 2).

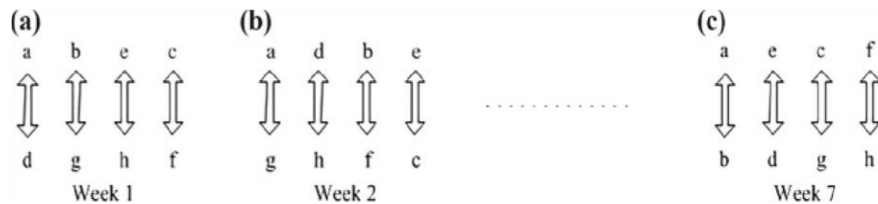


Figure. 3.2 A simple example of league championship scheduling

In LCA, a stochastic criterion of playing strength, which depends on the degree of fit of a team, is utilized to determine the winner or loser of the match. Note that in the basic version of LCA the outcome of the matches can only be win or loss (no tie). The teams' degree of fit refers to the proportion of playing strength, which is calculated based on the distance between the playing strength and the ideal reference point (the lower bound of the optimization problem).

Assuming that team i competes with team j at week t , the chance of each team to defeat another team can be expressed as (Kashan 2009) follows:

$$\frac{f(x_i^t) - \hat{f}}{f(x_j^t) - \hat{f}} = \frac{p_j^t}{p_i^t} \quad (3.1)$$

where x_i^t and x_j^t = formation of teams i and j at week t ; $f(x_i^t)$ and $f(x_j^t)$ = playing strength of teams i and j at week t ; \hat{f} = ideal reference point; p_i^t = chance of team i to defeat team j at week t ; and p_j^t = chance of team j to defeat team i at week t .

Because the chances of both teams to win the match are evaluated based on the specific point, the ratio of distance is identified as the team's winning portion. According to idealized rule 3, the relationship of the chances of teams i and j at week t can be expressed as follows:

$$p_i^t + p_j^t = 1 \quad (3.2)$$

Based on Eqs. (3.1) and (3.2), the chance of team i to defeat team j at week t is given by (Kashan 2014):

$$p_i^t = \frac{f(x_i^t) - \hat{f}}{f(x_i^t) + f(x_j^t) - 2\hat{f}} \quad (3.3)$$

In LCA, in order to specify the winner of the match, a random number between $[0,1]$ is generated randomly. If the generated number is equal to or less than p_i^t , team i defeats team j at week t . Otherwise, team j defeats team i at week t .

3.6 Setting Up a New Team Formation

Before applying any strategy to team i , in order to change the formation of team i at next week, coaches should identify strengths and weaknesses of the team and players

Chapter 3: League Championship Algorithm (LCA)

(individuals). Based on these strengths and weaknesses, coaches determine the formation of the team in next week to enhance the performance of the team. An artificial match analysis can be performed to specify the opportunities and threats. Strengths and weaknesses are internal factors while opportunities and threats are external factors. In LCA, the internal factors are evaluated based on the team's

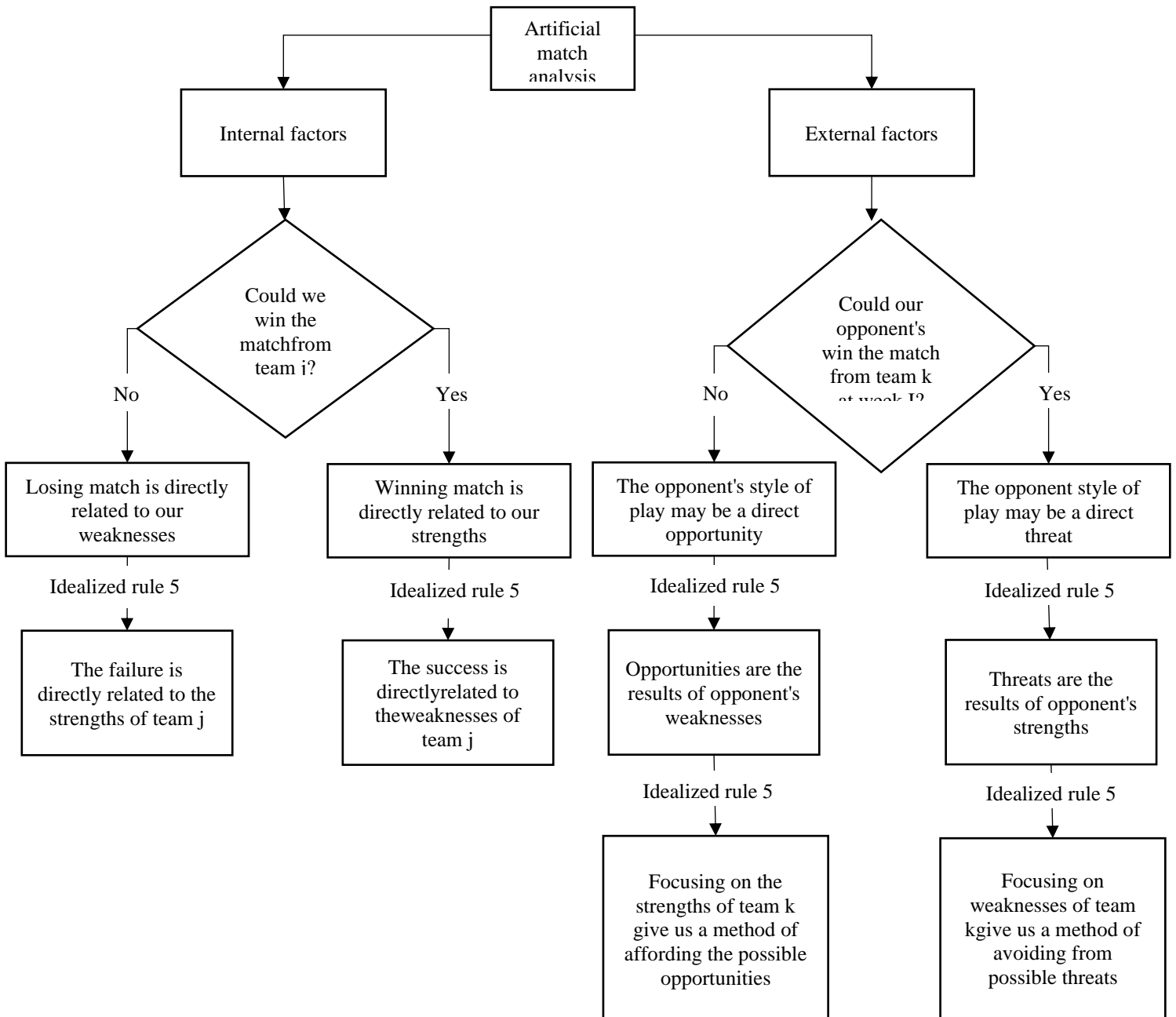


Figure. 3.3 Procedure of the artificial match analysis in LCA

Chapter 3: League Championship Algorithm (LCA)

performance at the last week (week t), while evaluating the external factors is based on the opponent's performance at week t . The artificial match analysis helps prepare team i for next week (week $t + 1$). In the modeling process, if team i wins (loses) the match at week t , it is assumed that the success (failure) is directly related to the strengths (weaknesses) of team i or weaknesses (strengths) of its opponent team j (idealized rule5). The procedure of modeling and evaluating the artificial match analysis for team i at week t is displayed in Figure. 3.3. The left side in Figure. 3.3 shows the evaluation of hypothetical internal factors and the right side shows the way of evaluating the external factors.

According to the results of the artificial match analysis applied to team i in order to determine its performance, the coach should take some possible actions to improve the team's performance. The possible actions (SWOT analysis) are shown in Table 3.2. The SWOT analysis is adjusted based on idealized rule 6. Table 3.2 shows different strategies (S/T, S/O, W/T, and W/O) that can be adopted for team i in different situations. For instances, if team i has won the last match and team l has lost its match at the last week, it is reasonable for team i to focus on strengths which give it more chance to win team l at next match. Therefore, adopting the S/O strategy for team i is efficient. Table 3.2 also displays,

	Adopt S/T strategy	Adopt S/O strategy	Adopt W/T strategy	Adopt W/O strategy
	Team i has won	Team i has won	Team i has lost	Team i has lost
	Team l has won	Team l has lost	Team l has won	Team l has lost
	Focusing on	Focusing on	Focusing on	focusing on
S	Own strengths or weaknesses of team j	Own strengths or weaknesses of team j	–	–
W	–	–	Own weaknesses	Own weaknesses

Chapter 3: League Championship Algorithm (LCA)

			or strengths of team <i>j</i>	or strengths of team <i>j</i>
O	–	Weaknesses of team <i>l</i> or strengths of team <i>k</i>	–	Weaknesses of team <i>l</i> or strengths of team <i>k</i>
T	Strengths of team <i>l</i> or weaknesses of team <i>k</i>	–	Strengths of team <i>l</i> or weaknesses of team <i>k</i>	–

Table 3.2 Hypothetical SWOT analysis derived from the artificial match analysis

in a metaphorical way, the SWOT analysis matrix which is used for planning in the future matches.

The aforementioned analysis must be performed by all participants at week *t* to plan for next match and choose a suitable formation for upcoming match. After adopting a suitable strategy for team *i* based on the SWOT matrix, all teams should fill their gaps. For instance, assume that in a soccer match team *i* has lost the match at week *t* to team *j* and the results of the match analysis process have specified that the type of defensive state (man-to-man defensive state) is the reason of loss. Therefore, a gap exists between the current sensitive defensive state and the state which ensures a man-to-man pressure defense at week *t*+1.

According to the league schedule, team *l* is the competitor of team *i* ($i = 1, 2, \dots, L$) at week *t*+1; team *j* is the competitor of team *i* at week *t*; and team *k* is the competitor of team *l* at week *t*. As aforementioned, X_i^t ; X_j^t and X_k^t , respectively, denote the formations of teams *i*, *j*, and *k* at week *t*. $(X_k^t - X_i^t)$ defines the gap between playing styles of teams *i* and *k*, which highlights the strengths of team *k*. This case applies when team *i* wants to play with team *l* at week *t*+1 and team *k* wins team *l* at week *t* by X_k^t 's formation. Therefore, if team *i* uses the playing style of team *k* at week *t* (X_k^t) to compete with team *l* at week *t*+1, it is highly possible for team *i* to win team *l* at week *t*+1. Similarly, $(X_i^t - X_k^t)$ is used if we want to 'focus on the weaknesses of team *k*'. In this case, team *i* should not use the playing

Chapter 3: League Championship Algorithm (LCA)

style of team k at week t against team l . $(X_i^t - X_j^t)$ and $(X_j^t - X_i^t)$ also can be defined. Due to the principle that each team should play with the best formation that is selected from playing experience up to now and by considering the results of the artificial match analysis in last week, new formation of team i at week $t+1$ $[X^{t+1}_i = (x^{t+1}_{i1}, x^{t+1}_{i2}, \dots, x^{t+1}_{in})]$ can be set up by one of the following equations:

If teams j and l have won the match at week t , the new formation of team i will be generated based on the S/T strategy:

$$\begin{aligned} \text{(S/T strategy): } x^{t+1}_{im} &= b_{im}^t + y_{im}^t (w_1 r_{1im} (x_{im}^t + x_{km}^t) + w_2 r_{2im} (x_{im}^t - x_{jm}^t)) & (3.4) \\ \forall m &= 1, 2, \dots, n \end{aligned}$$

If team i has won and team l has lost at week t , the new formation of team i will be generated based on the S/O strategy:

$$\begin{aligned} \text{(S/O strategy): } x^{t+1}_{im} &= b_{im}^t + y_{im}^t (w_2 r_{1im} (x_{km}^t + x_{im}^t) + w_1 r_{2im} (x_{im}^t - x_{jm}^t)) & (3.5) \\ \forall m &= 1, 2, \dots, n \end{aligned}$$

If team i has lost and team l has won at week t , the new formation of team i will be generated based on the W/T strategy:

$$\begin{aligned} \text{(W/T strategy): } x^{t+1}_{im} &= b_{im}^t + y_{im}^t (w_1 r_{1im} (x_{im}^t + x_{km}^t) + w_2 r_{2im} (x_{jm}^t - x_{im}^t)) & (3.6) \\ \forall m &= 1, 2, \dots, n \end{aligned}$$

If teams i and l have lost the match at week t , the new formation of team i will be generated based on the W/O strategy:

$$\begin{aligned} \text{(W/O strategy): } x^{t+1}_{im} &= b_{im}^t + y_{im}^t (w_2 r_{1im} (x_{km}^t + x_{im}^t) + w_2 r_{2im} (x_{jm}^t - x_{im}^t)) & (3.7) \\ \forall m &= 1, 2, \dots, n \end{aligned}$$

where m = number of team members; r_{1im} and r_{2im} = random numbers between $[0,1]$; w_1 and w_2 = coefficients used to scale the contribution of approach or retreat components; and y_{im}^t = binary variable that specifies whether or not the m th player must change in the new formation (only $y_{im}^t=1$ allows to change). Note that different signs in the parentheses are the consequence of acceleration towards the winner or recess from the loser. $y_i^t =$

$(y_{i1}^t, y_{i2}^t, \dots, y_{in}^t)$ denotes a binary change variable. The summation of the changes needed for next match ($y_i^t = 1$) is equal to q_i^t . Changes in all aspects of the team (players and styles) by coaches are not common (just a few changes in the team can be required). In order to calculate the number of changes in the team's formation for next match, a truncated geometric distribution is applied in LCA. The truncated geometric distribution lets LCA to control the number of changes with emphasis on the smaller rates of changes in B_i^t .

The truncated geometric distribution can be expressed as follows:

$$q_i^t = \left\lceil \frac{\ln(1-(1-p_c)^{n-q_0+1})r}{\ln(1-p_c)} \right\rceil + q_0 - 1: q_i^t \in \{q_0, q_0+1, \dots, q_0+n\} \quad (3.8)$$

where r = random number between $[0,1]$; p_c = control parameter [$p_c < 1, p_c \neq 0$]; and q_0 = the least number of changes. If $p_c < 0$, the situation is reversed so that by a more negative value of p_c , The emphasis in LCA is placed on a greater rate of change in the team's formation. q_0 is determined during the match analysis (note that the minimum value of q_0 is equal to zero). p_c in the truncated geometric distribution is the probability of success. In LCA, after calculating the value of q_i^t by using Eq. (3.8), the players of B_i^t are randomly selected and changed based on Eqs. (3.4)–(3.7).

3.7 Pseudo Code of LCA

Begin

Generate initial teams' formation randomly [$X_i^t = (x_{i1}^t, x_{i2}^t, \dots, x_{in}^t)$], $\forall_i = 1, 2, \dots, L$]

Generate league schedule for L teams

For $m = 1: L(S - 1)$

Evaluate the strengths for all teams

Calculate the chance of each team to defeat its competitors in next match (p_i^t)

Generate a random number between $[0,1]$ (R_n)

If $R_n \leq q_i^t$

Team i wins the match

Else

Team j wins the match

End if

Generate a random number between $[0,1]$ (r)

Calculate the number of changes in teams' best formation (B_i^t) for next match based on the truncated geometric distribution (q_i^t)

q_i^t players are selected randomly from B_i^t and changed by the SWOT matrix

If team i and team l have won

Select the S/T strategy

Else if team i has won and team l has lost

Select the S/O strategy

Else if team i has lost and team l has won

Select the W/T strategy

Else if team i has lost and team l has lost

Select the W/O strategy

End if

End for m

End

3.8 Conclusions

The league championship algorithm (LCA) has been introduced as a sport driven metaheuristic for numerical function optimization. LCA is a population based stochastic search methodology that mimics the sporting competitions in a sport league. At the heart of LCA is the artificial match analysis process where the new solutions are generated using a metaphorical SWOT analysis, which is typically followed by coaches during the planning for the next game. Some analysis was carried out to verify the rationale of the algorithm and the suitability of the updating equations, empirically. Some add-on modules

were also introduced into LCA with the aim of possibly enhancing the convergence speed of the algorithm toward the global minimum.

LCA is in its infancy, and much remains to be done to realize its full potency. It is therefore the author's hope that this paper inspires future works on developing LCA's theory and applications. Choosing a value for the control parameters of any optimization algorithm is often subjective, reflecting the user's experience and insight with a particular problem. To eliminate the need of the case based tuning of the control parameters, self-adaptive strategies could be employed in LCA as they are used in other evolutionary algorithms. Finally, the performance of LCA can be further tested on the real world engineering optimization problems addressed in the literature. Besides, a comparative study would be worth to conduct to measure the potency of LCA in comparison with other state of the art global optimization algorithms.

Chapter 4:

Simulation Results and Discussions

4.1 Introduction

An electrical distribution system (DS) represents the final stage in the electrical energy supply chain within power system operations, delivering electricity to individual customers through a radial network. In response to the restructuring of power system operation and planning, many power companies are investing in small-scale distributed power generation. Distributed Generation (DG) encompasses a wide range of systems, varying from fractions of kilowatts to megawatts. These systems can include conventional combustion generators powered by non-renewable energy sources, as well as renewable energy systems such as wind turbines, photovoltaic (PV) cells, microturbines, and small hydro turbines.

DG is defined as an electric power source that is connected directly to the distribution network or located on the consumer's side of the meter. DG offers several advantages over centralized power generation, including reduced transmission and distribution costs, decreased power losses, and improved voltage profiles. To maximize operational benefits, it is essential to optimally place and size DG during the planning phase of the distribution system. Improper placement and sizing can lead to increased power losses and result in voltage profiles that fall below acceptable limits.

The rise in active power loss translates to a loss of savings for utilities and a reduction in feeder utilization. Research indicates that approximately 70% [1] of power losses occur at the distribution level which can be categorized into technical losses (e.g., those resulting from line overloading or poor power factors) and non-technical losses (e.g., losses due to defective meters or incorrect tariffs). These losses significantly affect the financial performance and overall efficiency of the system. By integrating renewable energy-based DG units [2] for loss reduction, both energy sustainability aspects renewable energy and energy efficiency can be effectively addressed.

Key challenges in applying DG for loss reduction include determining proper locations, appropriate sizing, and effective operating strategies. In cases where the location is fixed for other reasons, incorrect sizing can lead to increased losses beyond those without DG. Therefore, optimal placement and sizing of DG are crucial to minimize overall system losses and enhance voltage profiles. Striving to draw maximum active power from a utility to boost profit from electricity sales can create imbalances between active and reactive power,

leading to voltage instability and potential collapse in critical scenarios. Properly sizing and placing shunt capacitors [3][4] can assist in correcting power factors, thus addressing the low power factor commonly associated with inductive loads, which contribute to higher power losses and voltage instabilities. The stability of voltage can be maintained by providing reactive power support at optimal locations in distribution systems .

Given the benefits of using both DG and capacitors in distribution networks, researchers have recently proposed various techniques to simultaneously determine the locations and sizes of both to enhance voltage stabilization and minimize power losses. utilized the Particle Swarm Optimization (PSO) algorithm [5] to identify the optimal locations and sizes for shunt capacitors and DG in IEEE standard networks with 12, 30, 33, and 69 buses, aiming to minimize losses.) employed the IEEE 33-bus network as a test system to demonstrate the advantages of using a Genetic Algorithm for locating DG and capacitors. applied the Bacterial Foraging Optimization Algorithm (BFOA) to a 33-bus network, comparing results across three scenarios: 1) only DG, 2) only Capacitors and 3) both DG and capacitors,

This study used the proposed LCA algorithm to calculate the optimal size of SC and PV-DG units in distribution systems. The voltage stability index was used as the objective function to find the best location and size for the DG units. Once the optimal-sized DG units were placed in the best location, various system performance metrics were calculated, such as minimizing real power loss, improving the voltage profile, and enhancing the voltage stability index. The LCA algorithm's results were compared to those of other algorithms after performing calculations on two test systems: the IEEE 33-bus and the 69-bus radial distribution system

4.2 Loss Sensitivity Factor

Based on LSF, DG installation locations can be discovered [17] The benefit of utilizing this approach is that it narrows the problem search space during optimization.

Fig. 1 depicts an illustration of a two-bus distribution system. The following calculation can be used to calculate the LSF at the line segment between buses i and k :

$$P_{ik-loss} = \frac{(P_k^2 + Q_k^2)R_{ik}}{(V_k)^2} \quad (4.1)$$

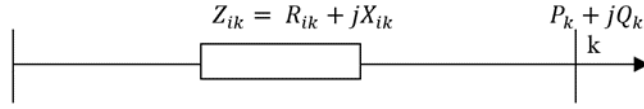


Figure 4.1. A two bus system one line diagrams Source: Authors, (2024).

4.3 Objective Function

The suggested objective function minimizes power losses, enhances voltage profiles, and increases the Voltage Stability Index. It can be solved to obtain the optimal DG locations and sizes.

$$F_t = w_1 f_1 + w_2 f_2 + w_3 f_3 \quad (4.2)$$

Where f_1 can be expressed as shown in the following equation:

$$f_1 = \frac{\sum_{i=1}^L (P_{LineLoss}(i))_{after\ DG}}{\sum_{i=1}^L (P_{LineLoss}(i))_{before\ DG}} \quad (4.3)$$

f_2 can be defined as the following equation:

$$f_2 = \frac{\sum_{i=1}^N |V_i - V_{i,ref}|_{after\ DG}}{\sum_{i=1}^N |V_i - V_{i,ref}|_{before\ DG}} \quad (4.4)$$

f_3 can be defined as:

$$f_3 = \frac{1}{VSI(k)_{after\ DG}} \quad (4.5)$$

Where VSI is formulated as the following Eq:

$$VSI(k) = |V_i|^4 - 4(P_k X_{ik} - Q_k R_{ik})^2 - 4(P_k R_{ik} - Q_k X_{ik})|V_i|^2 \quad (4.6)$$

$|w_1| + |w_2| + |w_3| = 1$ in this paper, w_1 is taken as 0.5 while w_2 as 0.25 and w_3 as 0.25

4.3.1 Constraints

➤ **Load Balancing Constraints**

The constraints for each bus are expressed as follows:

$$P_{g_{ni}} - P_{d_{ni}} - V_{ni} \sum_{j=1}^N V_{nj} Y_{nj} \cos(\delta_{ni} - \delta_{nj} - \theta_{nj}) = 0 \quad (4.7)$$

$$Q_{g_{ni}} - Q_{d_{ni}} - V_{ni} \sum_{j=1}^N V_{nj} Y_{nj} \sin(\delta_{ni} - \delta_{nj} - \theta_{nj}) = 0 \quad (4.8)$$

Where $n_i = 1, 2, 3, \dots, n_n$.

➤ **Voltage Constraints**

The considered range for the voltage of the buses is as follows:

$$V_{\min} \leq V_{ni} \leq V_{\max} \quad (4.9)$$

Where V_{\min} is the minimum voltage at bus n_i , V_{\max} is the maximum voltage at bus n_i .

➤ **DG Constraints**

The DG source that is utilized must conform to the permissible size and power factor within the specified range:

$$S_{\min}^{DG} \leq S_{NI}^{DG} \leq S_{\max}^{DG} \quad (4.10)$$

Where S_{\min}^{DG} is minimum apparent power at bus n_i , S_{\max}^{DG} is maximum apparent power at bus n_i and S_{NI}^{DG} is the apparent power at bus n_i

4.4 Results And Analysis Of Numerical Data

The proposed LCA algorithm is evaluated on both IEEE 33-bus and 69-bus radial distribution systems. To gauge its effectiveness, it is compared with the TLBO, HSA, and SOS algorithms. MATLAB is used to implement the LCA algorithm, aiming to determine the optimal size and placement of DG within the distribution network.

Algorithm: The League championship algorithm

```
1  To begin, set the league size (L) and the number of seasons
   (S). Additionally, assign the value of  $t = 1$ ;
2  create a league schedule;
3  Afterwards, generate a population of L solutions to initialize
   team formations. Determine the playing strengths of each
   team by evaluating their function or fitness value. It is
   important to note that the initialization of team formations
   should also serve as their current best formation;
4  While  $t$  is less than or equal to  $S$  multiplied by  $(L - 1)$ , or there
   has been no change in the last 100 iterations.
5      Identify the victor and loser of each team pairing at week
       $t$ , utilize a playing strength-based criterion based on the
      league schedule.
6       $t = t + 1$ ;
7      For  $i = 1$  to  $L$ 
8          Create a new formation for team  $I$  for the upcoming
          game, keeping in mind the team's best formation at the
          moment and the events of the previous week. Analyze
          the resulting arrangement's playing strength;
9          View the new formation as the team's current top
          arrangement if it is determined to be the most fitting
          one (i.e., the most excellent solution thus far for the
           $i$ th member of the population);

10     End for
11     If  $\text{mod}(t, L - 1) = 0$ 
12         Generate a league schedule;
13     End if
14 End while.
```

4.4.1 Only DG

➤ The IEEE 33-Bus Radial Distribution Network

The testing configuration outlined in [30] consists of a network featuring 33 buses and 32 branches. The system's total active and reactive power loads are 3.716 MW and 2.300 MVar, respectively. Distributed generation (DG) units vary in power output, with the largest unit at 3.4952 MVA and the smallest at 0.2 MVA. The DG penetration limit is set at 4.359 MVA, and the base voltage is maintained at 12.65 kV.

Chapter 4: Simulation Results and Discussions

Power flow calculations indicate that the system experiences active and reactive power losses of 210.1 kW and 143.14 kVAr, respectively. Using LSF factors, potential buses for DG placement have been identified. Table 1 provides the LSF values for each bus.

LSF	Bus No.	$\frac{V_{norm}(i)}{V(i)} = \frac{V}{0.95}$	Base Voltage
0.0173328	6	0.9994401	0.9494681
0.0139414	3	1.0346128	0.9828821
0.0138033	28	0.9826654	0.9335321
0.0103590	29	0.9740129	0.9253122
0.0103223	8	0.9813551	0.9322874
0.0080802	14	1.0188907	0.9679462
0.0080712	4	1.0267079	0.9753725
0.0060563	30	0.9702674	0.9217540
0.0047535	9	0.9746892	0.9259547
0.0047501	24	1.0238154	0.9726247
0.0045614	13	0.9595139	0.9115382
0.0045149	10	0.9685237	0.9200975
0.0037555	27	0.9947096	0.9449741
0.0030365	31	0.9658863	0.9175920
0.0028204	2	1.0494889	0.9970145
0.0027433	26	0.9974088	0.9475384
0.0026717	23	1.0308381	0.9792962
0.0023800	25	1.0203152	0.9692995
0.0022880	20	1.0451668	0.9929084
0.0013972	5	0.9571033	0.9092482
0.0013803	7	0.9957298	0.9459433
0.0013538	12	0.9660146	0.9177139

Chapter 4: Simulation Results and Discussions

0.0011808	17	0.9519908	0.9043912
0.0009111	16	0.9541467	0.9064393
0.0008107	15	0.9556014	0.9078213
0.0007965	11	0.9676092	0.9192287
0.0006456	32	0.9649225	0.9166764
0.0004473	18	0.9513452	0.9037779
0.0004155	21	1.0444252	0.9922039
0.0003599	22	1.0437542	0.9915665
0.0003317	19	1.0489327	0.9964861
0.0002027	33	0.9646238	0.9163927

Table 4.1. LSF values for the 33-bus system.

1. Predetermined number of DG units

The proposed solution has proven effective in addressing power loss reduction, especially when limited to 1, 2, or 3 DG units, as shown in Table 2. A comparison of results from the proposed technique with those from established methods—HSA [28], TLBO [29], and SOS [30]—indicates that the proposed method achieves lower total power losses. For the 33-bus test system, the LCA-based approach consistently outperforms the SOS, HSA, and TLBO methods in minimizing system power losses. Specifically, for a single fixed DG unit, the proposed method achieves a total loss of 109.07 kW, compared to 115.01 kW (SOS), 107.39 kW (HSA), and 124.695 kW (TLBO). With two fixed DG units, it reaches a total loss of 103.91 kW, outperforming the 107.39 kW achieved by HSA. For three fixed DG units, the

Chapter 4: Simulation Results and Discussions

proposed approach achieves 101.13 kW, compared to 104.26 kW (SOS), 135.69 kW (HSA), and 124.695 kW (TLBO).

Method	Number of DG Units	Optimal result			Loss (kW)
		DG size in MW (location)			
		DG1	DG2	DG3	
HSA	1	0.8491 (18)	-	-	144.23
	2	0.2012 (18)	0.6932 (17)	-	141.14
	3	0.1913 (18)	0.2133 (17)	0.5927 (16)	135.69
TLBO	1				
	2				
	3	1.1826 (12)	1.1913 (28)	1.1863 (30)	124.695
SOS	1	3.1322 (6)	-	-	115.01
	2	2.2861 (6)	0.8363 (28)	-	107.39
	3	2.2066 (6)	0.2 (28)	0.7167 (29)	104.26
LCA	1	2.0265 (14)	-	-	109.07
	2	1.1681 (14)	0.7232 (24)	-	103.91
	3	0.8523 (14)	0.1129 (24)	0.9012 (29)	101.13

Table 4.2. Results comparison of the 33-bus system with predetermined number of DG units

2. Optimal Number of DG Units

To determine the optimal number of DG units for the system, various configurations were tested, each with a different number of DG units, and their effects on active power loss were calculated. This iterative approach allowed each solution to correspond to a specific number of DG units, and the configuration with the lowest power loss was considered optimal. The evaluation spanned from 1 to 21 DG units, identifying the configuration that minimized power loss as the most suitable for the system.

Testing revealed that the minimum active power loss of 74.359 kW occurred with 12 DG units. This result aligns with the active power loss trends observed across other DG unit

Chapter 4: Simulation Results and Discussions

configurations. Thus, it can be concluded that the optimal configuration for the 33-bus system is 12 DG units, resulting in a total active power loss of 74.359 kW.

Table 3 displays the results of applying both the SOS and LCA methods to determine the optimal number of DG units. Although the LCA method achieves marginally lower power losses than the SOS method, both approaches identify the same optimal number of DG units. The proposed LCA-based method demonstrates high effectiveness in identifying the ideal location, size, and quantity of DG units for the IEEE 33-bus radial distribution system.

Power loss (KW)		Total DG Power Output (MW)	
SOS	LCA	SOS	LCA
76.967104	74.359012	2.509000089	2.50853254

Table 4.3. Results for the 33-bus system with 12 DG units obtained using both the SOS and LCA methods

Figure 2 illustrates the voltage profile curves after installing the optimal number of DG units using the SOS and LCA technics. The figure suggests that both approaches might have an identical impact on voltage profiles.

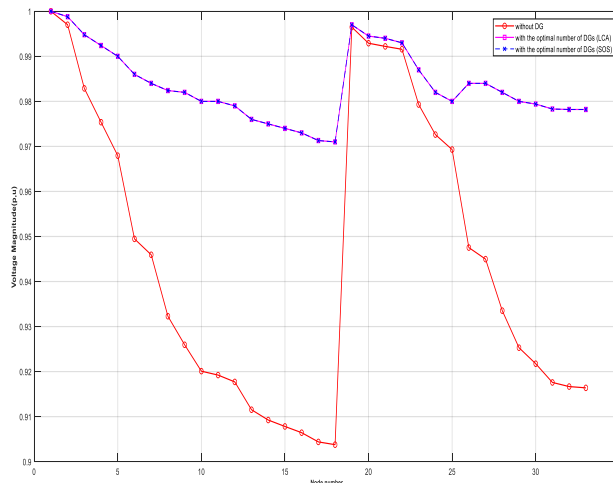


Figure 4.2. Voltage profile of the 33-bus system with optimal number of distributed generators

➤ The IEEE 69-Bus Radial Distribution Network

The next test system, as described in [30], is a radial distribution network with 69 buses, with a total load demand of 3.81 MW and 2.70 MVA_r. The system incurs active power losses of 225 kW and reactive power losses of 102.16 kVA_r. Distributed generation (DG) units in this system have capacities ranging from 0.2 MVA to 3.7248 MVA. The base voltage is set at 12.66 kV, and the DG penetration limit is capped at 4.656 MVA.

1. Predetermined Number of DG Units

The proposed approach effectively addresses the issue of determining the optimal configuration in scenarios where the number of DG units is predetermined. Table 4 compares the results of the proposed technique with existing methods, including HSA [30], TLBO [30], and SOS [30], and demonstrates that the proposed method achieves lower overall power losses than these alternatives.

For all cases with varying numbers of DG units, the proposed method outperforms HSA, TLBO, and SOS in minimizing system power losses. Specifically, for a single DG unit, the proposed method results in a total power loss of 110.12 kW, compared to 112.1 kW for HSA and 118.62 kW for SOS. With two DG units, it achieves a total power loss of 94.87 kW, outperforming HSA at 96.56 kW and SOS at 102.92 kW. For three DG units, the proposed approach yields a total power loss of 82.07 kW, compared to 86.66 kW for HSA, 82.172 kW for TLBO, and 82.07 kW for SOS.

In summary, the proposed LCA-based method effectively determines the optimal location, size, and number of DG units for the IEEE 69-bus radial distribution system.

Chapter 4: Simulation Results and Discussions

Method	Number of DG Units	Optimal result			Loss (kW)
		DG size in MW (placement)			
		DG1	DG2	DG3	
HSA	1	1.4363 (65)	-	-	112.10
	2	0.0544 (65)	1.5932 (64)	-	96.56
	3	0.0149 (65)	0.1416 (64)	1.6283 (63)	86.66
TLBO	1			-	
	2			-	
	3	0.9925 (17)	1.1998 (61)	0.7956 (63)	83.2
SOS	1	2.087 (57)	-	-	118.62
	2	0.3612 (57)	1.6948 (58)	-	102.92
	3	0.2588 (57)	0.2 (58)	1.5247 (61)	82.07
LCA	1	2.172 (11)	-	-	110.12
	2	0.3321 (11)	1.7284 (57)	-	94.87
	3	0.2061 (11)	0.1962 (57)	1.2741 (61)	81.74

Table 4.4. Evaluating of results for the 69-bus system with Predetermined number of DG units

2. Optimal Number of DG Units

The proposed technique was evaluated to assess the impact of varying DG unit counts on both active and reactive power losses. The results indicated that the minimum active power loss of 71.444166 kW was achieved with 8 DG units among the tested configurations.

Table 5 compares the proposed method with the SOS method in identifying the optimal number of DG units. Applying the LCA technique to the system with the ideal DG configuration resulted in lower total power losses than those achieved by the SOS method. Specifically, the active power losses obtained using the LCA and SOS techniques for the optimal DG configuration were 71.372133 kW and 71.444166 kW, respectively.

Power loss (KW)		Total DG Power Output (MW)	
SOS	LCA	SOS	LCA
71.444166	71.444166	2.437403138	2.393254123

Table 4.5. Results comparison for the 69-bus system with 8 distributed generation (DG) units.

Figure 4.3 displays the voltage profiles of the system's buses following the installation of the optimal number of DG units determined by the SOS and LCA methods. Both techniques markedly enhance the voltage levels at the buses, with nearly identical improvements resulting from both SOS and LCA methods.

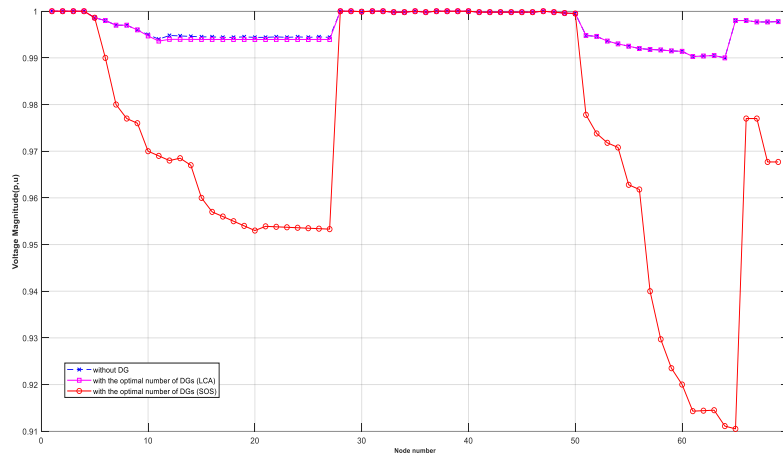


Figure 4.3. voltage profile of the 69-bus system with the optimal number of distributed generation (DG) units installed.

4.4.2 Only Capacitors

➤ THE IEEE 33-Bus Radial Distribution Network

1. Single Capacitor Placement

Table 6 displays the simulation results for the placement of a single capacitor utilizing the LCA technique. It includes the results from the base case, which does not incorporate any

Chapter 4: Simulation Results and Discussions

capacitors, along with two scenarios where a single capacitor is strategically positioned using the LCA method. The table outlines the optimal sizes and locations of the capacitors identified by this technique. In the base case, the power losses in the test system amount to 211 kW. By employing the LCA technique for capacitor placement, a reduction in losses of 27.91% is achieved.

Number of capacitors	Location Bus No.	Installed Capacity (MVar)	Loss in (kW)	Loss Reduction (%)
Without Capacitor	-	-	211.00	0.00
Single	31	1.29	152.10	27.91

Table 4.6. Single capacitor placement for 33-bus system.

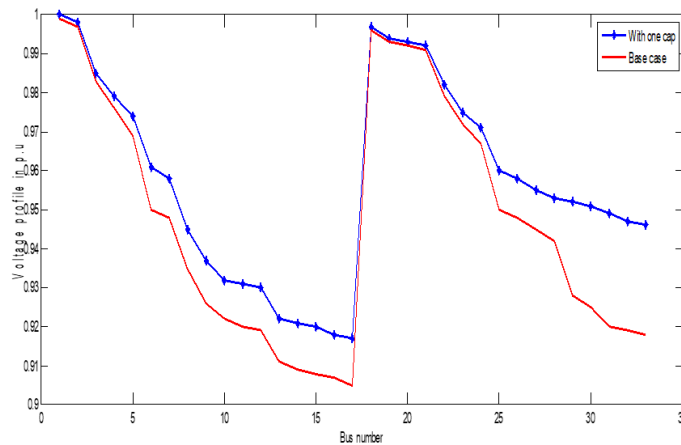


Figure 4.4 . Voltage profile improvement with single capacitor 33-bus.

Figure 4.4. shows the voltage profile improvement of the 33-bus radial distribution system with the installation of a single Capacitor using the LCA technique.

Chapter 4: Simulation Results and Discussions

2. Multi Capacitor Placements

Table 7 presents the simulation results for the 33-bus test system with various capacitor placements. It also includes the percentage reduction in losses achieved using multiple capacitors with the LCA technique. The results indicate that system losses decrease as the number of capacitors increases. However, the installation of capacitors is capped at four, as adding more leads to a decline in the system's voltage profile.

Number of capacitors	Installed Capacity (MVA _r) (Location Bus No)	Loss in (kW)	Loss Reduction (%)
Without Capacitor	-	211.00	0.00
2	C1 = 0.51 (11) C2 = 1.12 (29)	140.49	33.41
3	C1 = 0.42 (13) C2 = 0.53 (22) C3 = 1.06 (31)	139.31	33.97
4	C1 = 0.30 (9) C2 = 0.26 (13) C3 = 0.47 (24) C4 = 0.99 (31)	137.21	34.97
5	C1 = 0.12 (7) C2 = 0.29 (13) C3 = 0.56 (24) C4 = 0.21 (26) C5 = 0.89 (31)	136.70	35.21

Table 4.7. Multi capacitors placement for 33-bus system

➤ **The IEEE 69-bus radial distribution system**

1. Single Capacitor Placement

Table 4.7 provides the optimal sizes and locations for single capacitors, along with the percentage reduction in line losses for the IEEE 69-bus test system. It highlights the simulation results of placing a single capacitor using the LCA technique. The data shows that optimal placement of a single capacitor achieves a 32.70 % reduction in losses compared to the base case with LCA. Furthermore, the effectiveness of loss reduction improves as the number of DG and capacitor units increases.

Number of capacitors	Location Bus No.	Installed Capacity (MVar)	Loss in (kW)	Loss Reduction (%)
Without Capacitor	-	-	225.00	0.00
Single	61	1.92	151.41	32.70

Table 4.8. Single capacitor placement for 69-bus system.

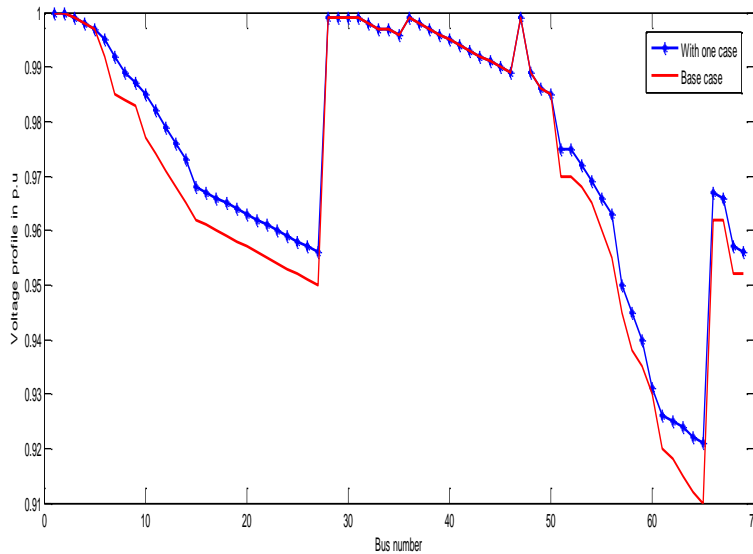


Figure 4.5. Voltage profile improvement with single capacitor 69-bus

Chapter 4: Simulation Results and Discussions

Figure 4.5 illustrates the voltage profile improvement of the IEEE 69-bus radial distribution system with single capacitor placement achieved through the LCA technique.

2. Multi Capacitor Placements

Table 4.9 displays the simulation results for the 69-bus test system with multiple capacitor placements and shows the percentage reduction in losses achieved through the use of multiple capacitors with the LCA technique.

Number of capacitors	Installed Capacity (MVar) (Location Bus No)	Loss in (kW)	Loss Reduction (%)
Without Capacitor	-	225.00	0.00
2	C1 = 0.32 (15) C2 = 1.22 (61)	147.38	34.45
3	C1 = 0.41 (12) C2 = 0.21 (21) C3 = 1.28 (61)	145.25	35.33
4	C1 = 0.38 (10) C2 = 0.27 (20) C3 = 0.61 (49) C4 = 1.27 (61)	144.50	35.78
5	C1 = 0.25 (12) C2 = 0.21 (19) C3 = 0.50 (51) C4 = 0.76 (55) C5 = 1.19 (61)	144.50	35.78

Table 4.9. Multi capacitors placement for 69-bus system

The figures clearly illustrate that increasing the number of installed capacitors improves the voltage profile and reduces system power losses. When determining the optimal number of capacitors, key considerations include the system's voltage profile, power loss, and voltage stability index. Based on these factors, the optimal number of capacitors is four for the 33-bus radial distribution system and three for the 69-bus radial distribution system.

4.4.3 Simultaneous PV-DG And Capacitors

➤ **The IEEE 33-bus radial distribution network**

Table 4.10 displays the simulation results for the 33-bus test system with Simultaneous PV-DG and Capacitors placements and sizes and shows the percentage reduction in losses achieved with the LCA technique and Grey Wolf Algorithm (GWA).

The number of PV-DG and Capacitors is fixed at three

	LCA	GWA
Capacitor Size in MVar (candidate Bus)	0.30(13) 0.55(22) 1.01(31)	0.30(33) 0.15(32) 0.45(31)
PV-DG Size in MW (Candidate Bus)	0.651(14) 0.113(24) 0.8913 (29)	0.868(18) 1.126(16) 1.098 (32)
V _{worst} in p.u. (Bus No)	0.989 (14)	0.989 (18)
PT, Loss (kW) (% Loss Reduction)	9.72 (95.39%)	10.56 (94.99%)

Table 4.10. Results of 33-bus Distribution System for Reconfiguration in the Presence of PV-DG and Capacitors.

➤ **The IEEE 69-bus radial distribution network**

Table 4.11 displays the simulation results for the 69-bus test system with Simultaneous PV-DG and Capacitors placements and sizes and shows the percentage reduction The number of PV-DG and Capacitors is fixed at three in losses achieved with the LCA technique and Grey Wolf Algorithm (GWA).

The number of PV-DG and Capacitors is fixed at three.

Chapter 4: Simulation Results and Discussions

	LCA	GWA
Capacitor Size in MVar (candidate Bus)	0.52(12) 0.33(21) 1.13(61)	0.60(22) 0.75(54) 0.75(65)
PV-DG Size in MW (Candidate Bus)	0.321(11) 0.191(57) 1.217 (61)	0.557(11) 0.448(18) 1.833 (59)
Vworst in p.u. (Bus No)	0.989 (53)	0.990 (50)
PT, Loss (kW) (% Loss Reduction)	2.13 (99.05%)	2.56 (98.86%)

Table 4.11. Results of 69-bus Distribution System for Reconfiguration in the Presence of PV-DG and Capacitors

Both the LCA and GWA show effective management of reactive power and distributed generation, with significant reductions in power losses. The results indicate a strong focus on enhancing grid performance and reliability, though there may be opportunities for further optimization, particularly in the GWA where slightly higher losses and a marginally lower voltage stability are observed.

4.5 CONCLUSION

This study presents a novel approach using the League Championship Algorithm (LCA) to optimize the placement and the size of PV distributed generators (PV-DGs) and Shunt capacitors in distribution networks. It specifically addresses the complexities involved in determining the ideal position, size, and number of DG units in radial distribution systems. The methodology prioritizes potential PV-DG and SC locations using a loss sensitivity factor and applies LCA to determine the optimal size for a set number of units. The configuration that achieves the lowest total power loss is selected as the optimal solution.

GENERAL CONCLUSION

Power systems can be divided into three main subsystems, namely, generation, transmission, and distribution. Of these three subsystems, distribution systems provide power to the various commercial, industrial and domestic customers via remote generation stations, with the generated power being transferred (through high-voltage transmission lines) to a load center. However, most distribution networks nowadays are defined as "active", which simply means that some of the power provided by these systems is generated by distributed generator (DG) units within the distribution system.

As a relatively new addition to distribution systems, DG improves overall system performance by reducing power loss and boosting system reliability and capacity.

The use of DG and capacitors also lengthens the life of infrastructure and is more environmentally friendly. However, to achieve these benefits, the Distributed Generators (DGs) must be placed at optimal locations and be optimally sized. Therefore, the integration of DGs into distribution networks is essentially an optimization problem formulated by system planner-designated constraints.

This thesis presents a methodology using the League Championship Algorithm (LCA) to determine the optimal placement and sizing of Photovoltaic Distributed Generation (PV-DG) units and Shunt Capacitors (SC) in radial distribution systems. The primary goal is to reduce power losses, improve voltage profiles, and enhance voltage stability by strategically integrating renewable generation sources and capacitors. Through simulation on IEEE 33-bus and 69-bus distribution systems, the study compares LCA's performance with other algorithms, showing that LCA achieves superior results in minimizing power loss and optimizing system stability.

Perspectives

There are several potential directions in which the present research could be extended. Some of these are listed below:

- The multi-objective optimization problem presented in this work could be applied to minimize the substation total emission productions or substation total electrical energy cost.
- The proposed strategy could also be utilized in other typical power system optimization problems

APPENDICES

Appendix I: IEEE 33-Bus Radial Distribution Network

Figure A.1 shows the configuration of the IEEE 33 Bus radial distribution system.

Substation

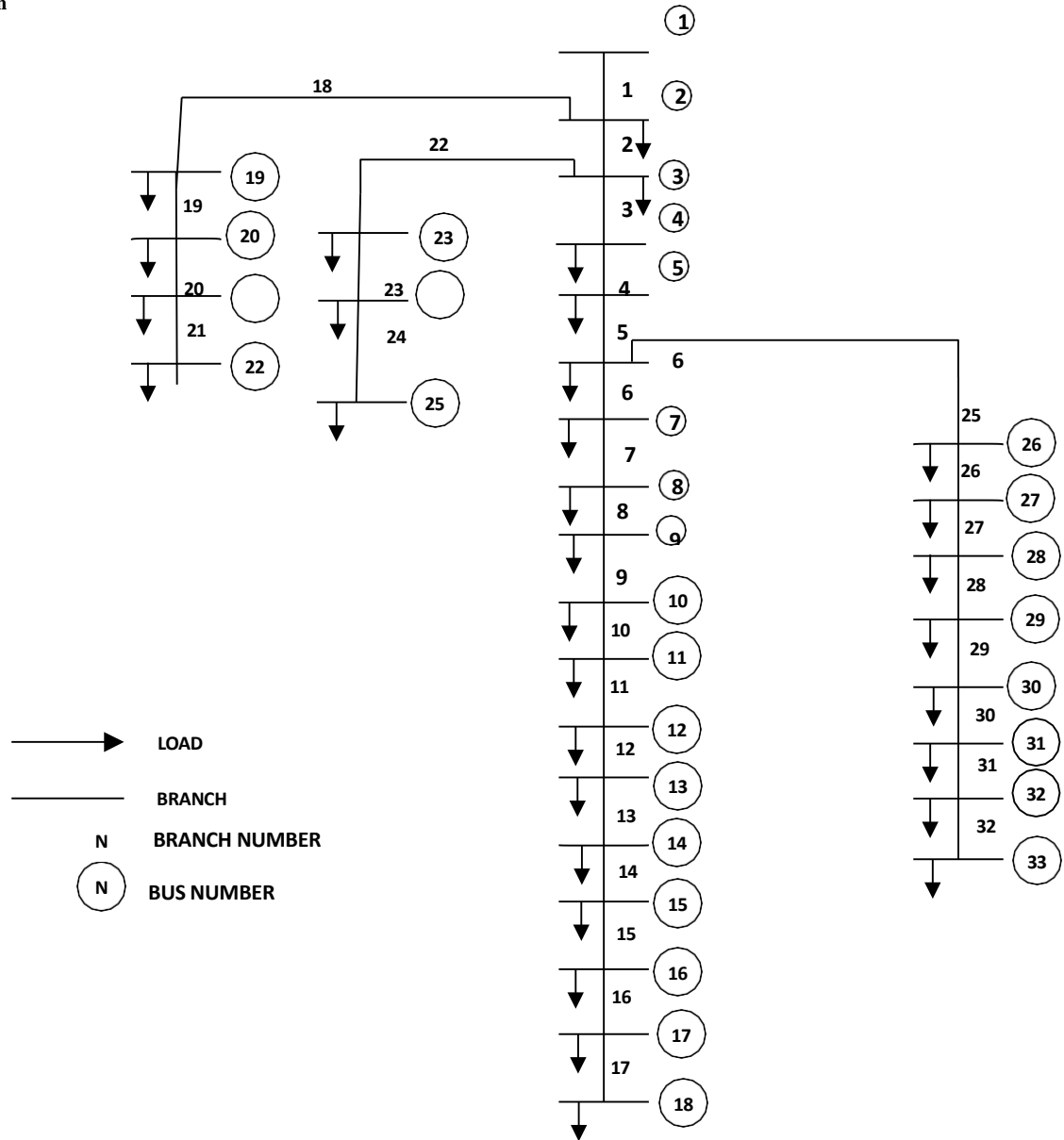


Figure A.1: IEEE 33-Bus radial distribution network.

Table A-1 shows the branch and bus data for the IEEE 33-bus radial distribution network.

Table A-1: IEEE 33-bus radial network parameters.

Sending Bus	Receiving Bus	R(Ohms)	X(Ohms)	load receiving bus P	at bus Q
1	2	0.0922	0.0477	100	60
2	3	0.4930	0.2511	90	40
3	4	0.3660	0.1864	120	80
4	5	0.3811	0.1941	60	30
5	6	0.8190	0.7070	60	20
6	7	0.1872	0.6188	200	100
7	8	1.7114	1.2351	200	100
8	9	1.0300	0.7400	60	20
9	10	1.0400	0.7400	60	20
10	11	0.1966	0.0650	45	30
11	12	0.3744	0.1238	60	35
12	13	1.4680	1.1550	60	35
13	14	0.5416	0.7129	120	80
14	15	0.5910	0.5260	60	10
15	16	0.7463	0.5450	60	20
16	17	1.2890	1.7210	60	20
17	18	0.7320	0.5740	90	40
2	19	0.1640	0.1565	90	40
19	20	1.5042	1.3554	90	40
20	21	0.4095	0.4784	90	40
21	22	0.7089	0.9373	90	40
3	23	0.4512	0.3083	90	50
23	24	0.8980	0.7091	420	200
24	25	0.8960	0.7011	420	200
6	26	0.2030	0.1034	60	25
26	27	0.2842	0.1447	60	25
27	28	1.0590	0.9337	60	20
28	29	0.8042	0.7006	120	70
29	30	0.5075	0.2585	200	600
30	31	0.9744	0.9630	150	70
31	32	0.3105	0.3619	210	100
32	33	0.3410	0.5302	60	40

System voltage is 12.66 kV

Appendix II: IEEE 69-Bus Radial Distribution Network

Figure A.2 shows the configuration of the IEEE 69 Bus radial distribution system.

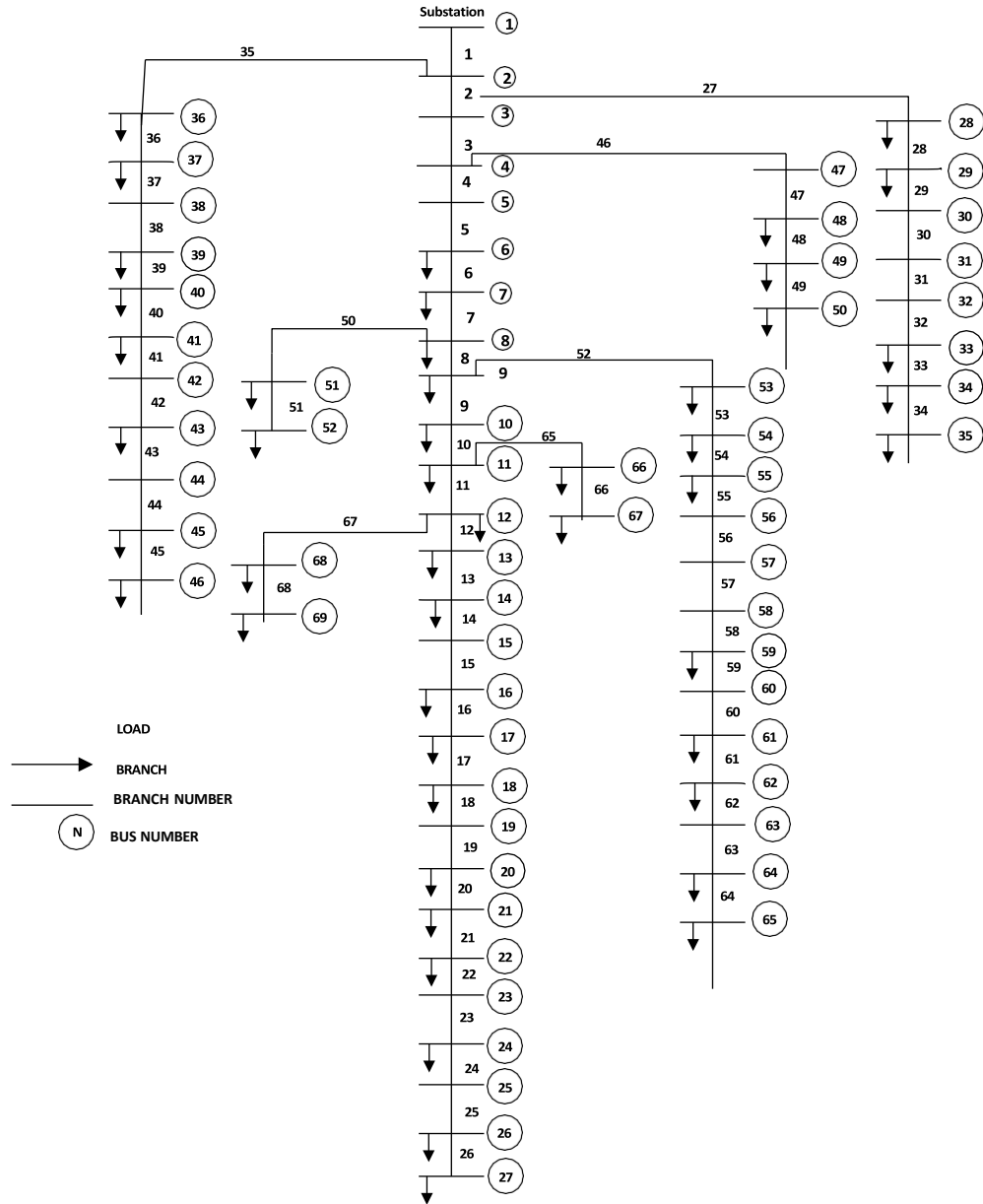


Figure A.2: IEEE 69-bus single line diagram

Table A-1 shows the branch and bus data for the IEEE 69-bus radial distribution network.

Table A-2: IEEE 69-bus system data.

Load at Receiving Bus

Sending Bus	Receiving Bus	R(ohms)	X(ohms)	P (kW)	Q(kVAr)	Sending Bus	Receiving Bus	R(ohms)	X(ohms)	P (kW)	Q(kVAr)
1	2	0.0005	0.0012	0	0	3	36	0.0044	0.0108	26	18.55
2	3	0.0005	0.0012	0	0	36	37	0.064	0.1565	26	18.55
3	4	0.0015	0.0036	0	0	37	38	0.1053	0.123	0	0
4	5	0.0251	0.0294	0	0	38	39	0.0304	0.0355	24	17
5	6	0.366	0.1864	2.6	2.2	39	40	0.0018	0.0021	24	17
6	7	0.3811	0.1941	40.4	30	40	41	0.7283	0.8509	1.2	1
7	8	0.0922	0.047	75	54	41	42	0.31	0.3623	0	0
8	9	0.0493	0.0251	30	22	42	43	0.041	0.0478	6	4.3
9	10	0.819	0.2707	28	19	43	44	0.0092	0.0116	0	0
10	11	0.1872	0.0619	145	104	44	45	0.1089	0.1373	39.22	26.3
11	12	0.7114	0.2351	145	104	45	46	0.0009	0.0012	39.22	26.3
12	13	1.03	0.34	8	5	4	47	0.0034	0.0084	0	0
13	14	1.044	0.345	8	5.5	47	48	0.0851	0.2083	79	56.4
14	15	1.058	0.3496	0	0	48	49	0.2898	0.7091	384.7	274.5
15	16	0.1966	0.065	45.5	30	49	50	0.0822	0.2011	384.7	274.5
16	17	0.3744	0.1238	60	35	8	51	0.0928	0.0473	40.5	28.3
17	18	0.0047	0.0016	60	35	51	52	0.3319	0.1114	3.6	2.7
18	19	0.3276	0.1083	0	0	9	53	0.174	0.0886	4.35	3.5
19	20	0.2106	0.069	1	0.6	53	54	0.203	0.1034	26.4	19
20	21	0.3416	0.1129	114	81	54	55	0.2842	0.1447	24	17.2
21	22	0.014	0.0046	5	3.5	55	56	0.2813	0.1433	0	0
22	23	0.1591	0.0526	0	0	56	57	1.59	0.5337	0	0
23	24	0.3463	0.1145	28	20	57	58	0.7837	0.263	0	0
24	25	0.7488	0.2475	0	0	58	59	0.3042	0.1006	100	72
25	26	0.3089	0.1021	14	10	59	60	0.3861	0.1172	0	0
26	27	0.1732	0.0572	14	10	60	61	0.5075	0.2585	1244	888
3	28	0.0044	0.0108	26	18.6	61	62	0.0974	0.0496	32	23
28	29	0.064	0.1565	26	18.6	62	63	0.145	0.0738	0	0
29	30	0.3978	0.1315	0	0	63	64	0.7105	0.3619	227	162
30	31	0.0702	0.0232	0	0	64	65	1.041	0.5302	59	42
31	32	0.351	0.116	0	0	11	66	0.2012	0.0611	18	13
32	33	0.839	0.2816	14	10	66	67	0.0047	0.0014	18	13
33	34	1.708	0.5646	9.5	14	12	68	0.7394	0.2444	28	20
34	35	1.474	0.4873	6	4	68	69	0.0047	0.0016	28	20

References

- [1] Wong L.A., Ramachandaramurthy V.K., Taylor P., Ekanayake J.B., Walker S.L., Padmanaban S. Review on the optimal placement, sizing and control of an energy storage system in the distribution network. *Journal of Energy Storage*, 2019, vol. 21, pp. 489-504. doi: <https://doi.org/10.1016/j.est.2018.12.015>
- [2] Hemmati R. Mobile model for distributed generations and battery energy storage systems in radial grids. *Journal of Renewable and Sustainable Energy*, 2019, vol. 11, no. 2, p. 025301. doi: <https://doi.org/10.1063/1.5079698>
- [3] Alharthi H., Alzahrani A., Shafiq S., Khalid M. Optimal allocation of batteries to facilitate high solar photovoltaic penetration. 9th International Conference on Power and Energy Systems (ICPES 2019), Perth, Australia, 2019. doi: <https://doi.org/10.1109/icpes47639.2019.9105479>.
- [4] A Ahmed H.M.A., Awad A.S.A., Ahmed M.H., Salama M.M.A. Mitigating voltage-sag and voltage-deviation problems in distribution networks using battery energy storage systems. *Electric Power Systems Research*, 2020, vol. 184, art. no. 106294. doi: <https://doi.org/10.1016/j.epsr.2020.106294>
- [5] Zhang Y., Xu Y., Yang H., Dong Z.Y. Voltage regulation- oriented co-planning of distributed generation and battery storage in active distribution networks. *International Journal of Electrical Power and Energy Systems*, 2019, vol. 105, pp. 79-88. doi: <https://doi.org/10.1016/j.ijepes.2018.07.036>
- [6] Benkhetta D, Rouina A, Necira A. Optimal Placement and sizing of DG Units Using LCA Algorithm. *EAI Endorsed Trans Energy Web* [Internet]. 2024 Jun. 24 [cited 2024 Oct. 29];11. Available from: <https://publications.eai.eu/index.php/ew/article/view/4345>
- [7] Benkhetta, D., Rouina, A., & Necira, A. (2024). The League Championship Algorithm (LCA) for optimal placement and sizing of shunt capacitors. *STUDIES IN ENGINEERING AND EXACT SCIENCES*, 5(2), e6975. <https://doi.org/10.54021/seesv5n2-124>
- [8] Gao J., Chen J.-J., Cai Y., Zeng S.-Q., Peng K. A two-stage Microgrid cost optimization considering distribution network loss and voltage deviation. *Energy Reports*, 2020, vol. 6, no. 2, pp. 263-267. doi: <https://doi.org/10.1016/j.egy.2019.11.072>
- [9] Luo L., Abdulkareem S.S., Rezvani A., Miveh M.R., Samad S., Aljojo N., Pazhoohesh M. Optimal scheduling of a renewable based microgrid considering photovoltaic system and battery energy storage under uncertainty. *Journal of Energy Storage*, 2020, vol. 28, art. no. 101306. doi: <https://doi.org/10.1016/j.est.2020.101306>.
- [10] A. Feliachi, "Optimal siting of power system stabilisers," in *IEE Proceedings C (Generation, Transmission and Distribution)*, 1990, pp. 101-106.
- [11] R. Fleming, M. Mohan, and K. Parvatisam, "Selection of parameters of stabilizers in multimachine power systems," *IEEE Transactions on power apparatus and systems*, pp. 2329-2333, 1981.
- [12] E. G. Shahraki, "Apport de l'UPFC à l'amélioration de la stabilité transitoire des réseaux électriques," *Université Henri Poincaré-Nancy 1*, 2003.
- [13] K. Hongesombut and Y. Mitani, "Implementation of advanced genetic algorithm to modern power system stabilization control," in *IEEE PES Power Systems Conference and Exposition*, 2004., 2004, pp. 1050-1055.
- [14] P. Kundur, "Power system stability," *Power system stability and control*, pp. 7-1, 2007.
- [15] N. P. Schmidt, "Comparison between IEEE and CIGRE ampacity standards," *IEEE*

- Transactions on Power Delivery, vol. 14, pp. 1555-1559, 1999.
- [16] B. Sørensen and G. Watt, "Trends in Photovoltaic Applications, Survey report of selected IEA countries between 1992 and 2005: Report IEA-PVPS T1-15: 2006," 2006.
- [17] A. Labouret and M. Villoz, *Energie solaire photovoltaïque vol. 3: Dunod Malakoff, France*, 2006.
- [18] K. Emery, Y. Hishikawa, and W. D. Warta, "Solar cell efficiency tables (Version 39)," *Progress in Photovoltaics: Research and Applications*, vol. 20, 2012.
- [19] T. Hammons, Y. Kucherov, L. Kapolyi, Z. Bicki, M. Klawe, S. Goethe, A. Tombor, Z. Reguly, N. Voropai, and V. Djangirov, "European policy on electricity infrastructure, interconnections, and electricity exchanges," *IEEE Power Engineering Review*, vol. 18, pp. 8-21, 1998.
- [20] S. Petibon, "Nouvelles architectures distribuées de gestion et conversion de l'énergie pour les applications photovoltaïques," *Université Paul Sabatier-Toulouse III*, 2009.
- [21] L. M. Fraas, "History of solar cell development," in *Low-cost solar electric power*, ed: Springer, 2014, pp. 1-12.
- [22] C. Bendel and A. Wagner, "Photovoltaic measurement relevant to the energy yield," in *3rd World Conference on Photovoltaic Energy Conversion, 2003. Proceedings of, 2003*, pp. 2227-2230.
- [23] D. King, B. Hansen, J. Kratochvil, and M. Quintana, "Dark current-voltage measurements on photovoltaic modules as a diagnostic or manufacturing tool," in *Conference Record of the Twenty Sixth IEEE Photovoltaic Specialists Conference-1997, 1997*, pp. 1125-1128.
- [24] A. C. Pastor, "Conception et réalisation de modules photovoltaïques électroniques," *INSA de Toulouse*, 2006.
- [25] S. Vighetti, "Systèmes photovoltaïques raccordés au réseau: Choix et dimensionnement des étages de conversion," *Institut National Polytechnique de Grenoble-INPG*, 2010.
- [26] S. Lyden, M. Haque, A. Gargoom, and M. Negnevitsky, "Modelling photovoltaic cell: Issues and operational constraints," in *2012 IEEE International Conference on Power System Technology (POWERCON), 2012*, pp. 1-6.
- [27] M. Abdulkadir, A. Samosir, and A. Yatim, "Modeling and simulation of a solar photovoltaic system, its dynamics and transient characteristics in LABVIEW," *International Journal of Power Electronics and Drive Systems*, vol. 3, p. 185, 2013.
- [28] P. de Assis Sobreira, M. G. Villalva, P. G. Barbosa, H. A. C. Braga, J. R. Gazoli, E. Ruppert, and A. A. Ferreira, "Comparative analysis of current and voltage-controlled photovoltaic maximum power point tracking," in *XI Brazilian Power Electronics Conference, 2011*, pp. 858-863.
- [29] M. A. De Brito, L. P. Sampaio, G. Luigi, G. A. e Melo, and C. A. Canesin, "Comparative analysis of MPPT techniques for PV applications," in *2011 International Conference on Clean Electrical Power (ICCEP), 2011*, pp. 99-104.
- [30] Chen J., Jiang X., Li J., Wu Q., Zhang Y., Song G., Lin D. Multi-stage dynamic optimal allocation for battery energy storage system in distribution networks with photovoltaic system. *International Transactions on Electrical Energy Systems*, 2020, vol. 30, no. 12, art. no. e12644. doi: <https://doi.org/10.1002/2050-7038.12644>
- [31] Wong L.A., Ramchandaramurthy V.K., Walker S.L., Taylor P., Sanjari M.J. Optimal placement and sizing of battery energy storage system for losses reduction using whale optimization algorithm. *Journal of Energy Storage*, 2019, vol. 26, art. no. 100892. doi: <https://doi.org/10.1016/j.est.2019.100892>.

- [32] Mukhopadhyay B., Das D. Multi-objective dynamic and static reconfiguration with optimized allocation of PV-DG and battery energy storage system. *Renewable and Sustainable Energy Reviews*, 2020, vol. 124, art. no. 109777. doi: <https://doi.org/10.1016/j.rser.2020.109777>.
- [33] MOHANDAS, N., R. BALAMURUGAN and L. LAKSHMINARASIMMAN. Optimal Location and Sizing of Real Power DG Units to Improve the Voltage Stability in the Distribution System Using ABC Algorithm United With Chaos. *International Journal of Electrical Power and Energy Systems*. 2015, vol. 66, iss. 1, pp. 41–52. ISSN 0142-0615. <https://doi.org/10.1016/j.ijepes.2014.10.033>.
- [34] Ahmadi B., Ceylan O., Ozdemir A. Voltage profile improving and peak shaving using multi-type distributed generators and battery energy storage systems in distribution networks. *55th International Universities Power Engineering Conference (UPEC 2020)*, Italy, 2020. doi: <https://doi.org/10.1109/upec49904.2020.9209880>.
- [35] ODA, E. S., A. A. ABDELSALAM, M. N. ABDEL-WAHAB and M. M. EL-SAADAWI. Distributed Generations Planning Using Flower Pollination Algorithm for Enhancing Distribution System Voltage Stability. *Ain Shams Engineering Journal*. 2015, vol. 8, iss. 4, pp. 593–603. ISSN 2090-4479. DOI: 10.1016/j.asej.2015.12.001.
- [36] Valencia A., Hincapie R.A., Gallego R.A. Optimal location, selection, and operation of battery energy storage systems and renewable distributed generation in medium–low voltage distribution networks. *Journal of Energy Storage*, 2021, vol. 34, art. no. 102158. doi: <https://doi.org/10.1016/j.est.2020.102158>.
- [37] Lu C., Gao L., Li X., Hu C., Yan X., Gong W. Chaotic-based grey wolf optimizer for numerical and engineering optimization problems. *Memetic Computing*, 2020, vol. 12, no. 4, pp. 371-398. doi: <https://doi.org/10.1007/s12293-020-00313-6>.
- [38] Mirjalili S., Mirjalili S.M., Lewis A. Grey wolf optimizer. *Advances in Engineering Software*, 2014, vol. 69, pp. 46-61. doi: <https://doi.org/10.1016/j.advengsoft.2013.12.007>
- [39] Settoul S., Chenni R., Hassan H.A., Zellagui M., Kraimia M.N. MFO Algorithm for optimal location and sizing of multiple photovoltaic distributed generations units for loss reduction in distribution systems. *7th International Renewable and Sustainable Energy Conference (IRSEC 2019)*. Morocco, 2019. doi: <https://doi.org/10.1109/irsec48032.2019.9078241>
- [40] Zellagui M., Settoul S., Lasmari A., El-Bayeh C.Z., Chenni R., Hassan H.A. Optimal allocation of renewable energy source integrated-smart distribution systems based on technical-economic analysis considering load demand and DG uncertainties. *Lecture Notes in Networks and Systems*. 2021, vol. 174, pp. 391-404. doi: https://doi.org/10.1007/978-3-030-63846-7_3
- [41] Belbachir N., Zellagui M., Lasmari A., El-Bayeh C.Z., Bekkouche B. Optimal PV sources integration in distribution system and its impacts on overcurrent relay based time-current-voltage tripping characteristic. *12th International Symposium on Advanced Topics in Electrical Engineering (ATEE 2021)*, Romania, 2021. doi: <https://doi.org/10.1109/atee52255.2021.9425155>
- [42] Lasmari A., Zellagui M., Hassan H.A., Settoul S., Abdelaziz A.Y., Chenni R. Optimal energy-efficient integration of photovoltaic DG in radial distribution systems for various load models. *11th International Renewable Energy Congress, (IREC 2020)*, Tunisia, 2020. doi: <https://doi.org/10.1109/irec48820.2020.9310429>.
- [43] Saleh K.A., Zeineldin H.H., Al-Hinai A., El-Saadany E.F. Optimal coordination of

- directional overcurrent relays using a new time-current-voltage characteristic. *IEEE Transactions on Power Delivery*. 2015, vol. 30, pp. 537-544. doi: <https://doi.org/10.1109/TPWRD.2014.2341666>.
- [44] Saremi S., Mirjalili S.Z., Mirjalili S.M. Evolutionary population dynamics and grey wolf optimizer. *Neural Computing and Applications*, 2015, vol. 26, no. 5, pp. 1257- 1263. doi: <https://doi.org/10.1007/s00521-014-1806-7>.
- [45] Zafar R., Ravishankar J., Fletcher J.E., Pota H.R. Multi- timescale model predictive control of battery energy storage system using conic relaxation in smart distribution grids. *IEEE Transactions on Power Systems*, 2018, vol. 33, no. 6, pp. 7152-7161. doi: <https://doi.org/10.1109/tpwrs.2018.2847400>
- [46] Bai L., Jiang T., Li F., Chen H., Li X. Distributed energy storage planning in soft open point based active distribution networks incorporating network reconfiguration and DG reactive power capability. *Applied Energy*, 2018, vol. 210, pp. 1082-1091. doi: <https://doi.org/10.1016/j.apenergy.2017.07.004>
- [47] Lei J., Gong Q. Operating strategy and optimal allocation of large-scale VRB energy storage system in active distribution networks for solar/wind power applications. *IET Generation, Transmission & Distribution*, 2017, vol. 11, no. 9, pp. 2403- 2411. doi: <https://doi.org/10.1049/iet-gtd.2016.2076>
- [48] H.R.E.H. BOUCHEKARA , M.A. ABIDO , A.E. CHAIB and R. MEHASNI . Optimal power flow using the league championship algorithm: A case study of the Algerian power system. *Energy Conversion and Management* 87 (2014) 58–70 <http://dx.doi.org/10.1016/j.enconman.2014.06.088H>.
- [49] A. KASHAN. 2014. League Championship Algorithm(LCA): An algorithm for global optimization inspired by sport championships. *Applied Soft Computing*. 16:171-200. <https://doi.org/10.1016/j.asoc.2013.12.005>
- [50] KOLLU, R., S.R RAYAPUDI and V. L. N. SADHU. A novel method for optimal placement of distributed generation in distribution systems using HSDO. *European Transactions on Electrical Power*. 2014, vol. 24, iss. 4, pp. 547–561. ISSN 2050-7038 <https://doi.org/10.1002/etep.1710>
- [51] SULTANA, S. and P. K. ROY. Multi-objective quasi-oppositional teaching learning based optimization for optimal location of distributed generator in radial distribution systems. *International Journal of Electrical Power & Energy Systems*. 2014, vol. 63, iss. 1, pp. 534–545. ISSN 0142-0615 <https://doi.org/10.1016/j.ijepes.2014.06.031>
- [52] J. L. Rueda, D. G. Colome, and I. Erlich, "Assessment and enhancement of small signal stability considering uncertainties," *IEEE transactions on Power Systems*, vol. 24, pp. 198-207, 2009..
- [53] T. J. Browne, V. Vittal, G. T. Heydt, and A. R. Messina, "A comparative assessment of two techniques for modal identification from power system measurements," *IEEE transactions on Power Systems*, vol. 23, pp. 1408-1415, 2008.
- [54] J. Hauer, "Application of Prony analysis to the determination of modal content and equivalent models for measured power system response," *IEEE transactions on Power Systems*, vol. 6, pp. 1062-1068, 1991.
- [55] J. F. Hauer, C. Demeure, and L. Scharf, "Initial results in Prony analysis of power system response signals," *IEEE transactions on Power Systems*, vol. 5, pp. 80-89, 1990.
- [56] S. P. Teeuwsen, I. Erlich, and M. A. El-Sharkawi, "Neural network based classification method for small-signal stability assessment," in *2003 IEEE Bologna Power Tech Conference Proceedings*, 2003, p. 6 pp. Vol. 3.

- [57] L. Chaib, A. Choucha, and S. Arif, "Optimal design and tuning of novel fractional order PID power system stabilizer using a new metaheuristic Bat algorithm," *Ain Shams Engineering Journal*, vol. 8, pp. 113-125, 2017.
- [58] Z. A. Obaid, L. Cipcigan, and M. T. Muhssin, "Power system oscillations and control: Classifications and PSSs' design methods: A review," *Renewable and Sustainable Energy Reviews*, vol. 79, pp. 839-849, 2017.
- [59] R. C. Eberhart and Y. Shi, "Comparing inertia weights and constriction factors in particle swarm optimization," in *Proceedings of the 2000 congress on evolutionary computation. CEC00 (Cat. No. 00TH8512)*, 2000, pp. 84-88.
- [60] J. Zhu, *Optimization of power system operation: John Wiley & Sons*, 2015.
- [61] Y. Abdel-Magid and M. Abido, "Optimal multiobjective design of robust power system stabilizers using genetic algorithms," *IEEE transactions on Power Systems*, vol. 18, pp. 1125-1132, 2003.
- [62] Y. Abdel-Magid, M. Abido, S. Al-Baiyat, and A. Mantawy, "Simultaneous stabilization of multimachine power systems via genetic algorithms," *IEEE transactions on Power Systems*, vol. 14, pp. 1428-1439, 1999.
- [63] S. Abe and A. Doi, "A new power system stabilizer synthesis in multimachine power systems," *IEEE Transactions on power apparatus and systems*, pp. 3910-3918, 1983.
- [64] M. E. Aboul-Ela, A. Sallam, J. D. McCalley, and A. Fouad, "Damping controller design for power system oscillations using global signals," *IEEE transactions on Power Systems*, vol. 11, pp. 767-773, 1996.
- [65] G. Andersson, "Modelling and analysis of electric power systems," *ETH Zurich*, pp. 5-6, 2008.
- [66] G. Andersson, "Dynamics and control of electric power systems," *Lecture notes*, pp. 227-0528, 2012.
- [67] J. R. Arredondo, "Results of a study on location and tuning of power system stabilizers," *International Journal of Electrical Power & Energy Systems*, vol. 19, pp. 563-567, 1997.
- [68] M. J. Basler and R. C. Schaefer, "Understanding power system stability," in *58th Annual Conference for Protective Relay Engineers*, 2005., 2005, pp. 46-67.
- [69] M. J. Basler, R. C. Schaefer, K. Kim, and R. Glenn, "Voltage regulator with dual PID controllers enhances power system stability," in *Hydrovision*, 2002.
- [70] P. Bornard, M. Pavard, G. Testud, and d. I. Réseaux, "de Transport: Réglages et Stabilité," *Techniques de l'Ingénieur, Traité Génie Electrique*, D4-092, 2005.
- [71] L. Cai, "Robust coordinated control of FACTS devices in large power systems," *Duisburg, Essen, Univ., Diss.*, 2004, 2004.
- [72] E. Lerch, D. Povh, and L. Xu, "Advanced SVC control for damping power system oscillations," *IEEE transactions on Power Systems*, vol. 6, pp. 524-535, 1991.
- [73] N. Rizoug, "Modélisation électrique et énergétique des supercondensateurs et méthodes de caractérisation: Application au cyclage d'un module de supercondensateurs basse tension en grande puissance," *Université des Sciences et Technologie de Lille-Lille I*, 2006.
- [74] P. L. Dandeno, A. N. Karas, K. R. McClymont, and W. Watson, "Effect of high-speed rectifier excitation systems on generator stability limits," *IEEE Transactions on power apparatus and systems*, pp. 190-201, 1968.
- [75] T. Nguyen-Phuoc, D. Vo-Ngoc and T. Tran-The, "Optimal number location and size of distributed generators in distribution systems by symbiotic organism search based method", *Advances in Electrical and Electronic Engineering*, vol. 15, no. 5, pp. 724-735,

2017. 0615 [https://doi.org/ 10.15598/aece.v15i5.2355](https://doi.org/10.15598/aece.v15i5.2355)
- [76] K. Rajalakshmi et al 2023 J. Phys.: Conf. Ser. 2601 012018M. G. H. Omran, S. Alsharhan, and M. Clerc, "A modified Intellects-Masses Optimizer for solving real-world optimization problems," *Swarm and Evolutionary Computation*, vol. 41, **pp. 159-166, 2018.**
- [77] Y. Sun, X. Wang, Y. Chen, and Z. Liu, "A modified whale optimization algorithm for large- scale global optimization problems," *Expert Systems with Applications*, vol. 114, pp. 563- 577, 2018.
- [78] Rezaei, H., Bozorg-Haddad, O., Chu, X. (2018). League Championship Algorithm (LCA). In: Bozorg-Haddad, O. (eds) *Advanced Optimization by Nature-Inspired Algorithms. Studies in Computational Intelligence*, vol 720. Springer, Singapore. https://doi.org/10.1007/978-981-10-5221-7_3